Dissertation

submitted to the

Combined Faculties for the Natural Science and for Mathematics

of the Ruperto-Carola University of Heidelberg, Germany

for the degree of

Doctor of Natural Science

presented by

Master in applied mathematics and physics: Evgeny Resnik

born in: Enakiewo, Ukraine

Oral examination: 12.12.2007

Impaired representation of space in the hippocampus of GluR-A knockout mice

Referees: **Prof. Dr. Bert Sakmann**

Prof. Dr. Heinz Horner

Co-adviser: **Dr. Mayank Mehta (Brown University, USA)**

SUMMARY

Um die Rolle der AMPAR vermittelten synaptischen Transmission bei der ortsabhängigen Aktivität hippokampaler CA1 Pyramidalzellen zu untersuchen, haben wir Aufzeichnungstechniken mit Mehrfach - Tetroden an sich freilaufenden Mäusen mit defektem GluR-A-Gen vorgenommen. Wir haben gefunden, dass bei den GluR-A Knockout Mäusen die ortsabhängige Aktivität der analysierten Nervenzellen beeinträchtigt war. Die Pyramidenzellen bildeten Aktivitätsfelder aus, die in im Vergleich zu Wildtypgeschwister Mäusen in GluR-A defizienten Mäusen signifikant größer (160-200%), weniger selektiv im Allgemeinen (73%), bezüglich der Richtung (39%) weniger stabil (53%) waren und weniger Information zur Position des Tieres trugen (47%). Trotz der beobachteten positiven Korrelation zwischen den Eigenschaften der Aktivitätsfelder und dem Grad der kognitiven Anforderung der drei hier untersuchten Verhaltensaufgaben, waren die räumlichen Aktivitätsdefizite der GluR-A Knockout Mäuse konsistent und unabhängig von deren Komplexität der Verhaltensaufgabe. Die Frequenz des hippokampalen Theta-Rhythmus war durch den Verlust des funktionellen GluR-A Gens leicht herabsetzt. Das relative Spike-Timing der Pyramidalzellen in Bezug auf den Theta-Rhythmus war jedoch normal. Diese Ergebnisse unterstreichen die Funktion der AMPA Rezeptoren mit GluR-A Untereinheit für eine korrekte, interne räumliche Repräsentation in der CA1-Region des Hippokampus, was wiederum für ein effektives Arbeitsgedächtnis wichtig zu seien scheint.

To investigate the role of AMPAR-mediated synaptic transmission in the place-specific firing of the hippocampal CA1 pyramidal cells, we have applied multiple tetrode recording techniques in freely behaving mice with a complete knockout of the GluR-A gene. We have found that place-specific activity of the neurons was significantly impaired in the GluR-A KO mice. The pyramidal cells in GluR-A KO mice formed firing (place) fields, that were: significantly larger (160-200%), less location selective (73%), less direction selective (39%), less stable (53%) and carried less information about the animal's position (47%) than those cells studied in wild-type mice. Despite the observed positive correlation between the firing field's properties and the degree of cognitive demands of three employed behavioral paradigms, the spatial firing defects were consistent across the paradigms independent from their complexity. We have also found that deletion of the GluR-A gene slightly reduced (5%) the frequency of the hippocampal theta rhythm, but did not affect relative timing of the pyramidal cell spikes in respect to the theta rhythm. These results demonstrate that GluR-A-containing AMPA receptors are necessary for the normal representation of space in the CA1 region of the hippocampus, which might be necessary for the flexible working memory system.

ACKNOWLEDGEMENTS

I want to take this moment to thank a number of people. First of all, my wife Olga, for her faith in me and her patience in dealing with me in these trying times; my 2-months old son Phillip, who has motivated me to take, finally, the last step and write the thesis; my parents for unconditional support, which made this easier than it could have been.

I would like to express my gratitude to Prof. Bert Sakmann for launching and further support of this long-lasting project despite many technical difficulties I had at the beginning. I am especially grateful to my advisor Dr. Mayank Mehta (Brown University, USA) for introducing me to a nice technique of extracellular recording in awake behaving mice, and for sharing his great experience in the analysis of experimental data.

I would like to thank Dr. Tansu Celikel, for the permanent support during all the time I worked in the Department of Cell Physiology, as well as for never sparing his time when I asked him to discuss the data or to read critically different parts of this dissertation. A special thanks to him for the collaboration in developing a new microdrive for chronic extracellular recording, after almost 1.5 years of unsuccessful efforts to record units with the original one.

I would like to thank also Prof. Peter Seeburg, Dr. Rolf Sprengel and Verena Bosch from the Department of Molecular Neurobiology who provided me with these nice dumb GluR-A knockout mice.

I am grateful to all members of the local Russian community: Prof. Dr. Nail Burnashev, Dr. Andrey Rozov, Dr. Alexandr Kolleker, Dr. Alexey Ponomarenko and Dr. Tatjana Korotkova, who helped me a lot with their experience and knowledge in both scientific and everyday life.

Thanks to all other members of the lab for creating such a friendly atmosphere in which it was a real pleasure to work.

The work presented in this thesis was supported by the Max Plank Society.

CONTENTS

1. INTRODUCTION

1.1. The hippocampus

The hippocampus is a part of the temporal lobe and belongs functionally to the limbic system (Squire et al., 2004). The name derives from its curved shape in coronal sections of the brain, which resembles a seahorse (Greek: hippo=horse, kampos=sea monster). The hippocampus has long been recognized as playing a vital role in formation of declarative memory, which describes the capacity to recollect facts and autobiographical events. The observations of Scoville and Milner (1957), showing that bilateral hippocampal removal as a treatment for epilepsy suffered by patient H.M. resulted in anterograde amnesia, explicitly identified the important role of the hippocampus and temporal lobe structures in memory. After hippocampal lesion, however, the patient was able to learn procedural tasks, suggesting that the non-declarative procedural memory system is independent from the hippocampus. In infrahumans the hippocampus is believed to be involved specifically in the spatial component of episodic memory (Morris et al., 1982; O'Keefe and Nadel, 1978), which can be easily tested experimentally. Therefore, the hippocampus of rats and mice has attracted attention as a model to study the mechanisms of hippocampus functioning and its role in behavior.

1.1.1. Gross anatomy

The rodent hippocampus is located along the rostro-caudal plane of the rodent brain in a way that, roughly, one end is near the top of the head (the dorsal hippocampus or septal pole) and another end near the bottom of the head (the ventral hippocampus or the temporal pole). The hippocampus consists of two C-shaped interlocking regions: the Ammon's horn (cornu ammonis, CA) and the dentate gyrus (fascia dentata, DG). A coronal section of the hippocampus reveals two layers of principal neurons in CA and DG: the pyramidal cells (statum [str.]. pyramidale) and the granular cells (str.granulosum), respectively (Ramón y Cajal, 1893). DG includes two more layers, one above str.granulosum: str.moleculare, where dendrites of granular cells arborize, and one below: the hilus, characterized by widely scattered polymorph neurons. The layers of CA, starting from the ventricular surface, are alveus, str.oriens, str.pyramidale, str.radiatum, str.moleculare and str.lacunosum. The latter two often combined into a single str.lacunosum-moleculare.

Ammon's horn can be further divided orthogonally to the layers into CA3, the area closest to the hilus of DG, and CA1 on the other end of the Ammon's horn, continuing through subiculum, pre- and parasubiculum to the entorhinal cortex (EC).

1.1.2. Cell types

As noted above, the cell bodies of hippocampal principal cells (i.e. granule cells of DG and pyramidal cells of CA) are located in str.granulosum and pyramidale. Granule cell dendrites stretch out to str.moleculare, while pyramidal cells have their main apical dendritic shafts in str.radiatum terminating in str.lacunosum-moleculare, and basal dendrites in str.oriens. Dendrites have numerous spines that are the postsynaptic elements of the synapses. Axons of pyramidal cells run in str.alveus where they emit numerous collaterals before leaving the hippocampus. All pyramidal and granule cells are excitatory as their primary neurotransmitter is glutamate.

The activity of pyramidal cells is modulated not only by extrinsic afferents but also by intrinsic ones coming from local inhibitory interneurons. They are fewer in number (10-20%) but greater in diversity (Freund and Buzsaki, 1996). Four main types of inhibitory interneurons that have been described in CA are γ-aminobutyric acid (GABA)-ergic and have their cell bodies in all five layers of the CA region.

Principal and interneurons can also be distinguished electrophysiologically: principal cells tend to fire wider action potentials, with a lower average frequency, may show strong firing rate adaptation, and often fire in bursts, compared to interneurons. However, the firing pattern of cells also varies as a function of the 'global state' of the hippocampus, reflected in hippocampal rhythms (see section about rhythms).

1.1.3. Connections with other areas

The principal cortical input to the hippocampus arrives via the perforant pathway from entorhinal cortex (EC), which receives monosynaptic inputs from higher-order sensory areas of each modality and pre-processed multimodal information from association areas (Figure 1.1). Cells in the layer II of EC project almost exclusively to the DG and CA3 subfield, while cells in layer III project to CA1 and subiculum. Due to the high density (~85%, Matthews et al., 1976) of EC synapses in DG and lack of feedback projections from the other subregions of hippocampus into DG, it is suggested that DG preferentially processes the information coming from the cortex into the hippocampus. EC

projections to hippocampus observe a rough topography: fibers from medial entorhinal cortex (MEC) terminate in the middle one-third of the molecular layer of DG and in the outer two-thirds of the molecular layer of CA1 close to the border with CA3. Fibers from lateral entorhinal cortex (LEC) terminate in the outer one-third of the molecular layer of DG and in the outer two-thirds of the molecular layer of CA1, but closer to the subicular border. An inverse terminal distribution is present in the subiculum, although considerable overlap occurs. The EC also projects to the contralateral hippocampal formation via dorsal hippocampal commissural fibers, which are smaller in number than those of the ipsilateral projections. Topographically, relatively small areas of the EC project to the extensive areas of the hippocampal formation (DG and CA) along its longitudinal and septotemporal axis. Lateral EC projects mainly to the dorsal part of the hippocampus, while medial EC to ventral part of the hippocampus. The entorhinal projections to the hippocampus are excitatory and use glutamate or aspartate as their neurotransmitter. The EC, in turn, receives projections from the subiculum and to a less extent from the entire longitudinal axis of CA1. Most of the fibers terminate in the deeper layers of the MEC, although weaker projections to LEC have been described. The subiculo-entorhinal pathway appears to be strictly ipsilateral.

The hippocampus has also extensive connections with other subcortical structures, among them are the other parts of the limbic system, thalamus and the brain stem reticular formation. Among the most important of these pathways are the reciprocal connections with septum: hippocampus receives cholinergic and GABAergic connections from the septum and both principal and interneurons send back their axons to the septum.

1.1.4. Internal circuitry

The hippocampus has an internal excitatory circuitry, often referred to as the hippocampal (trisynaptic) loop. Granule cells in DG receive synapses from the perforant path, and send mossy fibers terminating in str. radiatum on the proximal apical dendrites of CA3 pyramidal cells. CA3 pyramidal cell axons give recurrent collaterals to CA3 pyramidal cells and the Schaffer collaterals to CA1 pyramidal cells, terminating in the distal two-third of str. radiatum. Within all fields of the hippocampus a large number of interneurons are present. These interneurons often have extensive axon arborization, usually staying within the boundary of a given region. They can interact with many

hippocampal principal neurons modulating hippocampal activity both by feed-forward and feed-back inhibition (Lopes da Silva et al., 1990).

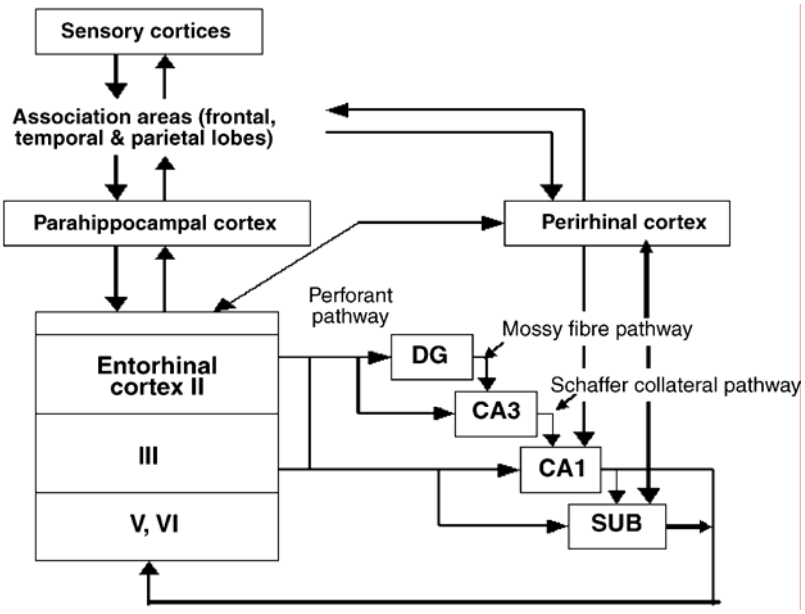

Figure 1.1. Extrinsic and intrinsic connections of the hippocampal formation. Adapted from O'Mara, (2005).

1.1.5. Synaptic plasticity and memory

Cajal (1913) originally hypothesized that information storage relies on changes in strength of synaptic connections between neurons that are active. Hebb (1949) supported this hypothesis and proposed that if two neurons are active at the same time, the synaptic efficiency of the appropriate synapse will be strengthened. The discovery of the long-term potentiation (LTP) provided a cellular model to test the hypothesis on how synapses are modified. The first full description of LTP by Bliss and Lømo (1973) reported that trains of high-frequency stimulation to the rabbit perforant path caused a sustained increase in efficiency of synaptic transmission in the granule cells of the dentate gyrus. This report, and others which followed during the 1970s, confirmed the Hebbian nature of this form of synaptic plasticity. The three well-described characteristics of LTP, cooperativity, associativity and input specificity (Bliss and Collinridge, 1993) and the durability of LTP (Abraham et al., 1995), have been identified as solid arguments that support the hypothesis that LTP may be a biological substrate for at least some forms of memory. Several other experimental observations have consolidated this view. Most notably, 1) LTP is most

easily demonstrable in the hippocampus, an area of the brain known to be fundamentally important in memory acquisition. 2) Rhythmic bursts of activity that induce LTP mimic naturally occurring theta rhythm recorded in the hippocampus during exploratory behavior (Diamond et al., 1988; Greenstein et al., 1988b; Larson et al., 1986b; Rose and Dunwiddie, 1986). 3) Inhibitors of hippocampal LTP also block hippocampal learning and retention of learned behavior (Morris et al., 1986). 4) Several biochemical changes that occur after induction of LTP also occur during memory acquisition (Frankland et al., 2001; Silva et al., 1998). 5) Hippocampal-dependent learning induces long-lasting changes in the synaptic strength of hippocampal synapses (Whitlock et al., 2006). These findings argue that memory consolidation requires induction of changes that resemble those, necessary for induction of LTP. However, it remains to be clearly shown that induction of LTP will result in some form of memory consolidation (Hölscher, 1999). Another interesting parallel between memory and LTP is related with the fact that LTP was shown to consist of distinct phases involving different molecular mechanisms. The early phase (E-LTP), which lasts 2–3 h, is independent of protein synthesis, while more persistent long-lasting LTP (L-LTP), which lasts several hours in vitro and weeks in vivo, requires gene expression and synthesis of new proteins (Frey et al., 1988; Huang et al., 1996). In analogy with LTP, two components of memory can be discriminated: short-term memory, which lasts for a few hours, and long-term memory, which persists for days and requires gene expression and new protein synthesis (for review see Davis and Squire, 1984).

Long-term changes in synaptic efficacy in the hippocampus can be induced by different patterns of stimulation. Among them the most widely used are presynaptic tetanization, pre- and postsynaptic stimulation pairing and theta burst pairing (TBP). Tetanization consists of a 1 s long high frequency (100 Hz) stimulation of presynaptic neurons (Figure 1.2A). Pairing protocol is a low frequency (0.7-1.5 Hz) presynaptic stimulation paired with prolonged (~3 min) postsynaptic depolarization at 0 mV, which aims to mimic postsynaptic action potential initiation upon presynaptic neural input to the postsynaptic neuron (Figure 1.2B). Theta-burst pairing is a theta rhythm-mimicking train of 5 bursts delivered at 5 Hz, with each burst consisting of 5 presynaptic EPSPs and postsynaptic action potentials paired at 100 Hz (Figure 1.2C). Although each of the protocols induces long-lasting synaptic changes, they differ in time course of expression of the early phase (0-5 min) LTP. After tetanic stimulation the peak increase in synaptic efficacy is expressed rapidly (1-3 min) after the stimulation and then drops gradually over

time (Malenka and Nicoll, 1999). Pairing protocol results in gradual saturating increase in synaptic efficacy without a large initial peak (Chen et al., 1999; Hoffman et al., 2002). Finally, theta-burst pairing generates a rapid potentiation of synaptic strength which then increases with time (Magee and Johnston, 1997; Pike et al., 1999). The difference in the time course of LTP expression induced by different protocols suggests different molecular pathways involved in expression of these different forms of LTP.

Since its discovery, there has been substantial progress in both characterizing LTP and understanding the cellular-molecular events underlying its induction, expression and maintenance. Among the most important advancements were 1) The discovery of its counterpart, long-term depression, LTD (Lynch et al., 1977), by which synaptic connections can weaken; 2) The description of both LTP and LTD in several synapses of the hippocampus and other brain regions, including neocortex and in several different preparations from in vitro to the freely behaving animal (Lynch, 2004; Martin et al., 2000).

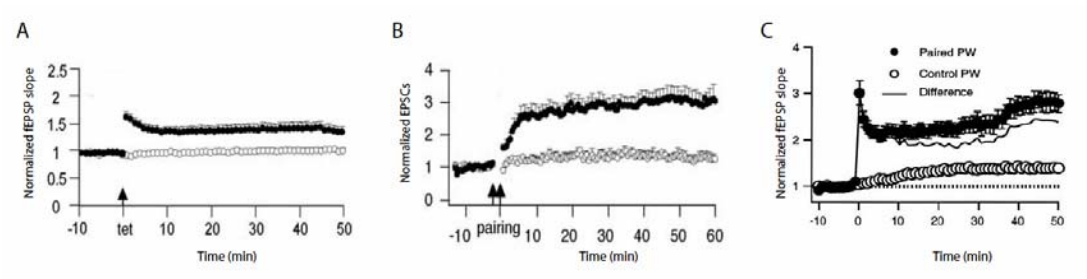

Figure 1.2. Characteristic traces of LTP induced by different protocols.
A) LTP induced by presynaptic tetanic stimulation at 100 Hz for 1s (adopted from Jensen et al., 2003). B) LTP induced by low frequency (0.7-1.5 Hz) presynaptic stimulation paired with prolonged (~3 min) postsynaptic depolarization at 0 mV (adopted from Jensen et al., 2003). C) LTP induced theta-burst pairing (adopted from Hoffman et al., 2002).

1.1.6. NMDA receptor and its role in synaptic plasticity and memory

Another fundamentally important finding was the observation that LTP in CA1 was inhibited by the competitive NMDA receptor antagonist AP5 and non-competitive NMDA channel blocker MK801 (Coan and Collingridge, 1987; Collingridge et al., 1983; Errington et al., 1987). These findings combined with the discovery that NMDA receptor activation leads to an influx of calcium through ligand- and voltage-sensitive calcium channels (Ascher and Nowak, 1986) resulted in a new insight on the possible role of NMDA receptor activation in LTP initiation. With the exception of mossy fiber-CA3

synapses, induction of LTP in all subfields of the hippocampus is NMDA receptor-dependent, although it has been shown that LTP in CA1 can be induced without the participation of NMDA receptors. Robust, NMDA independent LTP and LTD are also found in the dentate gyrus (Wang et al., 1997). In this case, the increase in postsynaptic calcium concentration is a consequence of activation of voltage-gated calcium channels, and therefore, calcium channel inhibitors suppress this form of LTP (Grover and Teyler, 1990). However, while the resultant increase in postsynaptic calcium concentration was both necessary and sufficient for expression of LTP, NMDA receptor activation, although required in many cases, was not sufficient to result in its induction (Bliss and Collinridge, 1993).

In parallel with the importance of NMDA receptor activation in induction of hippocampal LTP, it has been repeatedly shown that the NMDA receptor plays an essential role in the acquisition of 'spatial memories'. The first data that addressed this question were reported in 1986, when Morris and coworkers found that blocking the NMDA receptor with AP5 inhibited spatial learning. Later, Tsien et al. (1996) generated a mouse in which the NR1 subunit of the NMDA receptor was knocked out in CA1 and they reported that these mice exhibited impaired spatial memory, while nonspatial memory was intact, correlating with a deficit in LTP. Similarly, both spatial learning and LTP were impaired in mutant mice that lacked the NR2A subunit (Sakimura et al., 1995). Conversely, overexpression of the NR2B subunit yielded mice with enhanced LTP and enhanced learning and memory (Tang et al., 1999; Tang et al., 2001). These genetic correlations between LTP and some forms of learning and memory therefore support the initial findings of Morris et al. (1986). However, more recent studies have revealed that inhibition of the NMDA receptor only impairs spatial learning in task-naive animals, whereas pretraining in a spatial task overcomes the inhibition induced either by AP5 (Bannerman et al., 1995) or by another potent and specific NMDA antagonist, NPC17742 (Saucier and Cain, 1995), even when LTP in dentate gyrus was inhibited (Saucier and Cain, 1995). Interestingly, Bannerman et al. (1995) reported that pretraining in a nonspatial task induced a similar effect. It was subsequently shown that pretraining in a spatial learning task prevents disruption of a subsequent training session in spatial learning after saturation of LTP in the perforant path synapses (Otnaess et al., 1999). It was concluded that not all the components of spatial learning (at least in the Morris water maze) require NMDA receptor activation. It was proposed that spatial learning can take place in the

absence of LTP if episodic aspects (e.g. spatial cues in the environment where training took place) of the training context are familiar.

1.1.7. AMPA receptor and its role in synaptic plasticity and memory

The α-amino-3-hydroxy-5-methyl-4-isoxazole propionic acid (AMPA) receptors are glutamate-gated ion channels and are composed of four glutamate receptor subunits, GluR-A to GluR-D (also called GluR-1 to GluR-4) (Dingledine et al., 1999). The functional properties of AMPARs, their permeability to ions, their subcellular localization and trafficking depend on subunit composition, which varies depending on the brain region (Collingridge et al., 2004; Dingledine et al., 1999; Malinow and Malenka, 2002). In pyramidal cells of hippocampal CA1-CA3 regions and dentate gyrus granular cells of adult rodents, most AMPARs are GluR-A/B heteromers, some are GluR-B/C heteromers, and a few are GluR-A homomeric channels (Derkach et al., 2007; Petralia and Wenthold, 1992; Wenthold et al., 1996). In interneurons of hippocampal CA1 region AMPARs are assembled from GluR-A, -B, -C and GluR-D subunits (Jensen et al., 2003). AMPA receptor channels are permeable for cations and typically have rapid onset, offset, and desensitization kinetics (for a review see Gouaux, 2004; Sprengel, 2006; Sun et al., 2002). Calcium entry through AMPARs is modulated by the GluR-B subunit, which is subject to RNA editing such that the genomic glutamine (Q) codon for residue 607 can be changed to the arginine (R) codon (Jonas and Burnashev, 1995; Kask et al., 1998). Thus AMPAR-associated calcium permeability is low in pyramidal and granule cells of the hippocampus where there is a relatively high expression of AMPARs containing the GluR-B subunit with its edited Q/R site (Geiger et al., 1995).

The importance of AMPARs in fast excitatory synaptic transmission has been acknowledged for decades, and because of this, it has been recognized that modulation of AMPAR activity could significantly contribute to expression of LTP. LTP induction was shown to increase the number of postsynaptic AMPARs (Hayashi et al., 2000; Lissin et al., 1998) and conductance of the receptor-associated channels (Derkach et al., 1999; Benke et al., 1998). The discovery of silent synapses lacking AMPARs, and the evidence that LTP unsilences these synapses (Isaac et al., 1995; Liao et al., 1995) have convinced most researchers that LTP involves the activity-dependent rapid recruitment of synaptic AMPARs. Direct support comes from physiologically tagged AMPAR subunits (Hayashi et al., 2000; Liu and Cull-Candy, 2000; Shi et al., 2001) and experimentally uncaging

glutamate onto single spines (Bagal et al., 2005; Matsuzaki et al., 2004). It appears that there is a fairly constant turnover of GluR-B/C AMPARs at the synapse, whereas the trafficking of GluR-A/B AMPARs require neural activity (Shi et al., 2001). Interestingly, while LTP has been associated with an increased number of GluR-A-containing AMPARs in synapses, there is also evidence that NMDAR-dependent LTD is associated with a decrease in the corresponding AMPARs (Carroll et al., 1999).

The initial findings indicating an increase in AMPAR activity after LTP induction sparked some parallel investigations in tissue prepared from animals that underwent training in different behavioral paradigms. Tocco et al., (1991) reported that AMPAR, but not NMDAR binding was increased after training in a classical conditioning paradigm. A rapid and selective increase in the density of hippocampal AMPARs, in part due to increased GluR-A expression, was also reported after training in an inhibitory avoidance learning (Cammarota et al., 1998). While facilitation of AMPA-mediated responses was shown to improve memory (Granger et al., 1993; Staubli et al., 1994), inhibition resulted in retrograde amnesia of inhibitory avoidance training in rats (Cammarota et al., 1996; Cammarota et al., 1995; Jerusalinsky et al., 1992).

Production of mutant mice lacking a specific AMPAR or expressing a modified AMPAR subunit provided further insight into the role of AMPARs in synaptic plasticity and learning. Complete deletion of the GluR-B subunit in the entire mouse resulted in enhanced LTP in CA3-CA1 synapses accompanied with impaired performance in the Morris water maze (Jia et al., 1996). However, GluR-B knockout mice had poor motor coordination and low exploratory activity, which makes interpretation of the detected learning deficit difficult. The abnormal phenotype of GluR-B knockout mice is most likely mediated by pathological changes in the CNS induced by the enhanced cation influx through Ca^{2+}-permeable AMPARs. The function of the GluR-B subunit was investigated more specifically in mice with conditional GluR-B deletion in postnatal forebrain principal neurons (Shimshek et al., 2006). Forebrain-specific GluR-B knockout mice showed reduced basal CA1-CA3 synaptic transmission accompanied by increased synaptic excitability. Although tetanus-induced NMDAR-dependent LTP in CA3-CA1 synapses was unaffected in the forebrain-specific GluR-B knockout mice, the mice were impaired in hippocampal spatial working and reference memory on T-maze alternation and Y-maze tasks, respectively (Shimshek et al., 2006). The other subunit, GluR-C, is inserted into the synapses constitutively, however does not contribute to hippocampal function. Complete

knockout of GluR-C subunit from the forebrain had no effect on spatial reference memory as tested by the Morris water maze (Sanchis-Segura et al., 2006).

Considering that GluR-A-containing AMPARs are inserted into the hippocampal synapse in an activity-dependent manner, it is plausible that contribution of these receptors to the hippocampus-dependent behavior is more prominent compared to the other subunits. To test this hypothesis Zamanillo *et al.*, (1999) created a mutant mouse lacking GluR-A-containing AMPARs, which was then intensively investigated in multiple behavioral studies.

1.1.8. Electrophysiological and behavioral characterization of GluR-A knockout mice

Complete inactivation of the GluR-A gene mostly affected AMPARs in the hippocampus and amygdala, where GluR-A expression is high (Molnár et al., 1993). In the absence of GluR-A, in GluR-A-deficient mice (GluR-A KO), the expression of the other AMPAR subunits is not only delayed, but also the final expression level of GluR-A partners, like GluR-B and GluR-D, is reduced compared to wild-type mice (Jensen et al., 2003). Because GluR-B and GluR-D are the principal GluR-A partners in hippocampal AMPARs, absence of GluR-A leaves much of the GluR-B and GluR-D unassembled with a shorter half-life. Uncoupling with GluR-A also impairs the cellular localization of the other AMPAR subunits, as immunolabelling studies showed that GluR-B subunits are largely restricted to soma in the absence of GluR-A (Zamanillo et al., 1999).

Deletion of GluR-A leads to 10-fold reduction in somatic currents and 2-fold reduction in postsynaptic currents (EPSCs) mediated by AMPAR (Jensen et al., 2003; Zamanillo et al., 1999). Unlike the large difference in glutamate-activated synaptic currents, no difference was detected in field EPSPs (fEPSP) recorded extracellularly in CA1 dendritic layers (Zamanillo et al., 1999). The very low AMPAR currents in soma patches and relatively much higher AMPAR currents in synaptic measurements suggest that in CA1 pyramidal cells of GluR-A KO mice the remaining functional (GluR-B/C) AMPARs are mainly localized in synapses. Therefore, the strong somatically immunolabelled GluR-B in str. pyramidale of GluR-A KO brain slices must reflect unassembled or non-functional (low conductance) homomeric GluR-B channels (Jensen et al., 2003; Zamanillo et al., 1999). In addition, normal distance-dependent synaptic scaling

used by CA1 pyramidal cells to counter dendritic attenuation of EPSPs was lacking in GluR-A KO mice (Andrasfalvy et al., 2003; Magee and Cook, 2000).

Neither tetanus nor pairing protocols are able to induce LTP in CA3-CA1 synapses in adult (>P60) GluR-A KO mice (Zamanillo et al., 1999). The observation that the dendritic Ca^{2+} transients are not different between wild-type and GluR-A KO mice suggests that molecular mechanisms responsible for NMDA receptor-dependent LTP induction should be intact in the GluR-A KO mice. In the absence of GluR-A subunit, both AMPAR phosphorylation and incorporation processes, required for normal LTP expression, are strongly reduced (Barria et al., 1997). Thus, the expression, but not the induction, of the LTP is likely to be blocked in adult GluR-A KO mice (Zamanillo et al., 1999). Experimental support for this hypothesis came from the study which showed that GluR-A KO mice express slowly developing synaptic potentiation with a significantly reduced initial component after LTP induction with theta-burst pairing (Hoffman et al., 2002). The slow component of LTP becomes indistinguishable from that found in wild-type 25 min postinduction (Hoffman et al., 2002). Surprisingly, significant CA3-CA1 LTP could be induced in young (P14-P28) GluR-A KO mice either by tetanic stimulation or by pairing protocol (Jensen et al., 2003). During the following weeks the ability of these synapses to express LTP diminishes and at P42 it is no longer possible to induce LTP by tetanic stimulation or pairing protocol, similar to LTP reported for older (>P60) GluR-A KO mice (Zamanillo et al., 1999). This 'juvenile' GluR-A-independent form of LTP was shown to be NMDAR-dependent, postsynaptically expressed and, likely to rely on different molecular mechanism than GluR-A-dependent LTP in adult wild-types.

Considering that different forms of LTP might be relevant for different forms of information storage, one could expect that a specific LTP deficit might result in the impairment only of a certain memory type, while preserving others (Hoffman et al., 2002). Behavioral testing of GluR-A KO mice in a variety of hippocampus-dependent tasks provided evidence supporting this hypothesis. First of all, adult GluR-A KO mice are normal with respect to most of their behavioral patterns (Bannerman et al., 2004). Despite the lack of CA3-CA1 LTP, the GluR-A KO mice exhibit normal spatial reference memory performance in the Morris water maze, Y-maze and paddling pool escape task (Schmitt et al., 2004; Schmitt et al., 2003; Zamanillo et al., 1999). Nevertheless, GluR-A KO mice show a specific and profound spatial working memory impairment as tested on the T-maze alternation task and six-arm radial maze (Reisel et al., 2002; Schmitt et al., 2003).

Importantly, both LTP and spatial working memory can be partially restored by transgenic expression of GluR-A in the forebrain, providing direct evidence that GluR-A-containing AMPARs are critical for spatial working memory (Mack et al., 2001; Schmitt et al., 2005).

1.2. Rate coding: hippocampal place cells

Hippocampal place cells were discovered by O'Keefe and Dostrovsky (1971) as cells of the hippocampus that fire whenever the animal is in a particular location of the environment, the 'place field' of the cell. Soon the concept of 'Hippocampus as a Cognitive Map' (O'Keefe and Nadel, 1978) was established which stated that the role of the hippocampus is to construct a map of the environment which can then aid the animal to flexibly navigate through it, just as Tolman (1948) postulated the existence of such a map in the rat's brain. Since the first observations, experimental techniques became increasingly sophisticated (McNaughton et al., 1983a; McNaughton et al., 1983b; O'Keefe and Recce, 1993b), but the principle of place cell recording did not change much. The activity of single units (identified as single cells) is recorded from CA1-CA3 subregions while the rat is moving around in an environment, and the location of the rat is recorded each time a spike is fired by a cell. Spikes of a cell are thus assigned to spatial locations, and dividing the number of spikes in each spatial bin by the overall time the rat spent in that bin during exploration yields average firing rates as a function of position (Figure 1.3). Firing rate tuning curves obtained in this way usually have a center associated with high firing rates and a periphery where the cell tends to fire less, often approximated by a bell-shaped curve, but exceptions to this rule, such as 'double place fields', were also observed. Two properties of place cells have made them particularly appealing subjects for neuroscientific investigations: 1) Place cells appear to signal an abstract concept such as allocentric location (location in a world-based coordinate system) which is not directly related to either sensory input or motor output, in line with the anatomical location of hippocampus being remote from primary sensory or motor cortices, and thus seem to offer an opportunity to gain insight into higher cognitive functions on the level of single neurons; 2) Despite its abstractness, space is easily quantifiable and spatial correlates indeed appear to account even for quantitative properties of place cell firing (O'Keefe, 1999).

The aim of this section is not to give an exhaustive review of the vast literature that has been accumulated on place cells in the past decades, but rather to summarize their

basic characteristics, discuss correlation between place field quality and ability of the animals to learn spatial memory tasks and, finally, consider the role of synaptic plasticity in formation of both place fields and spatial memory.

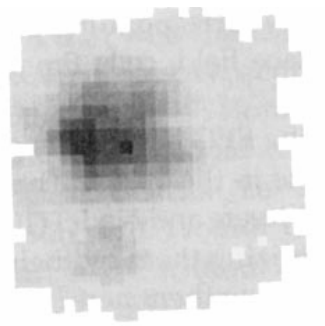

Figure 1.3. Place field in a small enclosed arena in which rats foraged for food that was randomly dropped in the arena. Darker shading indicates areas in which a higher rate of firing was seen. Adapted from Best *et al.*, 2001.

1.2.1. Evidence supporting that place cells are part of a cognitive map

Place cells were first identified electrophysiologically as complex burst cells (Ranck, 1973b), and later anatomically as the pyramidal cells in CA3 and CA1 (Fox and Ranck, 1975) and granule cells in the dentate gyrus (Jung and McNaughton, 1993). Hippocampal interneurons were described as theta cells (Fox and Ranck, 1975; Ranck, 1973b), firing at higher frequencies and more locked to theta rhythm. Place cells were observed in different environments, open fields, elevated platforms, linear, triangular, rectangular and circular tracks, T-, Y-, plus and radial mazes, where the rat was free to move in one, two, or in one case even three dimensions (Best et al., 2001; O'Keefe and Nadel, 1978; Redish, 1999; Sharp, 2002). They were also recorded during different behavioral protocols, from random exploration to the execution of highly stereotyped trained movement sequences. In any given environment only a small fraction of possible cells are active, estimates ranging between 15-30% (Thompson and Best, 1989; Wilson and McNaughton, 1993). The dedication of place cells to signaling spatial position is well demonstrated by the observation that the position of the animal can be predicted with a ~5 cm precision from the activity of approximately 100 cells in an environment (Brown et al., 1998; Wilson and McNaughton, 1993; Zhang et al., 1998). This, together with the several thousand pyramidal cells in CA1-CA3, indicates a high degree of redundancy, or robustness, in the place cell code.

Place cells do not seem to be dependent on any single modality (Maaswinkel and Whishaw, 1999; Mizumori et al., 1989; Poucet et al., 2000; Save et al., 2000), and robust place-specific activity was recorded in deafened and blind rats (Hill and Best, 1981; Save et al., 1998), in the absence of vestibular input during space flight (Knierim et al., 2000), and in the absence of self-motion cues (Foster et al., 1989). Furthermore, although place fields seem to be under the control of landmarks in the environment (see below), they do not depend on the presence of any single cue (O'Keefe and Conway, 1978). Yet, place cells quickly develop their place fields when the rat is placed into a new environment, although different results were obtained as to whether this happens within seconds (Hill, 1978) or takes several minutes (Wilson and McNaughton, 1993). Once established, place fields persist for practically as long as a stable recording can be obtained, in one case it was 153 days (Thompson and Best, 1990). Systematic manipulations of the environment revealed that on the one hand, small gradual changes in cue locations, such as the rotation of cue cards, or the platform under the rat, or scaling one or both sides of a rectangular arena, resulted in place field changes that preserved the geometrical relationship between environment (cues) and place fields (Muller and Kubie, 1987; O'Keefe and Burgess, 1996). On the other hand, more substantial or abrupt changes in environmental variables, such as scrambling of cues, lead to unpredictable changes in place cell activity ('remapping'), just as if the rat has been placed in a new environment (Kentros et al., 1998; Muller et al., 1987). It has also been observed that environmental cues may influence place fields differentially, depending on their proximity: proximal cues usually affect only those place fields that are in their immediate vicinity (Cressant et al., 1997; 1999; Muller et al., 1987). A number of important recent experiments have demonstrated quantitative differences in place cell behavior between hippocampal subfields. First, place field representations develop more rapidly in CA1 than CA3 (Leutgeb et al., 2004) and, second, small changes to a testing environment (such as modification of cues) cause larger changes in the place field representation in CA1 than that in CA3 (Lee et al., 2004; Vazdarjanova and Guzowski, 2004).

Place cells behave in a fashion that resembles sensory cells. However, the similarity between place cells and sensory neurons is only superficial and breaks down in two fundamental ways. First, the map of the environment is not topographic. Unlike sensory maps, neighboring place cells in the hippocampus do not have neighboring place fields in the environment (Guzowski et al., 1999; Kubie et al., 1992; Redish et al., 2001), although

there may be a slight tendency for clustering (Eichenbaum et al., 1989). This raises the question: Why should the organization of the spatial representation in the hippocampus be so different from sensory representations in neocortex? One possibility is that the hippocampus does not signal the stimulus pattern falling on a sensory receptive sheet, a sheet that has a relatively fixed set of connections from the periphery to the cortex. Rather, the hippocampus signals the position of the animal within the environment, and there is no constant relationship between the environmental surface and the hippocampal surface because different environments differ so dramatically in size and shape. Instead of a topographic map of the environment, the hippocampus may provide a topological map (Muller et al., 1996). In a topographic map, distance in the environment would be represented by distance between cells in the cell layer. In a topological map, distance in the environment might be represented by the strength of synaptic connections between pairs of place cells regardless of their location in the cell layer. Second, the analogy between place cells and sensory cells breaks down when the relationship between cell activity and sensory stimuli is examined. For instance, in rats and mice, rotating the primary visual cue in the experimental environment (for instance, a white cue card), causes place fields to rotate equally. Thus, the card has a powerful form of stimulus control over place cells. If place cells are properly thought of as sensory cells, removal of the card should disrupt place-cell firing. In fact, removal of the card leaves place fields intact, although they may rotate by an unpredictable amount inside the cylinder (Muller and Kubie, 1987). Thus, the hippocampal map of space appears to be a cognitive map, not a sensory map. The activity of its cellular components represents not specific sensory input but an abstract feature of the world - space.

1.2.2. Evidence challenging the cognitive map theory

Soon after the discovery of place cells it was recognized that the firing rate of these neurons may also depend on other variables than just the spatial location of the animal. In environments where the movement of the animal is restricted to one dimension, such as on a linear track, or in such parts of an environment, as the arms of a radial maze, a place cell can have a preferred direction of movement. In other words, when the animal is traversing its place field opposite to a cell's favored direction, the cell remains silent (Bostock et al., 1991; McNaughton et al., 1983a; O'Keefe and Recce, 1993a; Wiener et al., 1989). Direction-selective place fields were also demonstrated when the environment was two-

dimensional but the animal was trained to strictly follow given trajectories (Markus et al., 1995). In other studies the following parameters were also shown to influence firing rate of place cells: the running speed of the rat (Czurkó et al., 1999; McNaughton et al., 1983a; Wiener et al., 1989); finding an unexpected or not finding an expected object at a given location ('misplace cells';(O'Keefe, 1976); or approaching a goal independent of its spatial location (Gothard et al., 1996; Ranck, 1973b). These correlates, though not equivalent to location, are closely tied to spatial behavior, and thus may still be compatible with a predominantly spatial function of the hippocampus. However, a complete remapping of place fields can occur even in the same environment with unaltered cues, if the spatial task requirements changed, or as the animal executed subsequent stages of the same task (Markus et al., 1995; Wiener et al., 1989). Hippocampal cells change their firing rates in relation to task aspects even in non-spatial conditioning tasks (for review see Cohen and Eichenbaum, 1993; but see also critical review O'Keefe, 1999; Wallenstein et al., 1998). Surprisingly, place cell firing turned out to depend on past and future movement sequences of the animal in a portion of the environment where speed and direction of movement otherwise remained constant across trials (Wood et al., 2000). In a sophisticated study, specifically aimed to assess the degree to which hippocampal principal cells are bound to spatial or non-spatial variables, the influence of non-spatial variables was shown to be at least as strong as that of the location of the animal (Wood et al., 1999).

These and similar results led many researchers to hypothesize the existence of multiple reference frames in the hippocampus (Battaglia and Treves, 1998; Gothard et al., 1996; Samsonovich and McNaughton, 1997). Within a given reference frame, only small geometrical transformations of place cell firing are possible, though affecting all cells simultaneously. A complete remapping can occur due to changes in the environment or animal's behavior and it should result in a change in reference frame, when another 'map' is selected. However, even this multiple map scenario seems to be in disagreement with observations of partial remapping in some situations. Partial remapping resulted in some cells preserving their place fields, while others loosing them or developing new fields. It could occur in response to environmental manipulations (Tanila et al., 1997a), or in ambiguous environments where the rat could shuttle between two virtually identical boxes (Skaggs and McNaughton, 1998).

1.2.3. Place cells and spatial learning

If place cells provide the animal with a cognitive map, then performance in spatial tasks should depend on the integrity of place fields. Note that it is a different and more stringent criterion than just requiring hippocampal involvement in spatial behavior that was demonstrated by lesion studies (O'Keefe and Nadel, 1978; Redish, 1999). When rats were trained to select an arm of a radial maze indicated by cues that were rotated to another position before every trial, place fields followed the cues, as in the experiments discussed above, and in those few cases when place field transition did not occur properly the rat made an error selecting the arm corresponding to the incorrect place field map (O'Keefe and Speakman, 1987). In another study, septal lesion resulted in spatial working memory deficit on an eight-arm radial maze accompanied by unstable pattern of place cell firing across trials, although place field specificity (ratio between peak firing rate and averaged firing rate over the entire environment) was unaltered (Leutgeb and Mizumori, 1999). Lenck-Santini et al. (2001) have found that manipulations of the visual cues that caused place fields to change their configuration relative to standard one also resulted in a decrease in rat's performance in a spatial reference task on a Y-maze. Somewhat different, Puryear et al. (2006) have demonstrated that although darkness induced multiple changes in place field properties (remapping, reduced specificity and position stability), only the reduction in place field specificity was correlated with poor performance in a spatial working memory task on an eight-arm radial maze. Age-related performance deficit in hippocampus-dependent memory tasks in rats (Barnes, 1979; Gallagher and Burwell, 1989; Oler and Markus, 1998) may result from decreased sensitivity of the hippocampal place cells to respond to meaningful changes in the environment (Oler and Markus, 2000; Tanila et al., 1997a; 1997c). However, Barnes et al. (1997) found that when rats were removed from the environment between recording sessions, old rats had less consistent hippocampal representations when returned to the same environment.

A number of studies, however, point to a weak correlation between place field activity and performance in a spatial memory task. In the lesion study of Leutgeb and Mizumori (1999) described above, formation and basic properties of the place fields were unaltered, only trial-to-trial variability increased, and performance was still severely diminished. Choice accuracy was impaired in a working memory task on a radial maze when theta rhythm (see next chapter) was suppressed after septum inactivation, despite the preserved place fields in CA1 (but see also Brazhnik et al., 2003; Mizumori et al., 1989).

This can be explained if downstream brain structures decoding hippocampal output rely also on theta phase information, rather than purely on place cell firing (Jensen, 2001; 2005). Lesioning of DG did not disrupt place fields in CA3 and CA1, but greatly impaired spatial learning (McNaughton et al., 1989). Despite a contextual change to the environment that induced remapping of most place cells, navigational performance in a hippocampal-dependent tone-cued spatial task remained essentially intact (Jeffery et al., 2003). Similarly, reorganization of place fields of individual neurons was not always accompanied by behavioral impairments in experiments with pharmacological inactivation of the retrosplenial cortex (Cooper and Mizumori, 2001).

In summary, the relationship between the place cell properties and animal's performance in spatial memory tasks appears to be not consistent. Existence of intact CA1 place fields during periods of memory impairment indicates that place-specific cell firing might not be sufficient to support good performance on a spatial task (Bures et al., 1997). Recent studies using genetically modified mice that demonstrate a correlation between spatial learning, place field quality and synaptic plasticity will be discussed in the next section.

1.2.4. Place cells and synaptic plasticity

Given that the hippocampus is critical for spatial memory formation, and that its synapses are highly plastic, an important question is how the activity of place cells and hippocampal plasticity relate to each other. One of the approaches widely used to assess this question is to examine place cell activity when processes important for synaptic plasticity are modified or disrupted. If the pattern of place fields in a given environment arises as a result of experience-induced synaptic plasticity, then disruption of synaptic plasticity should produce effects on the place cell encoding of that environment. In general, the kinds of interventions that have been undertaken so far fall into three groups: pharmacological, electrophysiological and molecular genetic.

A number of studies have investigated the effect of pharmacological interventions on place fields. Kentros et al. (1998) found that application of the competitive NMDA receptor-antagonist CPP interfered specifically with the stability of the newly formed place fields without effect on the place fields developed prior to CPP injection. Place fields developed normally in the presence of the antagonist in a novel environment, but were not reliably reestablished on the next day (Kentros et al., 1998). Therefore it appears that

NMDAR-dependent synaptic plasticity is necessary for the formation of stable, long-term place representation. In contrast to early phase LTP (E-LTP), the late phase LTP (L-LTP) is known to require new protein synthesis (Morris et al., 2003). Similar to Kentros et al., Agnihotri et al. (2004) reported that inhibition of protein synthesis by anisomycin blocked long-term stability of the newly formed place fields across days. This finding suggests that long-term stability of place fields may require long-term (i.e. protein synthesis-dependent) LTP. In summary, pharmacological intervention targeted at LTP processes seems to affect long-term stability of place fields but not their formation per se.

Another way of altering hippocampal synapses is their electrical stimulation leading to a change in synaptic strength and in the connectivity of the system. In theory, induction of LTP that reaches its saturating amplitude should impair further plasticity and hence learning (Barnes et al., 1994; but see also Bliss, 1996; Moser et al., 1998). Dragoi et al. (2003) have demonstrated that inducing LTP in CA3 and CA1 synapses by electrical stimulation evoked a remapping and loss of existing place fields as well as development of new ones. Thus, alteration of the strength of hippocampal synapses was able to induce a new pattern of place field activity.

An important advancement in the molecular dissection of place cell plasticity and stability was done with the development of genetically engineered mice. In particular, the development of 'knock-out' mice lacking one or more of the genes implicated in synaptic plasticity, together with improved in vivo recording technologies, allowed to understand better the contribution of synaptic plasticity processes to the formation of spatial memory and place cell representation (Martin et al., 2000). All studies investigating the effect of genetic interventions on place cell activity fall into two groups based on the influence on hippocampal CA3-CA1 LTP: genetical modifications resulting in impaired LTP (Cho et al., 1998; McHugh et al., 1996; Nakazawa et al., 2002; Rotenberg et al., 2000; Rotenberg et al., 1996) and those resulting in enhanced LTP (Taverna et al., 2005; Yan et al., 2002).

Knocking out the NMDAR1 subunit of the NMDAR in the CA1 subregion has been found to produce little effect on many of the basic electrophysiological characteristics of both pyramidal cells and inhibitory interneurons (McHugh et al., 1996). Although the knockout animals showed no NMDAR-dependent CA3-CA1 LTP and poor spatial learning (Tsien et al., 1996), comparable numbers of cells with location-related firing were seen in control and mutant mice. Both groups of animals had place cells that were directionally selective on the linear track and stable across multiple exposures to the same

environment. However, place fields of the knockout mice were larger, more likely to have multiple peaks, and had more diffuse firing pattern than controls. Cells with overlapping fields, whose firing is usually correlated over short timescales, displayed uncorrelated firing in the mutant mice. The inference drawn from this is that downstream brain regions in these animals could not use correlations, if they normally do so, to learn about place. Furthermore, if the position of the animal was reconstructed based on the firing of place cells, it was found that as the number of cells included in the ensemble increased, the reconstruction error also increased. This indicates a loss of coherence in the ensemble spatial representation, likely reflected in the poor spatial learning of the animals.

Spatially restricted genetic alterations have also been targeted at NMDAR1 subunit in cells located in the CA3 subregion of the hippocampus (Nakazawa et al., 2002). Mice lacking NMDAR1 subunit in the CA3 subregion had impaired NMDAR-dependent LTP in recurrent collateral-CA3 synapses, but intact LTP in CA3-CA1 and mossy fiber-CA3 synapses. Nakazawa et al. tested the animals under a variety of conditions. The CA3 knockouts displayed normal acquisition and retrieval of spatial reference memory in the Morris water maze with a full cue set available. Under such conditions there was no significant difference between control and mutant place fields in terms of place field size or in-field firing rate. However, when the environment surrounding the animal was degraded (by removing all but one of the silent cues), not only retrieval of the spatial memory was impaired in the mutant mice, but impairment was also seen in the activity of their CA1 place cells (i.e. in cells downstream from the affected cells). Under partial cue conditions, mutant place cells showed significant reduction in place field size and in-field firing rate as compared to full cue conditions. In contrast to the CA1 NMDAR1 knockouts discussed above, there was no difference in the coordinated firing of pairs of cells with overlapping place fields. Influence of selective deletion of the NMDAR1 subunit in CA1 and CA3 subregions on hippocampal synaptic plasticity, place cells and spatial learning was well rewieved by Wilson and Tonegawa (1997), Tonegawa et al., (2003) and Nakazawa et al., (2004).

Genetic perturbations affecting LTP induction mechanisms also disrupt normal place cell activity. Mice expressing altered Ca^{2+}/calmodulin-dependent protein kinase (CaMKII) displayed normal tetanus-evoked CA3-CA1 LTP, but had a specific deficit in LTP when stimulation was in the 5-10 Hz frequency range, corresponding to theta rhythm in the hippocampal EEG. This specific deficit in hippocampal plasticity was accompanied by

impaired spatial reference memory and degraded place cell activity. First, CaMKII transgenic mice showed a significantly lower number of cells with place-related firing. Second, the existing place fields in the transgenic mice were enlarged and unstable across recording sessions separated by only a few minutes. Similarly, mice with blocked CaMKII autophosphorylation (αCaMKII^{T286A}) showed impaired NMDAR-dependent CA3-CA1 LTP, poor spatial learning in the Morris water maze (Giese et al., 1998) and unstable place fields which were significantly less selective (Cho et al., 1998). Cho et al. have also tested mice with a targeted disruption of the genes encoding the α and Δ isoforms of cAMP response element-binding protein (CREB$^{\alpha\Delta-}$). CREB$^{\alpha\Delta-}$ mice displayed somewhat normal tetanus-induced CA3-CA1 LTP, but smaller in amplitude relative to wild-type animals and decaying to baseline within 90 min after induction (Bourtchuladze et al., 1994). Furthermore, CREB$^{\alpha\Delta-}$ mice had a profound learning deficit in the Morris water maze, which, however, could be overcome by additional training with the increased intertrial interval (60 min instead of 1 min) (Kogan et al., 1997). As in case of the αCaMKII^{T286A} animals discussed above, spatial selectivity of place fields was lower in CREB$^{\alpha\Delta-}$ animals relative to the controls. Interestingly, place field stability was more affected in the αCaMKII^{T286A} than in the CREB$^{\alpha\Delta-}$ mutants, which correlates with the extent of deficit in LTP and spatial learning found in those animals (Cho et al., 1998).

Place cells have also been recorded in a strain of genetically modified mice that have reduced activity of the forebrain protein kinase A (PKA) (Rotenberg et al., 2000). PKA and other kinases phosphorylate receptors and membrane channels, thus altering their functional properties. Behaviorally, these mice showed spatial learning deficit in the Morris water maze (Abel et al., 1997). In these PKA KO mice there was near normal early-phase LTP, but impaired late-phase LTP in CA3-CA1 synapses of the hippocampus. As with acute pharmacological blockade of NMDARs (Kentros et al., 1998), the place fields in PKA mutants were stable and comparable to controls over short time periods (~1-2 hours), but lacked stability over 24 hours.

Taking into account that impaired synaptic plasticity seems to correlate with altered place cell activity and poor hippocampal-dependent spatial learning, it is of interest to check how place cells and spatial learning are affected by enhanced LTP. To our knowledge, there are only two studies of place cell properties in mutant mice with enhanced LTP in CA3-CA1 synapses: Yan et al., (2002) and Taverna et al., (2005). Yan et al., (2002) recorded place cells in knockout mice lacking AMPAR GluR-B subunit in the

entire organism (Jia et al., 1996). These animals exhibited a significantly elevated (2-fold) NMDA receptor-independent non-Hebbian LTP in CA3-CA1 synapses in response to tetanic stimulation. Furthermore, LTP appeared to be unsaturable and could be further increased with repeated tetanic stimulation in the mutants but not in control mice. Although GluR-B knockouts showed spatial learning deficit in the Morris water maze, hippocampal dysfunction is unlikely to explain all observed defects (Gerlai et al., 1998). Further behavioral testing revealed that complete deletion of GluR-B subunit in the mutant mice also resulted in an alteration in motor activity, motivation and sensitivity to sensory stimulation. Like the CaMKII mutants discussed above, the GluR-B knockouts had significantly fewer cells that showed location-related firing (~23%) compared to controls (~44%). The boundaries of the place fields were less defined in GluR-B knockouts compared to wild-type fields. Furthermore, mutant place fields were extremely unstable over 0.5-24 h between recording sessions. Nonspecific knocking out of the GluR-B gene in the mutant mice makes it difficult to link observed changes in long-term plasticity, spatial learning and place field quality. In addition to the enhanced non-Hebbian CA3-CA1 LTP in the hippocampus, potential impairments in other brain regions might also contribute to poor spatial representation of hippocampal place cells in GluR-B knockout mice. Nishi et al. (1997) created a mutant mouse with enhanced NMDAR-dependent CA3-CA1 LTP by means of selective deletion of the NOP_1/ORL_1/OP4 nociceptin receptor in the hippocampus (Manabe et al., 1998; Taverna et al., 2005). The NocR knockout mice learned the Morris water maze faster than wild-type animals, but reached the same level of spatial memory performance after ten days of training (Manabe et al., 1998). Surprisingly, similar to the mutants with impaired plasticity, the NocR knockouts showed significantly less number of cells with location-specific firing (~67%) compared to controls (~90%). Positional firing patters of place cells in NocR knockouts were more diffuse, more dispersed over the apparatus area and essentially less stable over a wide range of time periods relative to control mice (Taverna et al., 2005). It has been suggested that entorhinal neurons provide an important input to CA1, particularly during tasks that require the encoding of novel information (Brun et al., 2002; Jarrard et al., 1984; McNaughton et al., 1989; Mizumori et al., 1989). If so, poor place field tuning in the mutant mice might be a result of disturbed interplay between entorhinal and CA3 inputs (McHugh et al., 1996; Nakazawa et al., 2004).

In summary, the results indicate that NMDAR-dependent long-term plasticity in CA3-CA1 synapses is not required for the rapid establishment of place fields. Rather, LTP is needed for the fine-tuning of higher-order place field properties such as coherence, stability and synchronous firing (Jeffery and Hayman, 2004; Mayford et al., 1997; Nakazawa et al., 2004). Furthermore, there is no apparent relationship between direction of changes in LTP and place cell properties. For example, the quality of place fields became worse in mice with reduced (Cho et al., 1998; Kentros et al., 1998; McHugh et al., 1996; Rotenberg et al., 2000; Rotenberg et al., 1996) or enhanced LTP (Taverna et al., 2005; Yan et al., 2002). In other words, simple boosting of plastic changes is not sufficient to improve functioning of the hippocampal network (Taverna et al., 2005).

1.2.5. Cells with spatial correlates outside the rodent hippocampus

Cells with spatially selective activity were also described outside the hippocampus. It is important because the hippocampus may be part of a larger overall circuit for navigation. Place-related firing patterns have been observed throughout the hippocampal formation, including the entorhinal cortex (Fyhn et al., 2004; Hafting et al., 2005; Quirk et al., 1992; Sargolini et al., 2006), the presubiculum (Cacucci et al., 2004), postsubiculum (Sharp, 1996; 1999), parasubiculum (Cacucci et al., 2004; Taube, 1995), and subiculum (Sharp and Green, 1994).

Earlier studies have shown that principal cells in both the superficial and deep layers of the medial entorhinal cortex (MEC) have place fields, although these fields are significantly less place-specific than those of hippocampal place cells (Barnes et al., 1990; Mizumori et al., 1992; Quirk et al., 1992). Later, Fyhn and coworkers (2004) demonstrated that cells from superficial layers of MEC have sharply defined place fields comparable with hippocampal CA1 place fields. However, the number of subfields per cell was larger in MEC than in CA1, the subfields were slightly smaller and the peak rate was higher. However, the real step forward in characterizing MEC cell firing was done in 2005 when Hafting and coworkers placed rats in essentially bigger cylindrical environment than used so before (200 cm versus 50-80 cm diameter). Multiple firing fields of the pyramidal neurons in all principal layers of MEC turned out to be arranged in a strikingly regular, triangular, grid-like pattern that tessellates any two-dimensional environment explored by the animal (Hafting et al., 2005; Sargolini et al., 2006) . The firing pattern of each ‘‘grid cell’’ can be characterized by its spacing (the distance between neighboring vertices of the

grid), orientation relative to the environment, and spatial phase (the offset relative to a fixed position in the environment). The spacing of the grid increases from the dorsal to the ventral end of MEC (Fyhn et al., 2004; Hafting et al., 2005; Sargolini et al., 2006). Unlike place cells in the hippocampus, grid cells are active in all environments, regardless of external cues. The regular structure of the grid field and the environmentally invariant relationships among simultaneously recorded grid fields suggest that grid cells might be a part of a universal, path-integration-based spatial metric (Hafting et al., 2005; McNaughton et al., 2006; Sargolini et al., 2006).

Despite the fact, that many subicular cells were tonically active throughout the time that the animal was in the environment, they showed consistently higher rates in one or more regions. They also do not show topography-breaking remapping on transition into a different environment as hippocampal place cells do (Sharp, 2006). Space is also represented in the posterior cortex, but instead of being in a world-based coordinate system (allocentric) this representation is egocentric, i.e., its reference point is the individual (for review see Colby and Goldberg, 1999). Cells signaling the head direction of the animal were observed in several brain regions, including the subicular complex, thalamic nuclei, and other structures, most of them having close anatomical connections with hippocampus (for review see Sharp, 2006).

An important and much debated question is how much our knowledge on rodent place cells is applicable to other species, such as primates and humans. Although there is evidence for the involvement of the human hippocampus in solving spatial tasks (O'Keefe and Burgess, 1999), for a long time primate data on the single cell level seemed to be ambiguous: some investigators reported rodent-like place cells in monkey (Hori et al., 2003; Matsumura et al., 1999; Ono et al., 1991), while others described cells as “spatial view cells” that respond whenever the monkey looks at a given place in the environment (1999; Rolls et al., 1997). However, all of these studies were performed in monkeys restrained in a primate chair or motorized cab, with head fixed, although these restraining apparatuses were moveable in two dimensions either by the experimenter or the seated animal. Recently, Ludvig et al. (2004) have made an attempt to examine the electrical activity of hippocampal neurons in squirrel monkeys allowed to move freely, in three dimensions, in a relatively large space. They found a group of hippocampal complex-spike cells that had marked location-specific firing which was 7-46 times higher than the average firing rate over the entire environment. In a study in human epileptic patients, Ekstrom et

al. (2003) have revealed that ~24% of the hippocampal cells, recorded while the subjects navigated in a 'virtual town' presented on a computer screen, had place-specific firing.

Of particular importance is a recent finding by Ego-Stengel and Wilson (2006) that during spatial exploratory behavior on a linear track, inhibitory interneurons in the CA1 subfield of the hippocampus also show spatial selectivity and phase precession dynamics. They have demonstrated that the firing rate of interneurons is modulated reliably up and down around an ongoing baseline activity level for specific locations in the environment, producing robust place-specific increases or decreases in discharge. Consequently, over the course of a running period, the inhibitory cell firing rate is able to encode more information about space than the excitatory place cells.

1.3. Theta oscillation in the hippocampus

Neural oscillations were first described as periodic signals in the electroencephalogram (EEG) trace of humans (Berger, 1929). As with any time series data, EEG signals can also be transformed to the frequency domain and subject to power spectrum analysis, which yields in principle a continuous function showing the relative contribution of each frequency component to the signal. The observation that some frequencies in the EEG power spectrum are predominant compared to others, and that different frequencies dominate under different behavioral states, such as different stages of sleep and wakefulness (Dement and Kleitman, 1957), led to the classification of EEG frequencies as distinct rhythms. These rhythms are generally thought to reflect the synchronous activity of large populations of neurons, or synapses, and therefore offer a way of measuring large scale neural activity in a given region. Since that time, an enormous body of results has been published on theta oscillation, which will not be reviewed here in detail. For reviews on different aspects of theta see Bland, (1986); Kahana et al., (2001); Buzsaki, (2002); Stewart and Fox, (1990); Klimesch, (1999); Bland and Oddie (2001).

Below follows a brief summary of electrophysiological events characterizing theta rhythm, the ways it influences synaptic transmission in the hippocampus, its proposed generating mechanisms, behavioral correlates, and the possible functions it may play in cognitive processes.

1.3.1. Electrophysiological characterization of theta oscillation

Theta oscillation is a prominent, large amplitude (>1 mV) field potential oscillation, or EEG signal, in the 4-12 Hz frequency band in the rat hippocampus (Stewart and Fox, 1990). Although most easily recordable from rodents, it has also been demonstrated in several other species (Green and Arduini, 1954; Robinson, 1980), including humans (Bodizs et al., 2001; Niedermeyer, 1999). Theta can be recorded from all regions of the hippocampal formation. The phase and amplitude of theta changes according to the 'depth' of the extracellular recording site, i.e., the layer of the hippocampus in which it is recorded from (Bragin et al., 1995; Buzsáki, 1986; 1983; Winson, 1974), but not along the long axis of the hippocampus (Bullock et al., 1990; Fox et al., 1986). The average discharge rate of different cell types changes according to whether the hippocampus is in theta or non-theta mode: principal cell activity decreases, while most interneurons increase or do not change their firing rates during theta (Buzsaki et al., 1983; Csicsvari et al., 1999), although so-called theta-off interneurons that become silent under theta have also been found (Buzsaki et al., 1983; Csicsvari et al., 1999; Mizumori et al., 1990a). The activity of hippocampal principal cells as well as most of the numerous types of hippocampal interneurons was shown to be theta modulated (Csicsvari et al., 1999; Ego-Stengel and Wilson, 2007; Klausberger et al., 2003; Skaggs et al., 1996). Theta modulation is also observable at the level of membrane potential oscillations (Kamondi et al., 1998; Ylinen et al., 1995a). Note that this phase locking to a common 'clock signal' results in a unique order in which neurons of different classes tend to fire after each other during each theta cycle.

1.3.2. Rhythm generating mechanisms

Although many studies addressed the generating mechanisms of theta, the source of the rhythm has not been conclusively resolved (Buzsáki, 2002). The 'classic' theta model posits that the locus of rhythmogenesis is the medial septum-diagonal band of Broca (MS-DBB), and hippocampus merely follows its septal pacemaker input (Petsche et al., 1962). Consistent with this, single MS-DBB units were found to fire phase-locked to hippocampal theta in anesthetized animals (Petsche et al., 1962), even in the absence of inputs from the hippocampus (Vinogradova et al., 1980) or hippocampal theta (Stewart and Fox, 1989). Lesions of MS-DBB abolished theta throughout the entorhinal-hippocampal axis (Petsche et al., 1962; Vinogradova et al., 1980). In addition, GABAergic MS-DBB neurons selectively innervate GABAergic interneurons of the hippocampus (Freund and Antal,

1988), and thus are capable of rhythmically disinhibiting hippocampal pyramidal cells (Toth et al., 1997), that, together with the tonic depolarization provided by the cholinergic component of the septo-hippocampal projection (Frotscher and Leranth, 1985; Madison et al., 1987), could drive pyramidal cells at theta frequency. However, several findings challenge the validity of this view: MS-DBB units that fire phase-locked to theta in the freely behaving animal are not synchronized to each other, and their phase preferences have a wide distribution over the theta cycle (King et al., 1998). A detailed analysis of current generators in the hippocampus revealed a rhythm generator in CA3 (Kocsis et al., 1999), and in line with this study, theta could be induced in isolated hippocampal slices in vitro by the ACh agonist carbachol (Chapman and Lacaille, 1999a; Nunez et al., 1987), although its properties differed from the in vivo rhythm is many respects (Williams and Kauer, 1997). A recent study by Gillies et al. (2002) showed that theta could be induced by a metabotropic glutamate receptor agonist in the hippocampal slice consisting of CA1 only. This seemed to be a better in vitro model of atropine resistant theta, as the phase relationships of neurons belonging to different cell populations and the pharmacological profile of the oscillation were consistent with those recordable in vivo. Intrinsic oscillatory properties of pyramidal cells and of interneurons (Chapman and Lacaille, 1999b; Nunez et al., 1987), as well as possible intrahippocampal network mechanisms (Kiss et al., 2001; Orban et al., 2001) may also promote septum-independent theta generation. A 'pre-septal' scenario for theta genesis was also suggested, in which the septum itself is paced by other lower-level structures in the brain stem and the diencephalon (Vertes and Kocsis, 1997).

1.3.3. Behavioral correlates of theta oscillation

Because theta oscillation is not present continuously in the hippocampus, it is of interest to identify behavioral episodes of the animal that are accompanied by theta. Power in the theta band of hippocampal EEG was found to increase during all kinds of preparatory (as opposed to consummatory) behaviors: voluntary movement (Vanderwolf, 1969), orienting (Gavrilov et al., 1995), exploration of the environment (Komisaruk, 1970; Macrides, 1975) (even without vestibular inputs, Dees et al., 2001), and during rapid-eye-movement (REM) sleep (Jouvet, 1969). Theta was also found to be phasically coupled to sniffing (Forbes and Macrides, 1984) and other rhythmical behavior (Komisaruk, 1970). Frequency of theta was found to be correlated with the running speed of the animal

(McFarland et al., 1975; Shin and Talnov, 2001). Further behaviors often associated with theta are described among its cognitive correlates below.

However, theta oscillations recorded under different conditions have different characteristics. On the basis of pharmacological sensitivity to a muscarinic ACh receptor blocker, atropine, two types of theta could be distinguished: atropine-sensitive (in the anesthetized animal, and in the slice induced by carbachol) and atropine-resistant (in the awake, walking rat) (Kramis et al., 1975; Vanderwolf et al., 1975). The atropine-resistant component was shown to be sensitive to urethane, ketamine, and other NMDAR-blockers, as well as to the lesion of the entorhinal cortex, and thus seems to depend critically on an intact entorhinal input (Buzsáki, 2002; Buzsaki et al., 1983; Ylinen et al., 1995a). These two types of theta oscillations differ in frequency, in the phase relationship that cells maintain relative to the theta, and in the distribution of current sources and sinks as revealed by current source density analysis (reviewed in Buzsáki, 2002). It has recently been proposed that these two types of theta correspond to the 'learning' and 'recall' modes of hippocampus (Lisman and Otmakhova, 2001), but no direct experimental evidence has yet emerged that would support such a distinction.

1.3.4. Theta oscillation and cognitive processing

Part of the excitement about hippocampal theta oscillation is attributable to the finding that most behaviors associated with it seem to require at least some level of attention and presumably cognitive processing. Theta was shown to increase in intensity in a wide variety of behavioral tasks, such as during conditioning (Adey et al., 1960; Grastyan et al., 1966), tasks involving motor control (Buno and Velluti, 1977) or sensorimotor integration (Bland, 1986; Bland and Oddie, 2001). Furthermore, theta oscillations were found to reset at the presentation of a stimulus in a working memory task both in rat (Givens, 1996) and human (Tesche and Karhu, 2000), and bursts of hippocampal theta cycles were shown to be associated with the novelty-associated neocortical event-related potential in an auditory discrimination task (Brankack et al., 1996). The amount of theta (its power, frequency or duration) decreased during the course of conditioning (Adey et al., 1960; Grastyan et al., 1959), covaried with memory load (Tesche and Karhu, 2000) and performance in a conditioning task (Berry and Thompson, 1978; Seager et al., 2002). In humans, drugs widely used for the treatment of psychiatric and cognitive disorders were shown to affect hippocampal theta oscillation (Hajos et al.,

2003). However, these correlational studies can not give insight into whether theta merely correlates with performance in these tasks or it actively takes part in cognitive processes. To this end, manipulations that block or facilitate theta have also been carried out, and were shown to cause impairment (Givens and Olton, 1994; Givens and Olton, 1990; Mizumori et al., 1990b; Pan and McNaughton, 1997; Winson, 1978) or improvement (Kinney et al., 1999; Markowska et al., 1995) in performance in a variety of tasks, respectively.

1.3.5. Theta oscillation and synaptic plasticity

Consistent with many hints on the involvement of theta oscillation in cognitive processes (see above), theta oscillation was also found to modulate synaptic plasticity in the hippocampus. Indirect evidence came from studies demonstrating that stimulation consisting of a few pulses repeated at theta frequency (so-called theta burst stimulation), but not at lower or higher frequencies, were effective in inducing LTP (Greenstein et al., 1988a; Larson et al., 1986a). More direct evidence was provided by experiments in which LTP or LTD could be induced depending on that brief bursts of stimulation used for induction were delivered on the peaks or troughs of the theta cycle, respectively, in vitro (Huerta and Lisman, 1993, 1995), in vivo in anesthetized (Holscher et al., 1997; Pavlides et al., 1988) and freely behaving animals (Orr et al., 2001).

1.3.6. Theta phase precession and phase coding

A theta phase precession effect was first described by O'Keefe and Recce (1993a) in place cells recorded in the CA1 and CA3 subfields of the hippocampus of rats running on a linear track. In this study the authors recorded both the activity of individual pyramidal cells and ongoing theta oscillation. They revealed that as a rat traversed through a place field, the respective place cell fired progressively earlier relative to the ongoing theta rhythm. The overall phase shift between the first and the last spikes fired during a single pass could be as much as 360°. Importantly, the phase shift was more correlated with location than with time spent in the place field (Czurkó et al., 1999; O'Keefe and Recce, 1993a). Phase precession appeared in different environments, although its pattern was less obvious in open field where the rat could freely move in two-dimension than on one-dimension linear track (Skaggs et al., 1996). Interestingly, phase precession was shown to occur even during theta activity in REM sleep when spatial location of the animal does not

seem to be a relevant behavioral variable (Harris et al., 2002). In that study spike phase correlated with instantaneous firing rate, namely decreased as firing rate increased. The authors suggested that the spatial phase precession phenomenon might be a manifestation of a more fundamental principle governing the timing of pyramidal cell discharge. Mehta et al., (2002) also found that firing phase correlated well with firing rate as rats run on a linear track. Furthermore, the correlation between firing phase and an animal's position increased as the rats traversed the same place field repeatedly (Mehta et al., 2002). Furthermore, phase precession is stronger in the first half of a place field than in the second half (Mehta et al., 2002). Amplitude of hippocampal theta oscillation was found to be identical in young and aged rats, although theta frequency during awake behavior but not REM sleep was slightly reduced with age (Shen et al., 1997). Phase precession and the net phase shift during a traversal of a place field remained constant across age and experience (Mehta et al., 1997; Shen et al., 1997) and after application of the NMDAR antagonist CPP (Ekstrom et al., 2001; but see also Mehta and McNaughton, 1997).

In accordance with the proposed cognitive map function of the hippocampus (O'Keefe and Nadel, 1978) ensemble activity of place cells was found to be a good predictor of an animal's position in an environment (Brown et al., 1998; Wilson and McNaughton, 1993; Zhang et al., 1998). The phase precession phenomenon has led to the hypothesis that spatial information can also be represented by the phase at which a cell fires. Indeed, it was demonstrated that the accuracy of estimation of an animal's position can be improved by up to 40%, if theta phase of firing is taken into account (Jensen and Lisman, 2000). Furthermore, choice accuracy was impaired in a working memory task on a radial maze when phase information was unavailable due to the suppression of the theta oscillation, in spite of the preserved rate code in CA1 (Mizumori et al., 1989). This can be explained if downstream brain structures decoding hippocampal output rely on the phase code of place cell firing (Jensen, 2001; Jensen, 2005).

1.3.7. Other hippocampal rhythms

Theta is not the only rhythm in the hippocampus. Gamma oscillation is a fast (30-100 Hz) oscillation, often, but not exclusively cooccurring with theta (Csicsvari et al., 2003). Sharp waves are not rhythms in a strict sense, as they appear irregularly as large peaks in the hippocampal local field potential (hence their former name: large irregular activity), commonly recorded in CA1 str. radiatum, which reflect the synchronous activity

of large populations of neurons, thus leading to the most synchronized physiological mode of hippocampal dynamics (Buzsáki, 1986). Sharp waves occur only during non-theta behaviors, and it is this complementariness with theta, and their many opposing features, that led some researchers to hypothesize that these two 'rhythms' have distinct roles in memory encoding and consolidation (Buzsaki, 1996; Hasselmo, 1999). Ripples are very fast (200 Hz) oscillations riding on sharp waves, similarly as gamma waves are nested within theta cycles (Buzsaki et al., 1992). Recent studies demonstrated that sharp waves-ripples may also appear coordinated with neocortical oscillations (Siapas and Wilson, 1998; Sirota et al., 2003). Hippocampus thus possesses a variety of oscillations, probably tuned for different computations.

1.4. Aim of the thesis

The hippocampus has long been identified as a brain structure that is critical for spatial learning and navigation. One of the supporting evidence for this proposition is the existence of hippocampal place cells, whose activity is restricted to a given part of the environment called the "place field" (O'Keefe and Dostrovsky, 1971). The hippocampal synapses undergo long-lasting plastic changes, which are considered as an excellent candidate for hippocampally mediated storage of spatial (and other) forms of memory. It has been suggested that AMPA receptor, mediating fast glutamatergic synaptic transmission in the hippocampus, is the likely cellular correlate that regulates synaptic plasticity and spatial memory. Although the contribution of AMPA receptors to hippocampus-dependent spatial memory at the behavioral level has been well investigated, its role in the hippocampal cellular dynamics *in vivo* remains to be understood.

In the presented doctoral work, my overall aim was to study the role of AMPA receptor-mediated synaptic transmission and plasticity in the functioning of the hippocampal network *in vivo*. This work has been motivated by the previous findings that genetically engineered mice lacking GluR-A-containing AMPA receptors have a selective defect in a defined component of hippocampal LTP and an impairment in the acquisition of certain spatial learning paradigms.

I recorded the activity of single pyramidal cells from CA1 region of the hippocampus in the wild-type and GluR-A knockout mice as they performed behavioral tasks with different cognitive demands. I focused primarily on characterizing place-specific activity of the pyramidal cells as well as temporal relationship between their firing and hippocampal theta rhythm.

The results obtained in this work uncover the role of AMPA receptor-mediated synaptic transmission in the function of the hippocampal network, responsible for the formation of spatial memory in mice.

2. METHODS

2.1. Subjects

All experiments were carried out in wild-type (WT) and GluR-A knockout (GluR-A KO) age- and litter-matched male mice. In total 7 WT and 7 GluR-A KO mice were used in the study. Among these animals 7 WT and 7 GluR-A KO mice were recorded in the linear track experiments; 4 WT and 6 GluR-A KO mice were recorded in the open field experiments; 2 WT and 4 GluR-A KO mice were recorded in the T-maze experiments. GluR-A KO mice were generated as described in Zamanillo et al., (1999). Mice were housed individually and maintained on a 12-h light/dark cycle. They had ad libitum access to food and water unless otherwise specified. The mice were approximately 16-weeks old at the start of experiment. Most mice were experimentally naive at the start of the study, except 2 animals, which have been run in another behavior experiment ('gap crossing') not related with this project. The experimenter was blind to genotype during the entire experiment and data analysis. All experiments were conducted in accordance with the animal welfare guidelines of the Max Planck Society. All efforts were made to minimize the pain and discomfort of the experimental animals. License number was 35.9185.81/G-60/02.

2.2. Surgical implantation of microdrive

A custom microdrive was designed to allow targeting of a single brain region and independent adjustment of 4 individual tetrodes (see results section 3.1). Tetrodes were constructed of four 15-µm nichrome wires (Kanthal, Palm Coast FL), which were twisted and heat-fused together (Wilson and McNaughton, 1993). Tetrode tips were gold-plated to produce impedances of 200-300 kOm at 1 kHz (impedance tester Thomas Recording GmbH). The mice were anesthetized with intraperitoneal injection of a mixture of ketamine/xylazin (2 and 0.1 mg/10g, in Ringer solution) and placed in a custom-made stereotaxic apparatus. Body temperature was maintained by a temperature controller-regulated heating pad. Pain reflexes were regularly checked and, if necessary, additional anesthetic was given. The skin overlying the skull was resected and 1 mm burrhole was made stereotactically over the approximate position of the dorsal CA1 region of the left hippocampus (coordinates: anteroposterior, -2.5 mm; lateromedial, 1.5 mm relative to bregma). Two stainless steel screw were implanted over the opposite frontal cortex (for anchoring) and the cerebellum (for ground). The microdrive was then lowered into the

burrhole so that the tetrode tips rested 0.5 mm below the dural surface. One of the tetrodes left at that depth served as reference electrode. The borehole was covered with a warm agarose jelly. The microdrive and screws were anchored to the skull with dental cement (Paladur, Heraeus Kulzer GmbH). Animals were then removed from the stereotaxic apparatus and kept warm until recovered from anesthesia. Animals were allowed to recover for at least 7 days, until they returned to their preoperative weight (plus the weight of the installed microdrive, ~1.2 g).

2.3. Behavioral training and tetrodes adjusting

Following a week of recovery after the surgery, the mice were trained to run on a linear track and to perform a T-maze alternation task. Throughout the entire training and further recording the animals were food-deprived and maintained at ~85% of their postoperative ad libitum body weights. All behavioral manipulations were carried out in an electromagnetically shielded and curtained chamber (2.4 x 2.4 x 1.8 m). A custom-made light fixture (shielded 8W halogen lamp), set at the center of the chamber's ceiling and 2 m above the floor, provided consistent illumination (~2 Lux) of the entire floor. A video camera was mounted on the ceiling of the chamber for tracking head position of the animals. Two black paper triangles on internal walls of the chamber served as additional distal cues for animal navigation. Throughout the entire experiments the cues were maintained at a constant configuration. All behavioral arenas (linear track, open field, T-maze) were placed at the center of the chamber.

The linear track on which the animals ran back and forth for food reward (sweetened milk) located in the opposite ends of the track was used to make electrophysiological recordings while the animals exhibited highly stereotypic running behavior. The track (length 140 cm, width 3 cm) was made of wood and painted in black color. A single session on the linear track (≥10 laps) was followed by the training session in the T-maze alternation task. This task was used to measure spatial working memory performance of the mice (Reisel et al., 2002). The black wooden T-maze consisted of a start arm (110 x 3 cm) and two identical goal arms (70 x 3 cm). As a task reward sweetened condensed milk (diluted 50/50 with water) was delivered manually in special food wells located at the ends of the both goal arms. Each trial in the T-maze consisted of a sample run and a choice run (Figure 2.1). On the sample run, the animal was forced to run either left or right by the presence of a wooden block, according to a pseudorandom sequence (with equal numbers

of left and right turns per session, and with no more than two consecutive turns in the same direction). A reward was available in the food well at the end of the arm. Then, the block was removed, and the mouse was immediately placed again in the beginning of the start track and allowed to choose freely either arm. The animal was rewarded for choosing the previously unvisited arm, that is for alternation. Mice were run one trial at a time with an intertrial interval of ~ 30 s, during which they were placed in the small wooden box. Each daily session in the T-maze consisted of at least 10 trials. GluR-A KO mice have been shown to have a impaired performance in the T-maze alternation task: the mean percent correct responses was ~50% in GluR-A KO mice in contrast to 80-90% in WT mice (Reisel et al., 2002). The mice were given daily 1 training session in the T-maze over 5-10 days before the beginning of the electrophysiological recording.

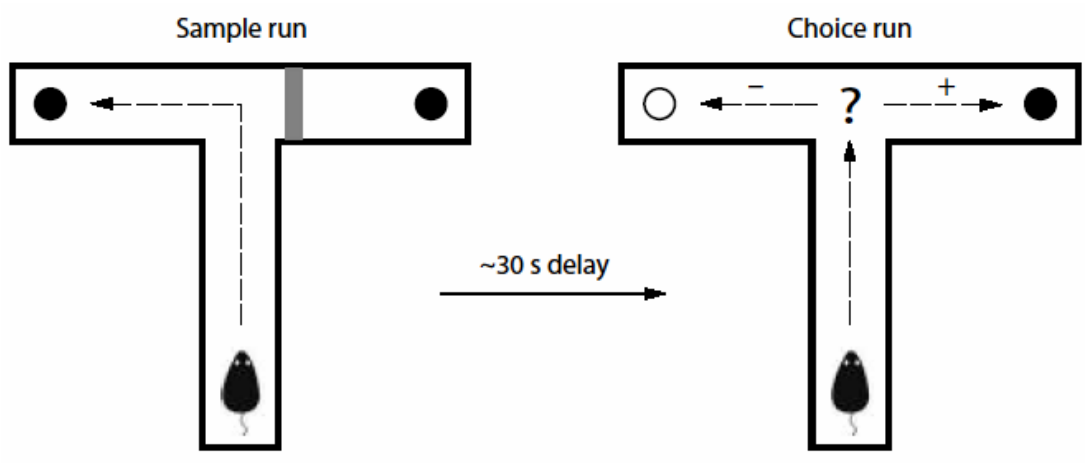

Figure 2.1. Schematic diagram of the T-maze alterantion task.
Each trial consists of a sample run and a choice run. For the sample run, one of two target arms of the maze is blocked, and the animal is forced to obtain the food reward from the unblocked arm. For the choice run, after a delay of ~30 s, both target arms are unblocked, and the animal is free to move into either arm. The animal is considered to have made the correct choice (+) if it visits the previously unsampled arm but incorrect (-) if it visits the previously sampled arm.

An open field was used to monitor place cell activity in a homogeneous environment and did not require pre-training. In this study the open field was a square wooden box (60 x 60 x 30 cm) painted in black. Box floor was covered with a white paper. Recording was made while the animals foraged for crumbled chocolate pellets randomly scattered over the open field. A single open field session lasted, at least, 20 min.

Throughout the training period, the tetrodes were advanced gradually over the course of many days to place the tetrodes in the pyramidal cell layer in CA1. Before each linear track session, the animal was connected to the acquisition system while resting on an elevated circular platform (d=20 cm). During 20-60 min EEG signal and activity of single cells (called 'units' in extracellular recording field) from all tetrodes were monitored. Immobility or slow-wave sleep (1-2 Hz) periods were recognized by examining the recording on-line and were easily distinguished from the periods of more regular theta activity (6-12 Hz) that accompanied movement. The tetrodes were advanced in 25 μm increments by turning each of three microdrive screws $1/8^{th}$ turn. The arrival of each tetrode into the hippocampus was recognized by several criteria, including the presence of 100-300 Hz "ripples" in the EEG (Buzsáki et al., 1992; O'Keefe, 1976; O'Keefe and Nadel, 1978), the polarity of "sharp waves" in the EEG (Buzsáki, 1986), and the sudden appearance, at the depth of about 1 mm below the dura, of multiple simultaneously recorded cells with a complex spike discharge (bursts of spikes with decreasing amplitude) while the animal in quiet waking state. Because most of cells are active during immobility and sleep states, whereas many cells are silent when the mouse is behaving in a given environment (Thompson and Best, 1989), the proportion of detectable cells could be determined using recording while the animal was on the platform.

2.4. Electrophysiological recording

After 5-10 days of training in the experimental environments (linear track and T-maze) electrophysiological recording was started. Animals were attached to a unitary gain head-stage preamplifier (HS-16; Neuralynx, Tuscon, AZ) via a cable suspended on the supporting metal string to avoid an additional load to the animal's head. Signals were filtered and differentially amplified against one channel of the dedicated "reference" tetrode by two Lynx-8 programmable amplifiers (Neuralynx). Whenever the amplitude of the spike signal exceeded a predetermined threshold, each tetrode channel acquired a 1 ms sample of data at a rate of 32 kHz. These spike samples were time-stamped, amplified by a factor of 5000-10000 and stored on a personal computer running Cheetah data acquisition software (Neuralynx). Additionally, signals from one channel of each tetrode were amplified by a factor of 2000-5000 and band-pass filtered in the 1-475 Hz range. These additional channels were used to record EEG signal continuously at a sampling rate of 2 kHz. The animal's position and its head direction were obtained by overhead video

tracking of two light-emitting diodes (of red and blue color) attached to the headstage. Video recording was made with spatial resolution of 0.25 cm/pixel in the linear track and the T-maze protocols and 0.14 cm/pixel in the open field protocol. Sampling rate of the video frame acquisition was 50 Hz.

On each training day, before the first behavioral testing session and after the last testing session, each animal was given a baseline rest/sleep period (20 min) on the elevated platform, during which multiple cells were recorded. The data that were collected during sleep were used to determine the stability of recordings that were made during behavioral sessions. Unstable cells were not analyzed. After the first sleep session and between successive behavioral protocols, the mouse was placed into a small wooden box (30x30x20 cm) for ~ 5 min. Daily recording session consisted of 10-30 laps on the linear track followed by 10-20 trials in the T-maze, and then 20-30 min of running in the open field.

2.5. Data analysis

The entire data processing and statistical analyses were performed in Matlab 7.0 (Mathwork). Analysis of place cell activity and theta rhythm was done for each behavioral paradigm independently. Normally distributed data were represented as mean ± SEM, otherwise - as median (25-75% interquartile range). Student's *t* test was employed to compare the differences between genotype groups of normally distributed data, Mann-Whitney rank sum test - for data that had not normal distributions, Rayleigh Z test - for circular theta phase data. To compare the differences between behavioral paradigms and genotypes, either 1-way ANOVA or 2-way ANOVA together with Holm-Sidak test for post hoc pairwise comparisons were applied. For all the statistical tests a p-value less than 0.05 was considered to be statistically significant.

2.5.1. Identification of recorded cells

Spike sorting was performed offline using graphical cluster-cutting software MClust-3.4 (Redish et al.). Peak, energy and valley were computed for each spike waveform on four tetrode channels. Individual cells (called 'units' in extracellular recording field) were isolated manually by displaying all two-dimensional projections of the multidimensional parameter space (consisting of the spike waveform peaks, energies and valleys) and applying boundaries to each apparent unit cluster. To estimate spike sorting quality I

checked visually how far was the cluster from noise and computed so called 'isolation distance', a measure which estimates the distance from the cluster to the nearest spikes from other clusters or noise (Harris et al., 2001; Schmitzer-Torbert et al., 2005). Only units with isolation distance >5 were considered. Pyramidal cells in the CA1 region were distinguished from interneurons using standard criteria (Buzsaki et al., 1983; Fox and Ranck, 1981; McNaughton et al., 1983a; Ranck, 1973a). The classification criteria for inclusion into the pyramidal cell category was that the cell must fire at least a small number of complex spike bursts during the recording session, be recorded simultaneously with other pyramidal cells (in stratum pyramidale), have spike width (peak to valley) of at least 250 ms, and have an overall mean firing rate of < 2.5 Hz during the behavioral recording session.

2.5.2. Quantification of basic firing properties of cells

To study whether GluR-A subunit deletion influences general firing properties of CA1 pyramidal cells, the following parameters were quantified: 1) Mean firing rate, defined as the total number of spikes emitted by a cell divided by the total duration of recording. 2) Bursting index, defined as the number of spikes that occurred within 20 ms divided by the total spike number. 3) Complex spike index, defined as the number of spikes with decreasing amplitude occurred within 20 ms divided by the total spike number. While bursting index defines a burst based on the interspike interval structure within the burst, complex spike index additionally requires a decrease in the amplitude of the successive spikes within a burst.

2.5.3. Quantification of spatial firing properties of cells

Several quantitative measures were used to describe and compare place-specific firing of the pyrmidal cells in wild type and transgenic mice. For each recording session, firing rate maps were computed to visualize mean firing rate of a given cell as a function of the animal's position. The recording environment was divided into a bin array, consisting of 0.5 x 0.5 cm squares. The total time spent in each bin and the total number of spikes occurred in each bin were accumulated for the session duration. The mean firing rate for each bin was calculated by dividing the corresponding number of spikes by the time spent in that bin. Only bins where the animal spent more than 0.1 s in total were used in subsequent calculations. The firing rate maps created in this way were smoothed using

2D gaussian filter with $\sigma_x = \sigma_y = 3$ cm for the T-maze and open field protocols and $\sigma_x = 3$ cm, $\sigma_y = 0.5$ cm for the linear track protocol. A velocity filter was used to eliminate spikes which occurred when the animal moved slower than 2 cm/s, to prevent contamination by cellular spiking related with non-theta state of the hippocampus (Vanderwolf et al., 1975).

To evaluate spatial properties of pyramidal cell firing the following parameters were computed: (1) Mean firing rate over the entire environment was defined as a ratio between the total number of spikes emitted by a cell and the total session duration. (2) Peak firing rate over the entire environment was defined as the maximum firing rate over all pixels; (3) Spatial selectivity was defined as the ratio between peak and mean firing rates F over the entire environment; (4) Firing field size was defined as a percentage of the total area it occupied in the environment i.e. the number of pixels where average firing rates exceeded 0.1 Hz divided by the total number of pixels visited by the animal; (5) Sparsity, another conventional measure of the spatial distribution of firing was calculated as the ratio between the square mean rate and the mean square rate:

$$\text{Sparsity} = \frac{F^2}{\sum_i P_i f_i^2},$$

where F is the mean firing rate over the entire environment, f_i is the firing rate in the pixel i, P_i is the probability for the animal being in the pixel i; (6) The stability of a firing field within the recording session was quantified by computing the cross-correlation between firing rate maps of the first and second halves of the recording session, termed similarity score. Similarity score was defined as a correlation coefficient (Pearson) r between the firing rates of two maps computed on a pixel-by-pixel basis and z-transformed (Fisher z-transformation, $Z=0.5*\ln((1+r)/(1-r))$) for statistical comparisons. (7) Run-specific firing field size was defined as the distance between right- and leftmost spikes on the linear track in a given run, normalized by the total track length; (8) Run-by-run fluctuation in a firing field location on the linear track was estimated by the amount of shift in the center of mass (COM) of the field from run to run, averaged over all runs. The COM of the firing field in a given run was computed by the formula:

$$\text{COM} = \frac{\sum_i f_i x_i}{\sum_i f_i},$$

where f_i is the firing rate in the pixel i, x_i is the linearized coordinate of the pixel i; (9) Coherence was used to measure the local smoothness of the firing profile (Muller and Kubie, 1989). The coherence was calculated in three steps. First, parallel lists were constructed for the firing rate in each pixel and average firing rate in its eight first-order neighbors. The average firing rate was the sum of the number of spikes in the neighboring pixels divided by the sum of the time spent in the neighboring pixels. Coherence was the Fisher z-transform of the Pearson's correlation coefficient between the two lists; (10) Directionality index (DI), a measure of the relative difference in the firing rate as the animal runs in opposite directions on the linear track, was calculated as :

$$\mathrm{DI} = \left| \frac{f_{LR} - f_{RL}}{f_{LR} + f_{RL}} \right| \cdot 100\%,$$

where f_{LR} and f_{RL} are the firing rates in the left-right and right-left directions, correspondingly; (11) Information content, a measure of the amount of information in the spike train about the position of the animal (bits/spike), was defined by formula (Skaggs et al., 1993):

$$I = \sum_i P_i \cdot \frac{f_i}{F} \cdot \log_2 (\frac{f_i}{F}),$$

where F is the mean firing rate over the entire environment, f_i is the firing rate in pixel i, P_i is the probability for the animal being in the pixel i.

2.5.4. Quantification of theta rhythm

Theta properties were evaluated in two ways: 1) based on the analysis of power spectrum of the EEG signal (PSD-based analysis); 2) based on the analysis of the EEG signal which was band-filtered in the theta (6-12 Hz) range (oscillation-based method). In the PSD-based analysis, fitting the Gaussian function to the 'theta' peak (in 6-12 Hz range) in a power spectrum allowed to estimate the dominant theta frequency (center of mass of the gaussian fit) and theta peak power (peak of the gaussian fit). Theta integral power was determined as an integral of the spectrum over the range of 6-12 Hz, normalized by the total power in the 1-400 Hz range. Frequency of theta rhythm has been shown to be positively correlated with animal's speed in rats (McFarland et al., 1975; McNaughton et al., 1983a; Zhang et al., 1998). Therefore, for each recording session, regression and correlation analyses were used to examine the relationship between the running speed of

the animal and parameters of the theta rhythm. In this analysis, the animal speed, theta frequency, theta peak power and theta integral power were determined every 1 s. There were two food reward locations on the linear track, where the EEG changed from predominantly theta to large irregular activity (LIA) when the mice stopped to eat (Vanderwolf et al., 1975). Therefore, to prevent the contamination of theta rhythm by LIA, the all data where the speed was <2 cm/s at least for 1 s were excluded from the analysis. In order to match speed ranges across the animals, the measurements when the speed was > 30 cm/s (the highest speed common for all the animals), were also eliminated. To avoid complexities in the further analysis due to the ambiguous theta - speed relationship found in the current study, intercepts of the corresponding regression lines in a given session were used as a mean theta frequency and mean theta power in the session. The intercepts reflected values of the theta parameters without the influence of any movement. As an additional control, the frequency and amplitude of theta rhythm were estimated also by the oscillation-based method. In this method occurrences of theta oscillation were automatically identified in the EEG recording by using the theta/delta power ratio (Csicsvari et al., 1999) and only theta periods lasting more than 2 s were used for the analysis. The positive peaks of the theta waves were detected by differentiating the filtered EEG and searching for the convexity. The time between two contiguous positive peaks was defined as the period of theta waves. Theta frequency was defined as the inverse of the theta period. Theta amplitude was defined as the height of the positive peaks in the filtered EEG to the baseline (μV).

2.5.5. Theta phase analysis

The phase-relationship between cell activity and theta rhythm was calculated in the following manner. Each spike that occurred in the presence of theta rhythm was assigned a phase, according to the fraction of the time between the theta peaks at which it occurred. Specifically, the phase assigned to a spike at time t was $360°*(t-t_0)/(t_1-t_0)$, where t_0 and t_1 are the times of the preceding and following peaks of the filtered EEG signal respectively. Only cells which fired at least 50 spikes in the presence of theta were included in the phase analysis. A cell was considered as theta modulated if it showed a nonuniform unimodal distribution of its spike's phases relative to hippocampal theta rhythm. Nonuniformity was tested using the Rayleigh's statistic, $Z=nR^2$, where n is the number of spikes and R is the mean resultant length (the magnitude of the vector that results when each spike is

represented as a vector on the unit circle whose angle relative to some fixed point is given by the spike's phase and the vectors are all summed together). The probability that the null hypothesis of sample uniformity holds is given by $p = e^{-Z} [1 + (2Z - Z^2)/(4n) - (24Z - 132Z^2 + 76Z^3 - 9Z^4)/(288n^2)]$. For $n > 50$, the approximation $p = e^{-Z}$ is adequate (Fisher, 1993). Thus, a cell was considered modulated if its Z was greater than 6 ($p<0.05$).

2.6. Histology

Following completion of the experiments the mice were deeply anesthetized and electrolesion (200 µA for 4 s via each tetrode wire in respect to the ground wire) was done to confirm proper location of the tetrodes. After transcardial perfusion with 10% paraformaldehyde selected hippocampal sections (150 µm) were stained using Cytochrom C (Figure 2.2).

Figure 2.2. Coronal section showing a tetrode location in CA1 area of mouse hippocampus.

3. RESULTS

3.1. Development of a microdrive for chronic recording in behaving mice

In order to study activity of hippocampal neurons in awake behaving mice we designed a device which would allow chronic extracellular recording from multiple tetrodes for extended periods of time in freely moving animals. Such a device (or microdrive) should meet several requirements: 1) Small size and low weight. This is obviously of a particular importance when the animal of interest is small (adult mice weigh about 25-30 g). 2) Precise electrode advancement and repositioning: The drive should allow fine and independent movement of the electrodes it carries for large distances within the brain. The drive should ideally allow the electrodes to be removed from the brain to allow healing of the electrode tracks before repositioning the electrodes for consecutive recordings. 3) Stability over time. Ideally, most unit recordings should be stable over a period of 24 h or longer. Even if the scientific question does not require analyzing the neural activity throughout such long periods, building a drive that allows stable recordings would decrease the probability of the recorded unit to be lost during the recording period. 4) Simple implantation. Rapid implantation decreases the duration of the surgery and reduces the recovery from the surgery.

In collaboration with Tansu Celikel (MPIMF, Cell Physiology Department) I have developed a light (~1.2 g) and compact (11 x 11 x 15 mm) microdrive, which contains 4 independently movable (step size >~25 μm) tetrodes and permits day-to-day adjustment of dorsoventral position in the brain (Figure 3.1). Special effort was made to reduce the size and weight of the entire device so that it does not disturb the free movement of mice. The microdrive has successfully been tested for recordings not only from the hippocampus, but also from the barrel cortex, while mice were freely exploring the environment or solving a spatial learning task.

3.2. Study of spatially selective activity of CA1 pyramidal cells on a linear track

A linear track, on which the animal runs back and forth repeatedly for food does not require intensive animal training and provides a highly stereotyped behavior. Therefore, the linear track was chosen as the primary behavioral paradigm to study spatial properties and theta phase dynamics of CA1 pyramidal cells in GluR-A KO mice. Figure 3.2 shows a representative trajectory of the mouse superimposed with spikes from three difference pyramidal cells recorded simultaneously while the mouse was running on the track.

3.2.1. Basic electrophysiological properties of neurons are not altered in GluR-A KO mice

I recorded the activity of 129 CA1 pyramidal cells from 7 WT mice and 93 CA1 pyramidal cells from 7 GluR-A KO mice while the animals continuously ran on the linear track. Among these neurons, only 75 cells in wild-type mice and 58 cells in knockouts met the unit selection criteria (well isolated cluster, ≥100 spikes, mean firing rate > 0.1 Hz).. Subsequent analysis was performed only on these units.

I first evaluated the basic firing characteristics of the cells (Figure 3.3) and found that pyramidal cells of GluR-A KO animals are largely indistinguishable from those of the control animals. Median firing rate of the pyramidal cells was 0.8 Hz (IQR=0.5-1.1 Hz) in control and 0.7 Hz (IQR=0.5-1.3 Hz) in knockout mice (p=0.7, Mann-Whitney rank sum test, Figure 3.3A).

It is well known that pyramidal cells can fire bursts of action potentials in vivo. It has been speculated that this burst-firing pattern is necessary for the induction of plastic changes in synapses (Buzsáki, 1986; Chrobak and Buzsáki, 1996). To study if bursting activity was altered following deletion of GluR-A containing AMPA receptors, I quantified bursting index (BI) and complex spike index (CSI), two commonly used indices of bursting activity in hippocampus (Harris et al., 2001; McHugh et al., 1996; Tropp Sneider et al., 2006). While bursting index defines a burst based on the interspike interval structure within the burst, complex spike index additionally requires a decrease in the amplitude of the successive spikes within a burst. Comparisons of the bursting activity across the two genotypes showed that the median BI of the pyramidal cells was 40 (IQR=32-46) and the median CSI was 11 (IQR=7-19) in both control and GluR-A KO animals give exact number for BI and CSI (accurate upto 1 decimal place) for WT and KO (p=0.8, Mann-Whitney rank sum test, Figure 3.3B and C). These results suggest that basic neuronal firing characteristics, firing rate and firing pattern in a burst, appear to be independent from GluR-A mediated neuronal activity during linear track exploration.

3.2.2. Place-specific firing of CA1 pyramidal cells is impaired in GluR-A KO mice

The initial classification of positional firing patterns was done by visual inspection of two-dimensional firing rate maps where mean firing rate of a given cell was studied as a function of the animal's position. Difference in the precision of spatial firing patterns

across the two genotype studied is clearly visible in Figure 3.4 on which firing rate maps for 10 representative WT (B) and 10 GluR-A KO (E) cells are shown. The primary difference between the two genotype's firing maps was that place fields recorded in wild-type animals usually had a single salient peak while place fields of the cells recorded in knockout animals were much more diffuse with multiple peaks (see figures ??).

Figure 3.1. A mouse with implanted microdrive
A microdrive carrying four independently adjustable four-channel tetrodes was fixed to the skull of the mouse directly above the hippocampus (2.0 mm L, 1.5 mm P bregma coordinates), allowing large numbers of individual cells to be recorded during behavior.

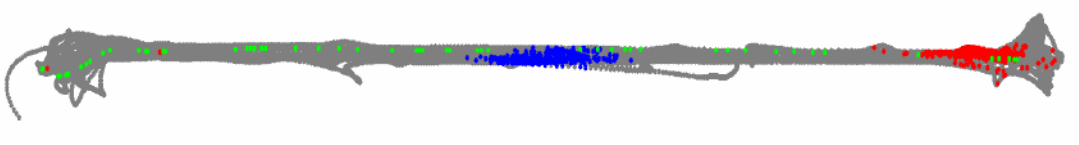

Figure 3.2. Example of the mouse's trajectory on a linear track.
Locations of spikes from three different cells (red, blue, green) recorded simultaneously are superimposed on the mouse's trajectory (gray).

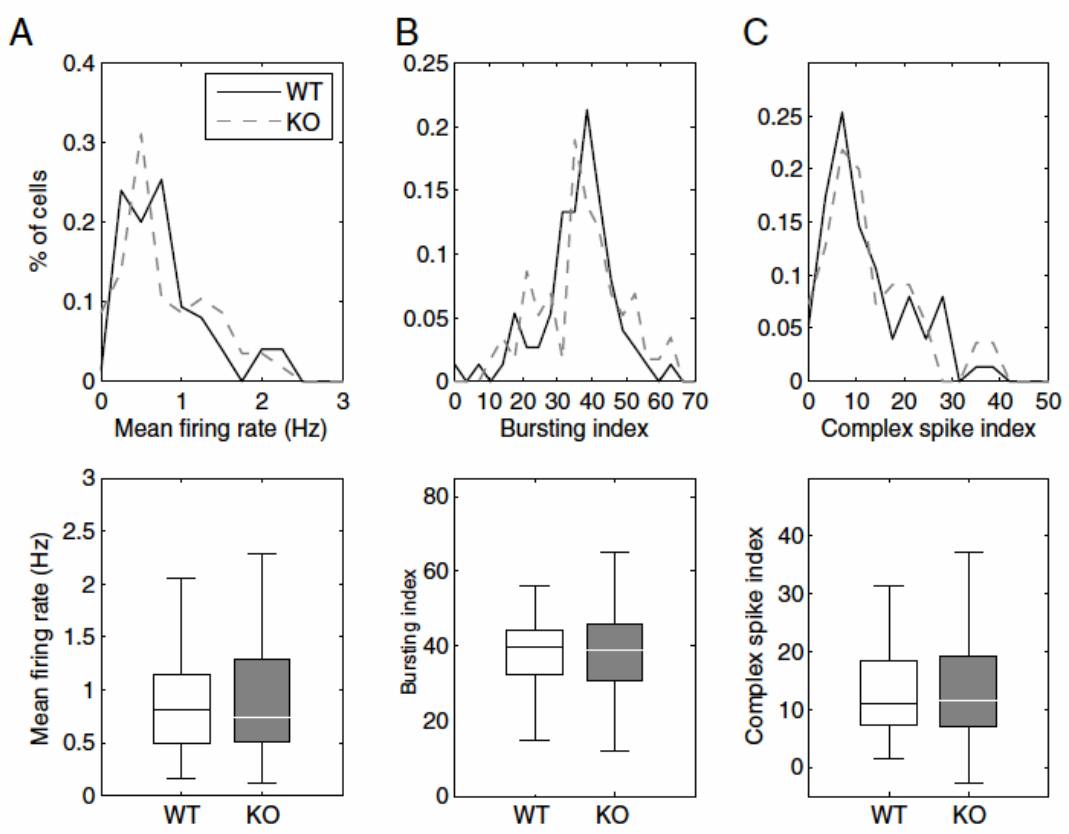

Figure 3.3. Unaltered basic electrophysiological properties of pyramidal cells in GluR-A KO mice.

Top row) Distributions of the mean firing rate (A), bursting index (B) and complex spike index (C) values for the WT (black solid line, n=75) and GluR-A KO (gray dashed line, n=58) pyramidal cells. Bottom row) Median values (horizontal lines inside boxes), interquartile range (boxes), upper and lower limits of the distributions from the corresponding upper panels. Statistical evaluation was done by a Mann-Whitney rank sum test ($p<0.05$).

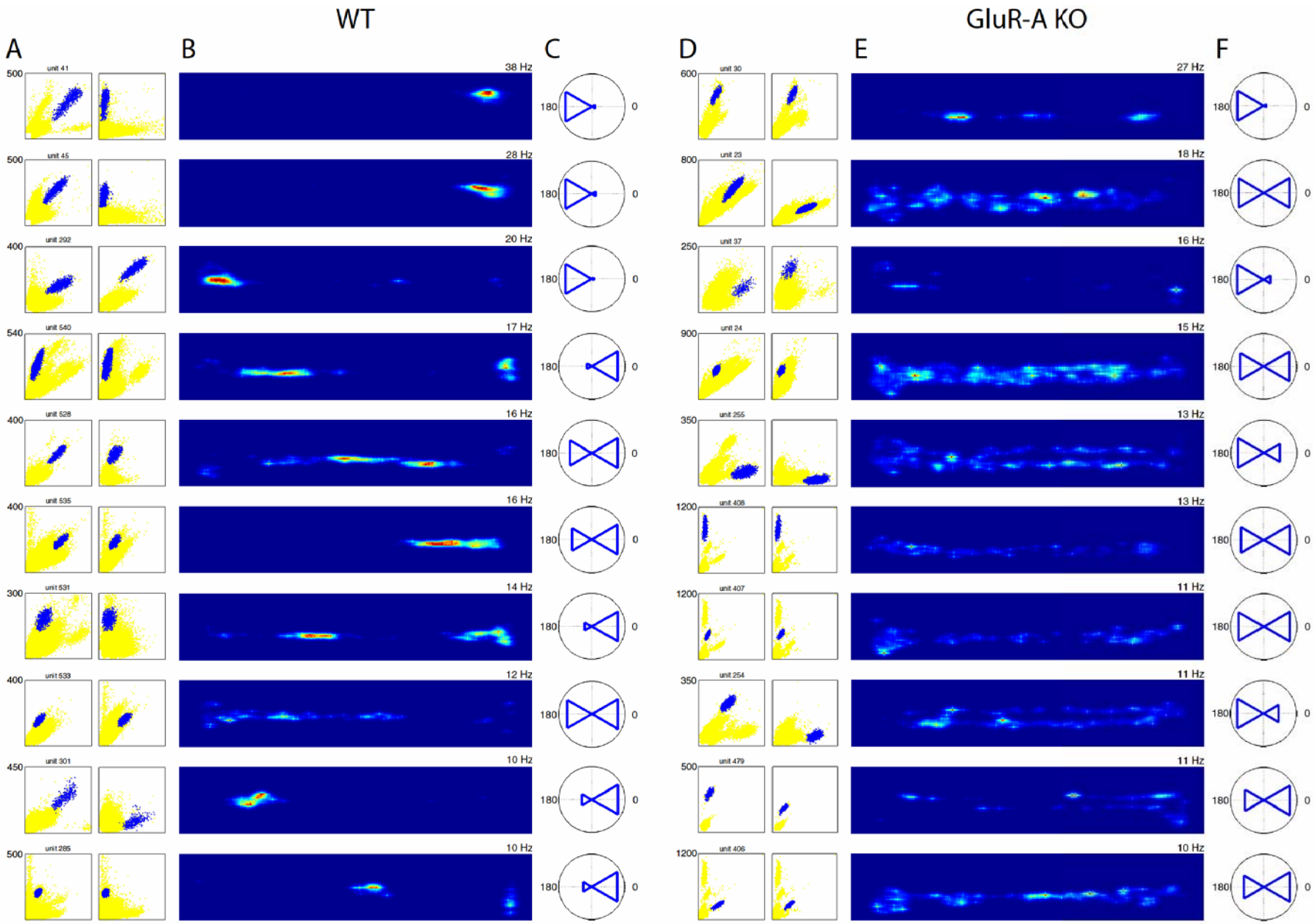
WT
GluR-A KO
A
B
C
D
E
F
500 unit 41
38 Hz
500 unit 45
28 Hz
400 unit 292
20 Hz
540 unit 540
17 Hz
400 unit 528
16 Hz
400 unit 535
16 Hz
300 unit 531
14 Hz
400 unit 533
12 Hz
450 unit 301
10 Hz
500 unit 285
10 Hz
600 unit 30
27 Hz
800 unit 23
18 Hz
250 unit 37
16 Hz
900 unit 24
15 Hz
350 unit 255
13 Hz
1200 unit 408
13 Hz
1200 unit 407
11 Hz
350 unit 254
11 Hz
500 unit 479
11 Hz
1200 unit 406
10 Hz
180
0

Figure 3.4. Impaired place-specific firing of CA1 pyramidal cells in GluR-A KO mice.
Data from WT mice are shown in the left column (A,B,C) and data from the GluR-A KO mice - in the right column (D,E,F). Different rows show data from different cells recorded in different sessions and tetrodes. A) Separation of extracellular action potentials (spikes) when the animal ran on the linear track. Each dot represents peak amplitude of a spike recorded on two of the four tetrode channels. Blue dots represent spikes from an individual isolated neuron. The scale of x and y-axes is the same and shown in the upper left corner in μV. Two adjacent panels show the same isolated neuron in two different combinations of the four tetrode channels. B) Firing rate of the isolated neurons in (A) as a function of the animal's position on the linear track (top-down view). Red indicates maximum firing rates, which are different for each cell and shown in the upper right corners, and dark blue indicates no firing. C) Firing rate of the isolated neurons in (A) as a function of the animal's head direction in polar coordinates. Polar angle represents the head direction and the radial distance represents firing rate of the neuron for that direction. D,E,F) Similar data as (A,B,C), but from GluR-A KO mice. By visual inspection, it is clear that activity of the CA1 pyramidal cells in GluR-A KO mice is spatially unselective and less direction-modulated as compared to WT mice.

3.2.3. Firing fields are notably less selective in GluR-A KO mice

To evaluate how selective is spatial firing of the pyramidal cells I computed the ratio between peak and mean firing rates over the entire environment for each cell. The peak/mean firing rate ratio contrasts in-field firing of a cell with its background discharge and can also be interpreted as a signal-to-noise ratio of the cell's signaling. Figure 3.5 depicts the difference in peak/mean firing rate ratio found between WT and GluR-A KO mice. The spatial selectivity of the pyramidal cells, measured by the peak/mean firing rate ratio, was significantly lower in GluR-A KO animals (Md=19, IQR=14-26) as compared to WT animals (Md=26, IQR=20-39) ($p<0.001$ give the exact p value, Mann-Whitney rank sum test). Furthermore, the reduced spatial selectivity was largely due to decreased peak firing rate of the knockout cells (WT: Md=12 Hz, IQR=8-17 Hz; KO: Md=10 Hz, IQR=7-13 Hz; $p=0.014$, Mann-Whitney rank sum test), while mean firing rate was unaltered (see previous section). If this was true, then the difference in peak firing rates between WT and KO should be the same as ratio of peak/mean between WT and KO. How do you getout of that? Thus, deletion of GluR-A-containing AMPARs made firing fields less distinct from the background activity resulting in spatially unselective neural activation in the CA1 region of the hippocampus.

3.2.4. Firing fields are notably larger in GluR-A KO mice

The decreased spatial selectivity of the knockout cells was accompanied by an increase in the firing field size. The firing field size was expressed as a percentage of the total area it occupied on the track: number of pixels (spatial resolution: 0.5 x 0.5 cm/pixel) where average firing rates exceeded 0.1 Hz divided by the total number of pixels visited by

the animal (Figure 3.6A). The median firing field size was 0.29 (IQR=0.21-0.56) in GluR-A KO mice and 0.18 (IQR=0.14-0.24) in WT mice ($p<0.001$ give exact p value at all places, Mann-Whitney rank sum test)

I also computed sparsity, another parameter widely used to describe how cell firing is distributed across space (Figure 3.6B). Median sparsity was 0.4 (IQR=0.2-0.5) for GluR-A KO mice and 0.2 (IQR=0.1-0.3) for WT mice, which was significantly smaller than the sparsity of cell firing in the knockout mice ($p<0.001$, Mann-Whitney rank sum test). These results confirm the previous conclusion (see section 3.2.3) that deletion of GluR-A-containing AMPAR significantly reduces the tendency for place cells firing to be tightly confined to a certain region in space.

3.2.5. Firing fields are less stable in GluR-A KO mice

The previous results show that impaired GluR-A mediated postsynaptic excitation alters place fields in the CA1 region of the hippocampus. I next asked whether the firing patterns of the knockout cells, although being diffuse, are maintained over time, as the cognitive map theory would require for normal performance in spatial memory tasks. I assessed the short-term stability of place cells within a single session, which lasted usually 15-30 min, after splitting the session into two equal parts and computed firing rate maps for each part. Figures 3.7A and 3.7B illustrate the range of stability for wild-type and knockout place cells, respectively. As the figure shows, in wild-type mice the place cells were stable; their fields remained in approximately the same position throughout the session. By contrast, the positional firing patterns of the knockout cells changed during the session.

The stability of firing fields in the knockout mice can be quantified by computing the cross-correlation between firing rate maps for two halves of the recording session, termed similarity score. Similarity score was defined as a correlation coefficient (Pearson) between the firing rates of two maps computed on a pixel-by-pixel basis and z-transformed (Fisher) for statistical comparisons. Histograms of similarity values for the wild-type and knockout cells are shown in Figure 3.7C. The median similarity score for the knockout cells (Md=0.5, IQR=0.3-0.7) was slightly, although significantly, lower than that for wild-type cells (Md=0.6, IQR=0.4-0.9) ($p=0.007$, Mann-Whitney rank sum test). Due to systematic changes in the place cells within the first 3-4 trials, you should exclude those data and compute similarity between trials 4-7 and 8-11. Further, stability should be calculated with firing rate maps in 1D not 2D.

Small difference in the similarity score between genotypes can be explained by the fact that firing patterns of the knockout cells spread almost over the entire environment. As a result, variability of the firing patterns in the knockout cells was mostly related with spatial redistribution of pixels with peak firing rates within a large firing field with stable boundaries rather than with the change in the location of the entire firing field. Similarity score is, therefore, not sensitive enough to detect such fine alterations in the firing rate distribution. Furthermore, the large firing fields of the knockout cells could arise either as a result of summed up scattered firing in individual runs or via normal focused firing in each run, which, however, fluctuates along the track across runs. To distinguish these possibilities I computed firing fields of the cells for individual runs (so called, run-specific firing fields). Figures 3.8A and 3.8B show representative firing patterns of one wild-type (A) and one knockout (B) cell in four individual trials when the mice were running from left to right. As the figures show, the WT cell spiking was restricted to a very narrow region of the track. In contrast, spikes generated by the GluR-A KO cell were scattered along the track and changed their position in each successive run. To quantify diffuse firing of the knockout cells in individual runs I calculated the size of the run-specific firing fields, averaged across all runs (Figure 3.8C). Run-specific firing field size was defined as the distance between right- and leftmost spikes on the track in a given run, normalized by the total track length. Distributions of averaged run-specific field size values for wild-type and knockout place cells are shown in Figure 3.8C. Run-specific firing fields of the knockout cells (Md=0.48, IQR=0.25-0.61) were significantly larger than those of the wild-type cells (Md=0.15, IQR=0.04-0.34) ($p<0.001$, Mann-Whitney rank sum test). Run-by-run fluctuations in a firing field location were estimated by the amount of shift in the center of mass (COM) of the field from run to run, averaged over all runs (Figure 3.8D). Because directionally selective cells have different activity in left- and right-directed runs, only runs in the direction associated with higher firing rate were used for the calculation of the COM shift. Distributions of COM shift values for wild-type and knockout place cells are shown in Figure 3.8D. Amplitude of the COM fluctuations between successive runs in the knockout cells (Md=17 cm, IQR=13-27 cm) was significantly higher than that in the wild-type cells (Md=9 cm, IQR=3-20 cm) ($p<0.001$, Mann-Whitney rank sum test). Thus, positional firing of the pyramidal cells in GluR-A KO mice was unstable over short (15-30 min) time intervals even when the mouse was continuously on the recording track.

Furthermore, diffuse positional firing of the GluR-A KO cells became apparent already in individual runs and changed across runs.

3.2.6. Firing fields have more irregular structure in GluR-A KO mice

If firing rate of a cell is highly correlated with position, changes in rate between neighboring pixels should be small, and the firing rate in a given pixel should be highly correlated with that of its neighbors. Therefore, place fields are well-ordered structures in the sense that they are consistent, graded, location-related variations in firing rate. To examine integrity of the firing fields structure in GluR-A KO mice I computed spatial coherence, a measure of the orderliness in the firing rate (Muller and Kubie, 1989). The coherence was calculated in three steps. First, parallel lists were constructed for the firing rate in each pixel and average firing rate in its eight first-order neighbors. The average was the sum of the number of spikes in the neighboring pixels divided by the sum of the time spent in the neighboring pixels. Coherence was the Fisher z-transform of the Pearson's correlation coefficient between the two lists. Figure 3.9 shows the distributions of coherence values for control and knockout animals. Mean coherence of the pyramidal cells was 2.12±0.04 in WT and 1.83±0.03 in GluR-A KO mice (mean±SEM, $p \leq 0.001$, Student's t test). Thus, firing fields in GluR-A KO mice revealed less coherence, i.e. impaired location-related gradient of the firing rate as compared to WT mice.

3.2.7. Firing fields show less directional selectivity in GluR-A KO mice

When rats or mice are placed on a linear track, many CA1 place cells display directional selectivity: they only fire when the animal is running in one of the two directions (McHugh et al., 1996; McNaughton et al., 1983a). I therefore examined the data for impairment in the directional selectivity of the place cells in GluR-A KO mice. Figure 3.10A shows examples of the direction dependent activity of one WT cell (upper row) and one GluR-A KO cell (bottom row) when the animals were running on the linear track. To quantify directional selectivity I defined a directionality index, which is a measure of the relative difference in firing rate as the animal runs in opposite directions and lies in the range from 0 (nondirectional) to 100% (strongly directional). Figure 3.10B shows the distributions of directionality index values for control and knockout animals. Both groups showed a certain degree of directional selectivity, but the cells recorded in knockout mice were significantly less direction selective and had a tendency to fire action potentials in a

direction independent manner (WT: Md=46%, IQR=20-75%; KO: Md=18%, IQR=10-39%, p<0.001, Mann-Whitney rank sum test).

3.2.8. GluR-A KO cells convey less information about animal's location

Location-specific discharge of the pyramidal cells was further quantified using a previously described information-theoretic measure, termed an information content (Skaggs et al., 1993). The information content measures the specificity of cell firing by quantifying the amount of information in the spike train about the position of the animal, measured in bits per spike. It was calculated as

$$I = \sum_i P_i \cdot \frac{f_i}{F} \cdot \log_2 (\frac{f_i}{F}),$$

where F is the overall mean firing rate, f_i is the firing rate in pixel i, P_i is the probability for the animal being in the pixel i. More spatially specific firing leads to a larger value of this measure. Figure 3.11 shows the distributions of information content values for control and knockout animals. Indeed, pyramidal cells in GluR-A KO mice carried approximately 2 times less information about animal's location (Md=0.9, IQR=0.5-1.7) than WT cells (Md=1.9, IQR=1.2-2.6) (p<0.001, Mann-Whitney rank sum test). Thus, the impaired location-specific firing of the GluR-A KO cells was also demonstrated by the reduction in the amount of information about the animal's position conveyed by the cells.

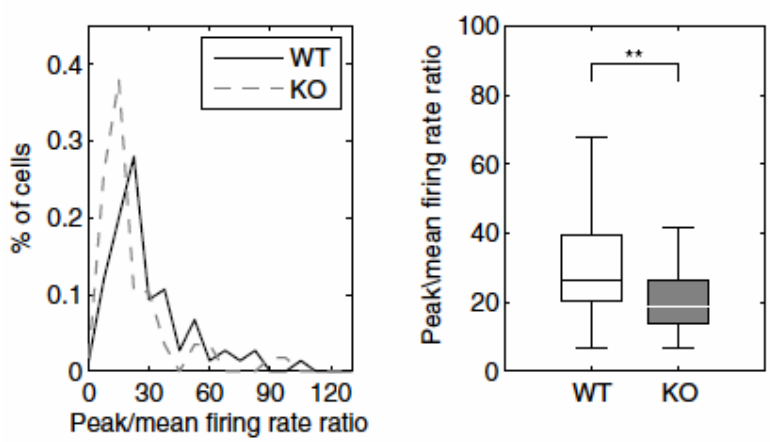

Figure 3.5. Reduced spatial selectivity of the firing fields in GluR-A KO mice.
Ratio between overall peak and mean firing rates was computed for each cell to evaluate spatial selectivity of its firing. Left panel) Distributions of the peak/mean firing rate ratio values for the WT (black solid line, n=75) and GluR-A KO (gray dashed line, n=58) pyramidal cells. Right panel) Median values (horizontal lines inside boxes), interquartile range (boxes), upper and lower limits of the distributions from the left panel. Statistical evaluation was done by a Mann-Whitney rank sum test (**p<0.001). The firing fields of the GluR-A KO pyramidal cells were less distinct from the background activity (i.e. spatially unselective) than those of the WT cells.

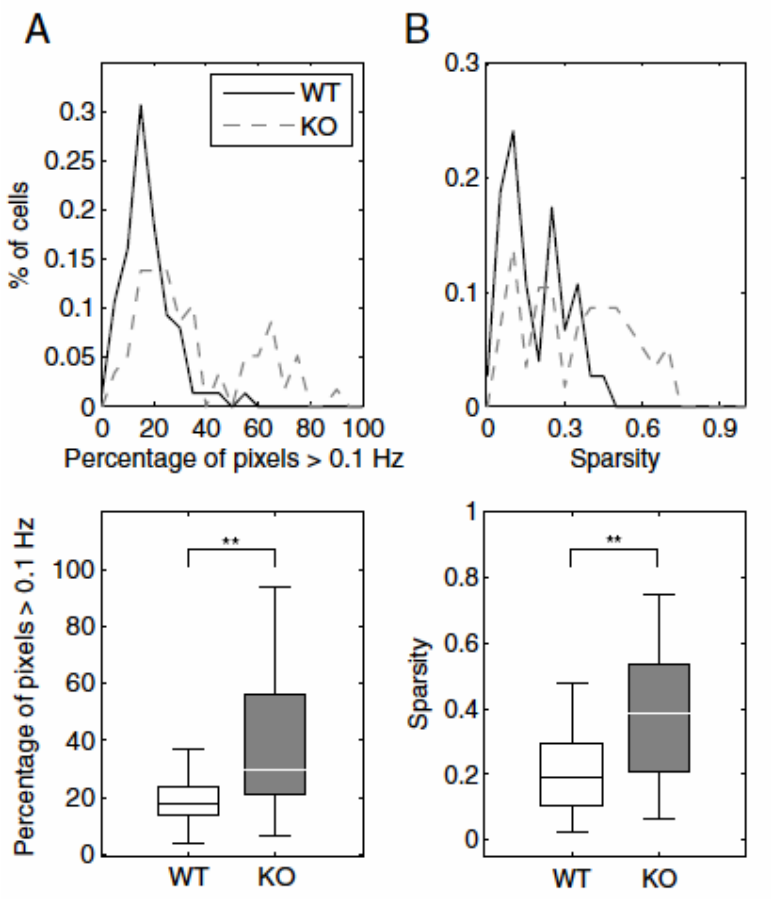

Figure 3.6. Larger firing fields in GluR-A KO mice.
To evaluate the size of the area where the cells fired the following parameters were quantified: percentage of the pixels in which the average rate of firing exceeded 0.1 Hz (A) and sparsity (B). Top row) Distributions of the percentage of the pixels > 0.1 Hz (A) and sparsity (B) values for the WT (black solid line, n=75) and GluR-A KO (gray dashed line, n=58) pyramidal cells. Bottom row) Median values (horizontal lines inside boxes), interquartile range (boxes), upper and lower limits of the distributions from the corresponding upper panels. Statistical evaluation was done by a Mann-Whitney rank sum test (**p<0.001). The pyramidal cells in GluR-A KO mice were active in significantly larger portion of the environment compared to the cells in WT mice.

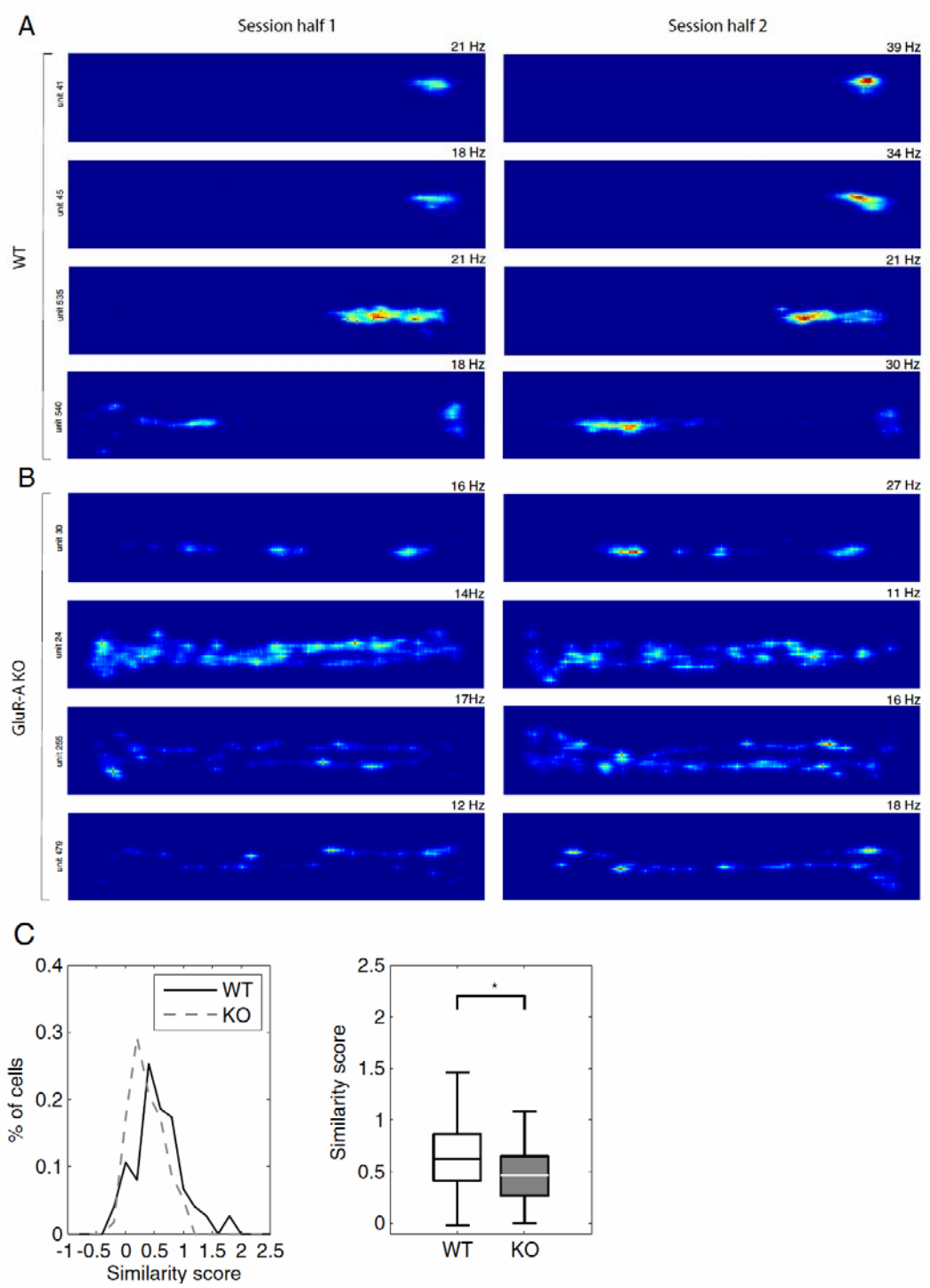
A
Session half 1
Session half 2
WT
21 Hz
39 Hz
18 Hz
34 Hz
21 Hz
21 Hz
18 Hz
30 Hz
B
GluR-A KO
16 Hz
27 Hz
14Hz
11 Hz
17Hz
16 Hz
12 Hz
18 Hz
C
WT
KO
% of cells
Similarity score
Similarity score
WT
KO
*

Figure 3.7. Reduced stability of the firing fields in GluR-A KO mice within a session.
To assess stability of positional firing of the place cells as the animal ran on the linear track, similarity score between firing rate maps of two session halves was calculated. Similarity score was defined as a Pearson's correlation coefficient between the firing rates of two maps computed on a pixel-by-pixel basis and z-transformed (Fisher) for statistical comparison. Right and left columns show firing rate maps from the first and second halves of the same session, correspondingly. Different rows show data from different cells recorded from WT (A) and GluR-A KO (B) mice. Red color in the firing rate maps indicates maximum firing rates, shown in the upper right corners. C) Left panel shows distributions of the similarity score for the pyramidal cells in control (black solid line, n=75) and mutant mice (gray dashed line, n=58). Right panel shows median values (horizontal lines inside boxes), interquartile range (boxes), upper and lower limits of the distributions from the left panel. Statistical evaluation was done by a Mann-Whitney rank sum test (*p=0.007). The spatial firing patterns of the GluR-A KO pyramidal cells were less stable within a single session on the linear track.

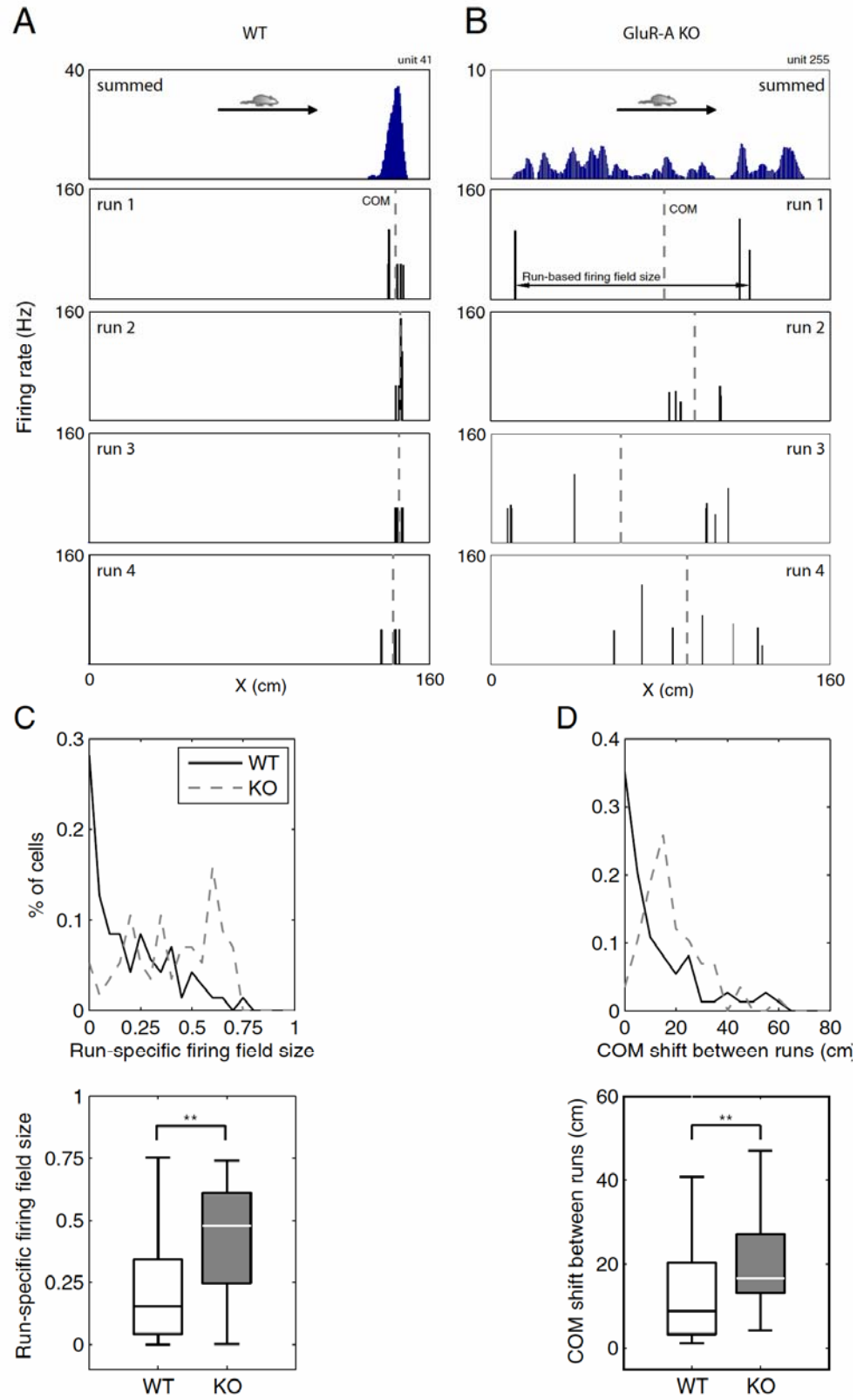
A
WT
unit 41
summed
run 1
COM
run 2
run 3
run 4
Firing rate (Hz)
X (cm)
B
GluR-A KO
unit 255
summed
run 1
COM
Run-based firing field size
run 2
run 3
run 4
X (cm)
C
WT
KO
% of cells
Run-specific firing field size
D
COM shift between runs (cm)
Run-specific firing field size
COM shift between runs (cm)
WT
KO

Figure 3.8. Firing fields in GluR-A KO mice are diffuse in individual runs and alter from run to run.
Mean size of the run-specific firing fields was calculated to evaluate how diffuse were firing patterns of the knockout cells in individual runs on the linear track. Mean size of the run-specific firing field was defined as the distance between right- and leftmost (first and last) spikes on the track in each run, averaged over all runs. Run-by-run fluctuation in the location of the firing field was estimated by the amount of shift in the center of mass (COM) of the field from run to run, averaged over all runs. A) Upper panel shows firing rate of a WT neuron as a function of the linearized animal's position on the track, summed over all right-directed runs. Four bottom panels show linearized firing fields for the same WT neuron computed individually for the first four right-directed runs in the same session. Vertical dashed lines depict the centers of mass (COM) of the firing fields in individual runs. B) Similar data as (A), but from GluR-A KO mice. Note scattered spiking of the GluR-A KO cell in the individual runs in contrast to local spiking of the WT cells. Furthermore, COM of the run-specific firing fields in GluR-A KO mice fluctuated across runs in contrast to relatively stable COM in the WT cell. C) Upper panel shows distributions of the mean run-specific field size values for CA1 pyramidal cells in control (black solid line, n=75) and mutant mice (gray dashed line, n=58). Lower panel shows median values (horizontal lines inside boxes), interquartile range (boxes), upper and lower limits of the distributions from the upper panel. D) Upper panel shows distributions of the run-by-run COM shift values for CA1 pyramidal cells in control (black solid line, n=75) and mutant mice (gray dashed line, n=58). Lower panel shows median values (horizontal lines inside boxes), interquartile range (boxes), upper and lower limits of the distributions from the upper panel. Statistical evaluation was done by a Mann-Whitney rank sum test (**p<0.001). Thus, positional firing of the GluR-A KO cells was unstable within a single recording session (15-30 min). Furthermore, diffuse positional firing of the GluR-A KO cells became apparent already in individual runs and changed across runs.

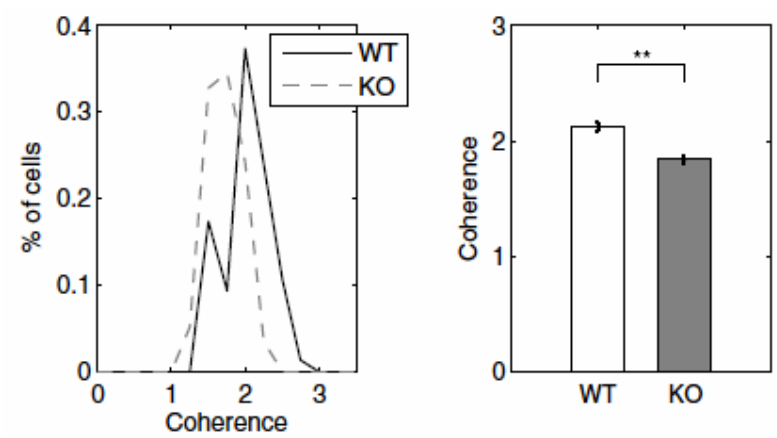

Figure 3.9. Irregular structure of the firing fields in GluR-A KO mice
Spatial coherence was computed to examine integrity of the firing field structure in GluR-A KO mice. Left panel) Distributions of the coherence values for the WT (black solid line, n=75) and GluR-A KO (gray dashed line, n=58) pyramidal cells. Right panel) Bars represent mean±SEM values of the distributions from the left panel. Statistical evaluation was done by a Student's *t* test (**p<0.001). Firing fields in GluR-A KO mice showed less coherence, i.e. impaired location-related gradient of the firing rate as compared to WT mice.

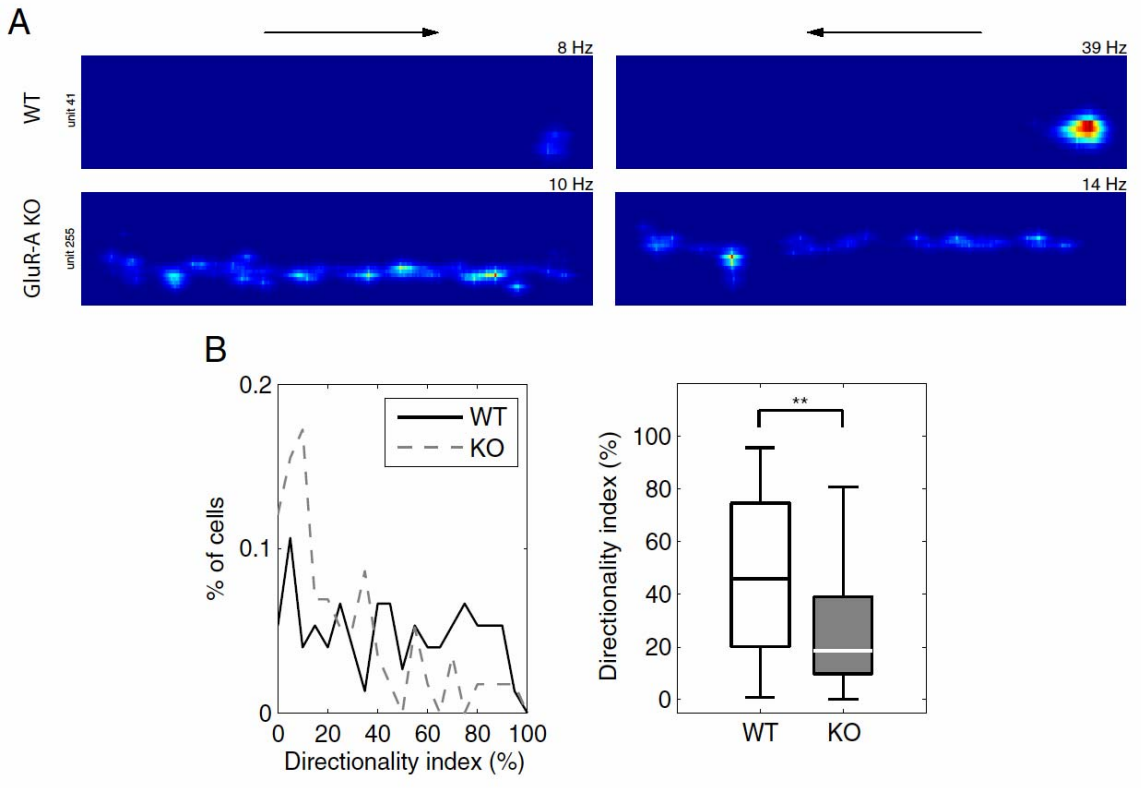

Figure 3.10. Firing fields show less directional selectivity in GluR-A KO mice.
Directional selectivity of the cells was quantified by computing directionality index, a measure of the relative difference in firing rate as the animal runs in opposite directions and lies in the range from 0 (nondirectional) to 100% (strongly directional). A) Right and left columns show firing rate maps calculated separately for right- and left-directed runs of the same session, correspondingly. Upper and bottom rows show data from one WT and one GluR-A KO cells, correspondingly. Red color in the firing rate maps indicates maximum firing rates, shown in the upper right corners. Note that the WT cell was almost silent when the animal was running from left to right (upper left panel) and discharged at high frequency in the opposite direction (upper right panel). B) Left panel shows distributions of the directionality index values for the pyramidal cells in WT (black solid line, n=75) and GluR-A KO (gray dashed line, n=58) mice. Right panel shows median values (horizontal lines inside boxes), interquartile range (boxes), upper and lower limits of the distributions from the left panel. Statistical evaluation was done by a Mann-Whitney rank sum test (**$p<0.001$). The GluR-A KO pyramidal cells showed significantly less directionally tuned spiking compared to the WT cells.

.

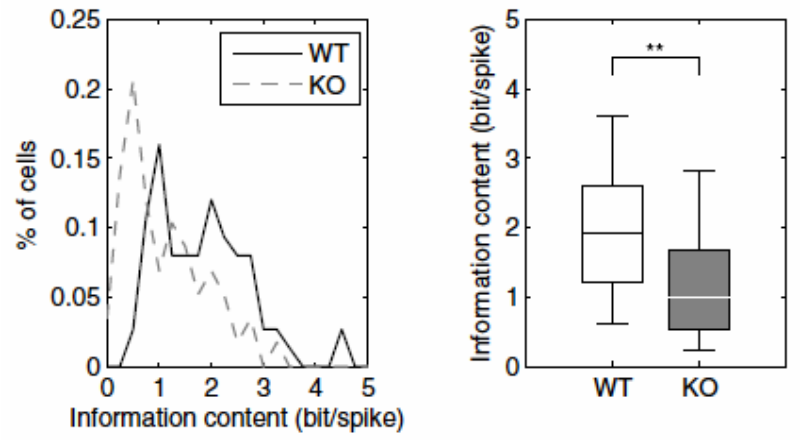

Figure 3.11. GluR-A KO cell convey less information about animal's location.
Location-specific discharge of the pyramidal cells was quantified by computing spatial information content, a measure representing the amount of information about the animal's location conveyed by a train of spikes (bit/spike). Left panel) Distributions of the information content values for the WT (black solid line, n=75) and GluR-A KO (gray dashed line, n=58) pyramidal cells. Right panel) Median values (horizontal lines inside boxes), interquartile range (boxes), upper and lower limits of the distributions from the left panel. Statistical evaluation was done by a Mann-Whitney rank sum test (**$p<0.001$). The pyramidal cells in GluR-A KO mice carried significantly less information about animal's location compared to the cells in WT mice.

3.2.9. Defective firing fields are not due to reduced peak firing rate in GluR-A KO mice

Visual inspection revealed that a relatively small subgroup of WT cells with high peak firing rate (>20 Hz, the highest rate common for the cells from both genotypes, and <45 Hz) possessed more selective and compact firing fields, which could, in principle, be a source of the found differences in the firing pattern parameters between the genotypes. To examine this possibility I restricted comparison of the firing parameters to only cells with a peak firing rate of ≤20 Hz (n(WT)=60; n(KO)=57). Figure 3.12 shows those of the analyzed parameters whose correlation with the peak firing rate in either genotype was statistically significant ($p<0.05$, Mann-Whitney rank sum test). Even after removing the cells with high peak firing rate, the differences in most of the spatial firing properties of WT and GluR-A KO cells were still statistically significant. The only parameter which became statistically indistinguishable between genotypes after recalculation was the similarity score ($p=0.2$, Mann-Whitney rank sum test), suggesting that stability of place fields is predominantly expressed in those cells with high firing rates. These results show that the impaired place-related firing of the pyramidal cells in GluR-A KO mice cannot be attributed to a decreased signal-to-noise ratio due to reduced peak firing rate.

3.2.10. Defective firing fields are not due to altered motor activity in GluR-A KO mice

Spiking rate of the CA1 pyramidal cells in both genotypes increased with the increasing speed of movement (Figure 3.13A), as previously reported (Czurkó et al., 1999; Ekstrom et al., 2001; Huxter et al., 2003; McNaughton et al., 1983a). To ensure that the detected impairments in place cell firing in GluR-A KO mice were not due to non-specific change in motor activity, I compared mean animal speed (Figure 3.13B) and linearized speed profiles along the track in both directions (Figure 3.13C) between genotypes. Mean speed was computed, first, for individual runs (track length divided by the time spent to run from one end to another), and, then, averaged across all runs, all sessions and, finally, all animals within each genotype. The same averaging procedure was used for calculation of the mean speed profile. Mean speed values on the track were similar for WT (22.5±0.3 cm/s) and GluR-A KO (21.9±0.6 cm/s) mice ($p=0.4$, Student's t test). Pixel-by-pixel comparison of the linearized speed profile revealed that GluR-A KO mice ran a bit faster (~1.1 times) in the beginning of the right-directed runs and in the middle of the left-directed runs ($0.0001 \leq p \leq 0.2$, Student's t test) (Figure 3.13C). In accordance with the speed-modulation of the firing rate observed in the present study (Figure 3.13A), the 1.1 times increase in running speed of GluR-A KO mice has a negligible influence on the firing rate of their cells. Thus, reduced peak firing rate of the pyramidal cells in GluR-A KO mice can not be attributed to a small increase in running speed of the knockouts.

3.2.11. Defective firing fields are not due to poor cell isolation in GluR-A KO mice

An important step in spike-train analysis is the isolation of single cells (called 'units' in extracellular recording field) on the basis of extracellular features. Multiple factors such as variability of spike amplitude and waveform result in different errors in unit isolation. A major problem with all currently used unit isolation methods is that their reliability cannot be verified independently. Therefore, it is possible that diffuse firing of the pyramidal cells in GluR-A KO mice relative to WT mice is due to poor isolation of units in the knockout animals, rather than due to specific defects in the hippocampal network function. In other words, if some spikes of other cells were erroneously included into the cluster during isolation stage, it could lead to a diffuse firing pattern of that cell. I have made a number of efforts to exclude this possibility.

Isolation quality of a unit can be qualitatively estimated by visual inspection of separation of its cluster from noise or neighbor clusters in each combination of four tetrode channels (projection). Figure 3.14A shows an example of completely (right panel) and partly (left panel) separated clusters in a given projection. Furthermore, cluster separation can be quantified by computing the 'isolation distance' measure which estimates the distance from the cluster to the nearest spikes from other clusters or noise (Harris et al., 2001; Schmitzer-Torbert et al., 2005). It is defined as the Mahalanobis distance from the cluster center within which as many spikes belong to the specified cluster as to others (see Methods). Median isolation distance for the clusters studied was 20 (IQR=14-27) in WT and 25 (IQR=18-38) in GluR-A KO animals (p=0.003, Mann-Whitney rank sum test, Figure 3.14B). Thus, the quality of unit isolation in the knockouts was even slightly higher than that in the controls and therefore the differences between mentioned in the WT and KO cannot be attributed to differences in spike sorting.

Considering that the analyzed pool of units included units with different isolation quality (Figure 3.14B), I examined whether medians and dispersions of the computed parameters as well as detected genotype-related differences are invariable as lower quality units were removed from the pool. Towards this goal, the units were categorized on the basis of their isolation quality as determined by visual inspection. Units whose clusters were completely separated from other spikes in at least two more projections were assigned to a category 1 ('best isolation', n(WT)=6, n(KO)=14). Units whose clusters were completely separated only in one projection were assigned to a category 2 ('good isolation', n(WT)=29, n(KO)=28). Units whose clusters were not completely separated in any of six projections were assigned to a category 3 ('weak isolation', n(WT)=40, n(KO)=16). Figure 3.15 shows changes in the parameter statistics when only 'weak' (category 3) or both 'weak and 'good' (categories 3 and 2) units were removed from the analyzed unit pool. Compute the difference between WT and separately for each of the 3 categories best, good and weak. Do not mix categories. The medians were not statistically different between unit categories as tested by Kruskal-Wallis one way analysis of variance on ranks (p>0.2). The genotype-related differences were still statistically significant after removing 'suspicious' (category 3) units, but became insignificant after removing both 'suspicious' and 'good' (categories 3 and 2) units. Lack of significant differences in the parameter values between genotypes in the 'best' (category 1) units can be due to a very small number of cells left (n=6 in WT and n=14 in GluR-A KO mice). To have an

additional and more objective control for the unit quality influence, I repeated the same analysis, but with the isolation distance as a unit quality estimator (Figures 3.16). Units with isolation distances >40 were assigned to a category 1 ('best isolation', n(WT)=7, n(KO)=13), with isolation distances in the range of 20-40 - to a category 2 ('good isolation', n(WT)=30, n(KO)=27), and with isolation distances <20 - to a category 3 ('weak isolation', n(WT)=38, n(KO)=19). The results of both visual inspection- and isolation distance-based analyses were in agreement with each other.

Thus, the quality of unit isolation was similar for the pyramidal cells in WT and GluR-A KO mice. Furthermore, the impairments found in spatial firing of the GluR-A KO cells were preserved even when stricter criteria for unit selection were applied, provided that each genotype group has enough number of cells (>10).

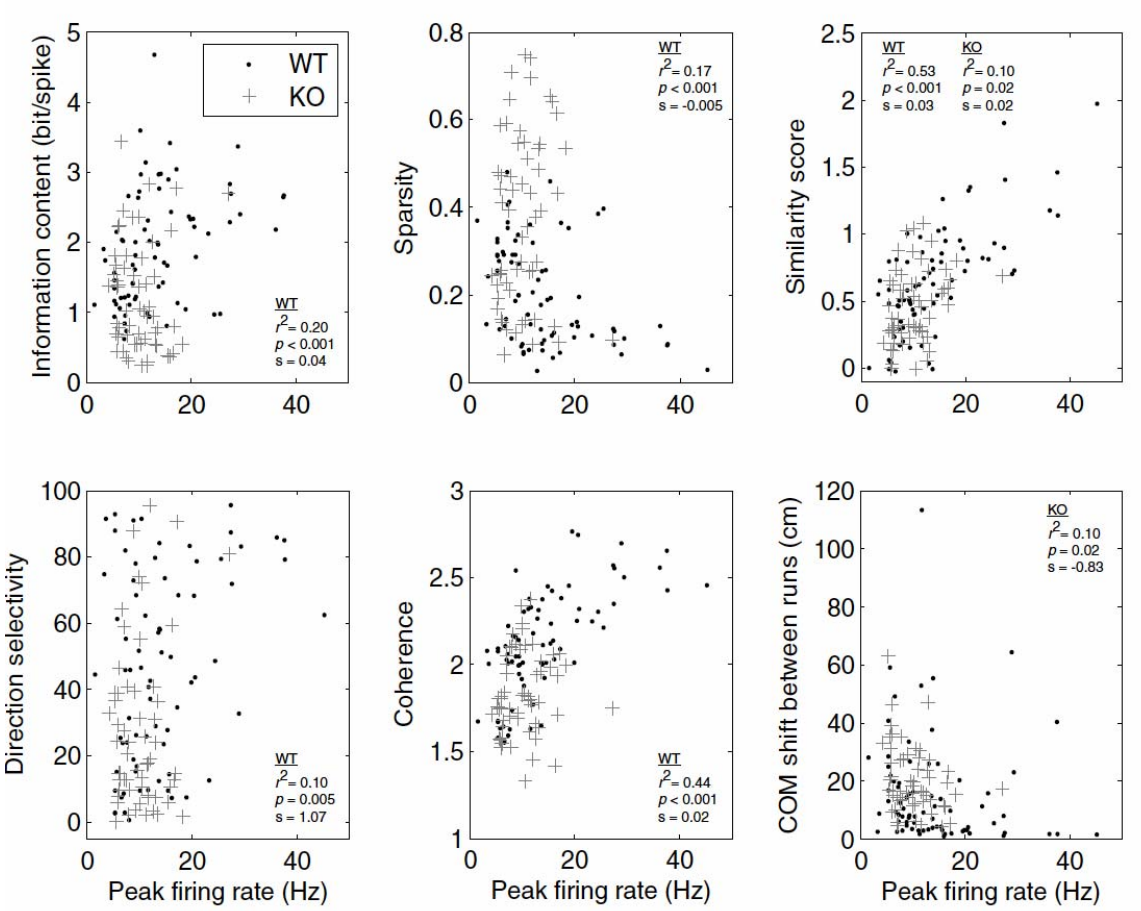

Figure 3.12. Correlation of the firing field properties with the peak firing rate
Only parameters whose correlation (Pearson) with the peak firing rate in either genotype was statistically significant ($p<0.05$) are shown. Each dot represents a single WT cell, while each cross – a single GluR-A KO cell. Squared correlation coefficients (r^2), p-values and linear fit slope values (s) are shown in each panel. Note that small fraction of the WT cells with the peak firing rates > 20 Hz can, in principle, account for the differences in the firing properties between genotypes.

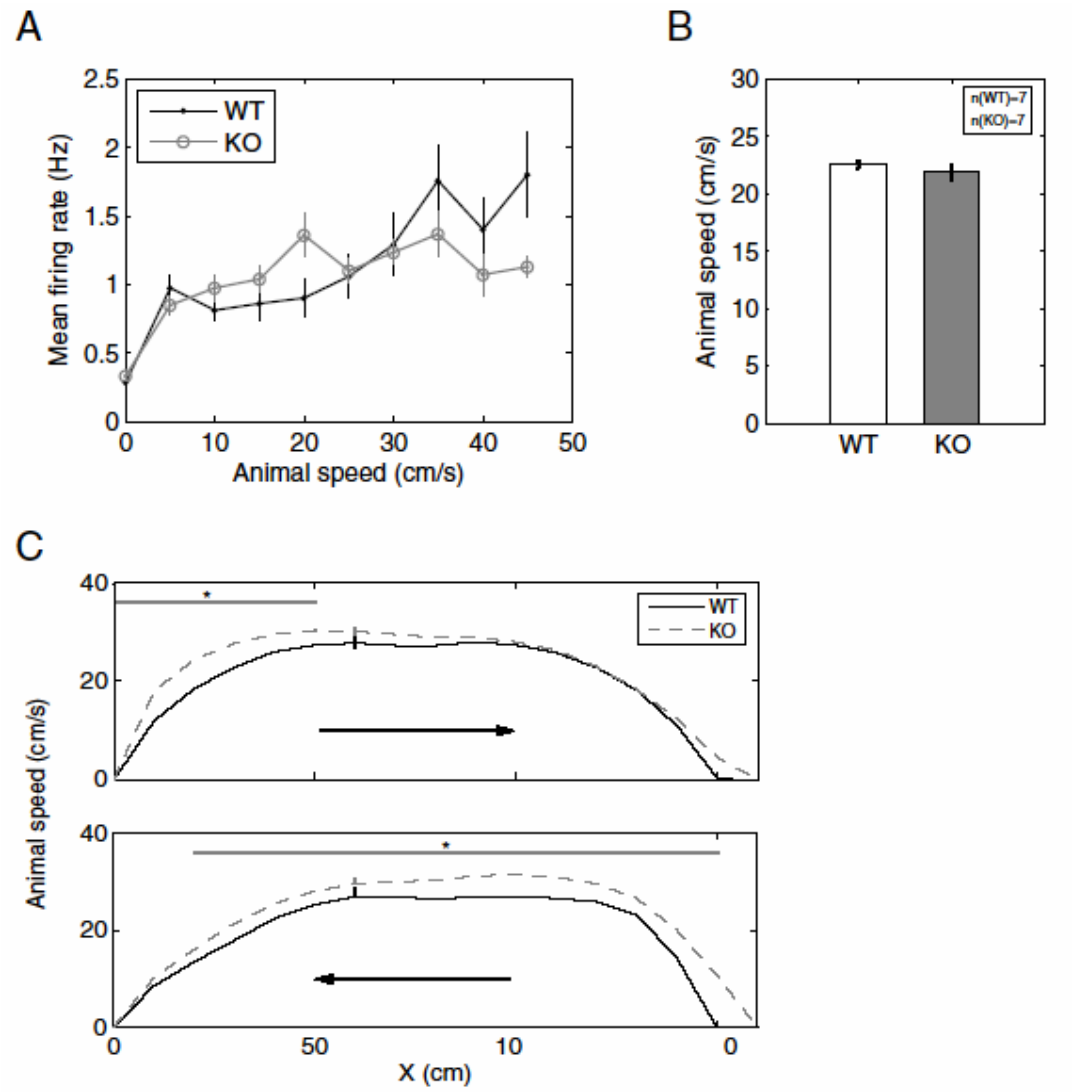

Figure 3.13. Similar running speed in WT and GluR-A KO mice.
A) Mean firing rate of the WT (black line with dots, n=75) and GluR-A KO (gray line with circles, n=58) pyramidal cells as a function of running speed of the animal on the linear track. Data are represented as mean±SEM. B) Mean running speed on the linear track was not different in WT (22.5±0.3 cm/s, n=7) and GluR-A KO mice (21.9±0.6 cm/s, n=7) (Student's *t* test, p=0.4). C) The running speed of the mice in both directions is shown as a function of linearized x position on the track, averaged across all runs and sessions for WT (black solid line) and GluR-A KO mice (gray dashed line). Two vertical bars on the speed curves represent standard error of the mean in that x position. Gray horizontal lines above the speed curves depict x positions where the difference in running speed was significant ($p<0.05$). GluR-A KO mice ran a bit faster (~1.1 times) in the beginning of the right-directed runs and in the middle of the left-directed runs (Student's *t* test, pixel-by-pixel comparison, $0.0001 \leq * p \leq 0.2$).

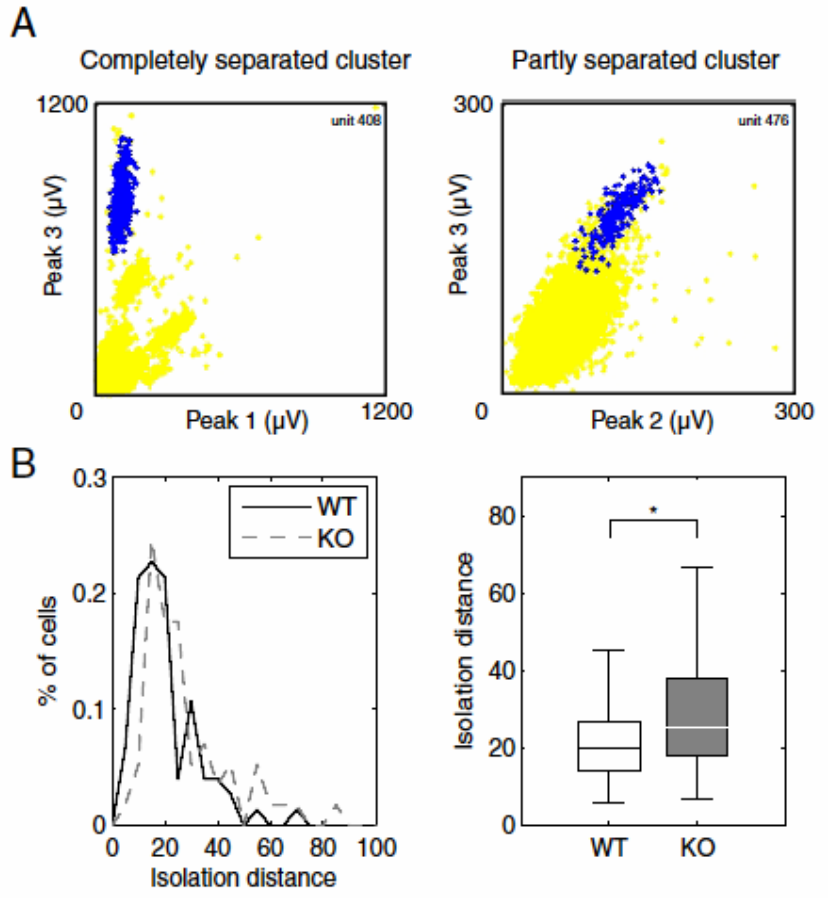

Figure 3.14. Similar isolation quality of the cells in WT and GluR-A KO mice.
A) Examples of two different cells with completely (left panel) and partly (right panel) separated clusters in a given combination of the tetrode channels. Each dot represents peak amplitude of a spike recorded on two of the four tetrode channels. Dark dots represent spikes from an individual isolated neuron. B) Cluster separation can be quantified by computing the 'isolation distance' measure, estimating the distance from the cluster to the nearest other cluster. Left panel) Distributions of the isolation distance values for the WT (black solid line, n=75) and GluR-A KO (gray dashed line, n=58) pyramidal cells. Right panel) Median values (horizontal lines inside boxes), interquartile range (boxes), upper and lower limits of the distributions from the left panel. Statistical evaluation was done by a Mann-Whitney rank sum test (*p=0.003). Isolation quality of the GluR-A KO cells was slightly, but statistically significantly, higher than that of the WT cells.

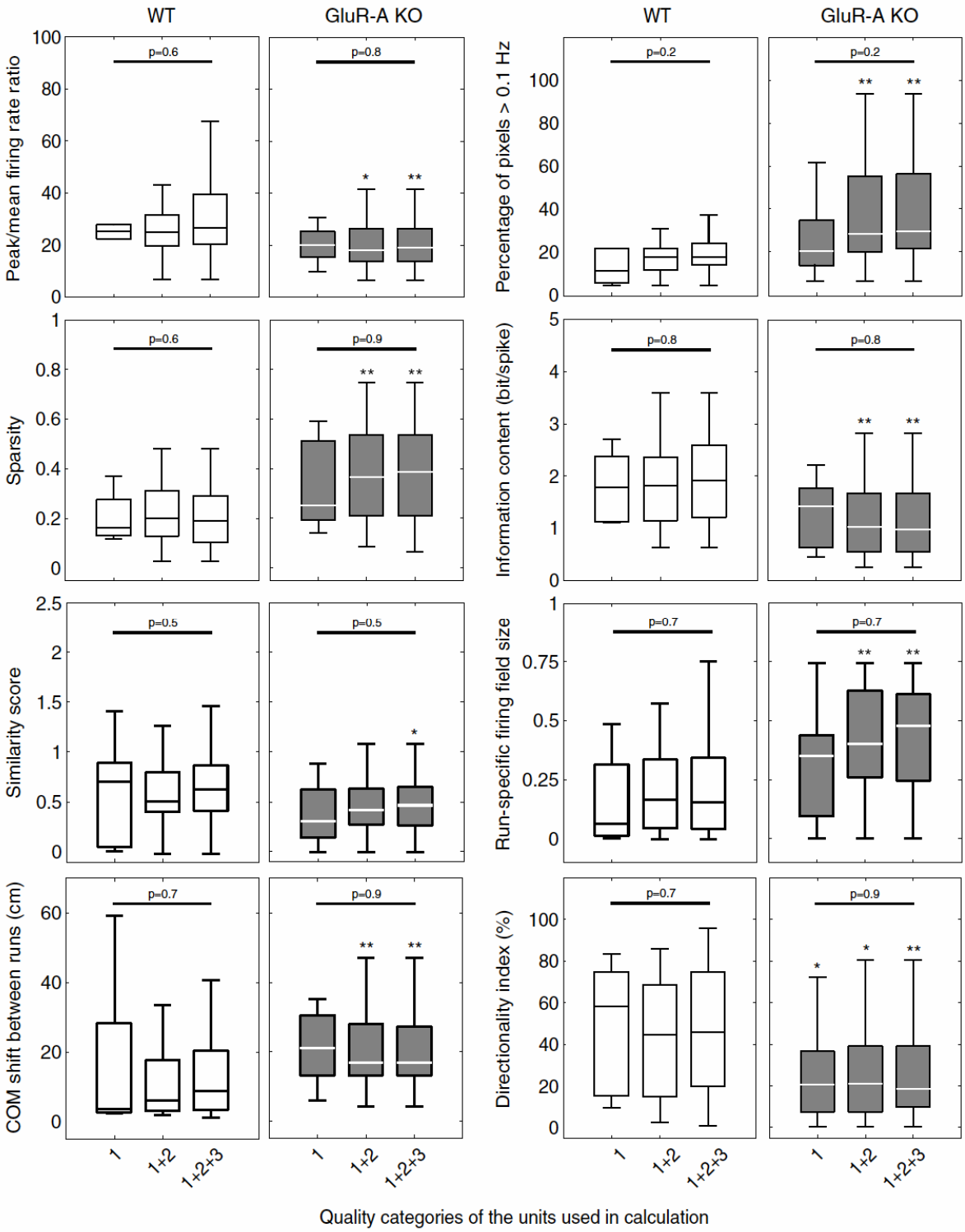
WT
GluR-A KO
WT
GluR-A KO
Peak/mean firing rate ratio
Percentage of pixels > 0.1 Hz
Sparsity
Information content (bit/spike)
Similarity score
Run-specific firing field size
COM shift between runs (cm)
Directionality index (%)
p=0.6
p=0.8
p=0.2
p=0.2
p=0.6
p=0.9
p=0.8
p=0.8
p=0.5
p=0.5
p=0.7
p=0.7
p=0.7
p=0.9
p=0.7
p=0.9
1
1+2
1+2+3
Quality categories of the units used in calculation

Figure 3.15. Change in the parameter statistics when cells of different isolation quality are analyzed (isolation quality was estimated visually).

Each horizontal pair of panels shows descriptive statistics of a certain firing parameter calculated for the cells of different isolation quality in WT (left panel within the pair, open bars) and GluR-A KO (right panel within the pair, filled bars) mice. Descriptive statistics is represented by median values (horizontal lines inside boxes), interquartile range (boxes), upper and lower limits of the values distribution. All the cells in each genotype were categorized on the basis of their isolation quality so, that the quality worsened from the category 1 ('best isolation') to the category 3 ('weak isolation'). Isolation quality of the cells was estimated by visual inspection of their clusters (see Figure 3.14A). X axis labels depict three groups of cells used in the analysis: '1' – only cells from the category 1; '1+2' – only cells from the categories 1 and 2; '1+2+3' – cells from all three categories. Horizontal lines with p-values above the median boxes show results of statistical comparisons across the groups of cells within a given genotype (Kruskal-Wallis one way analysis of variance on ranks). Asterisks above the median boxes show results of statistical comparisons across the genotypes within a given cellular group (Mann-Whitney rank sum test, *$p<0.05$; **$p<0.001$).

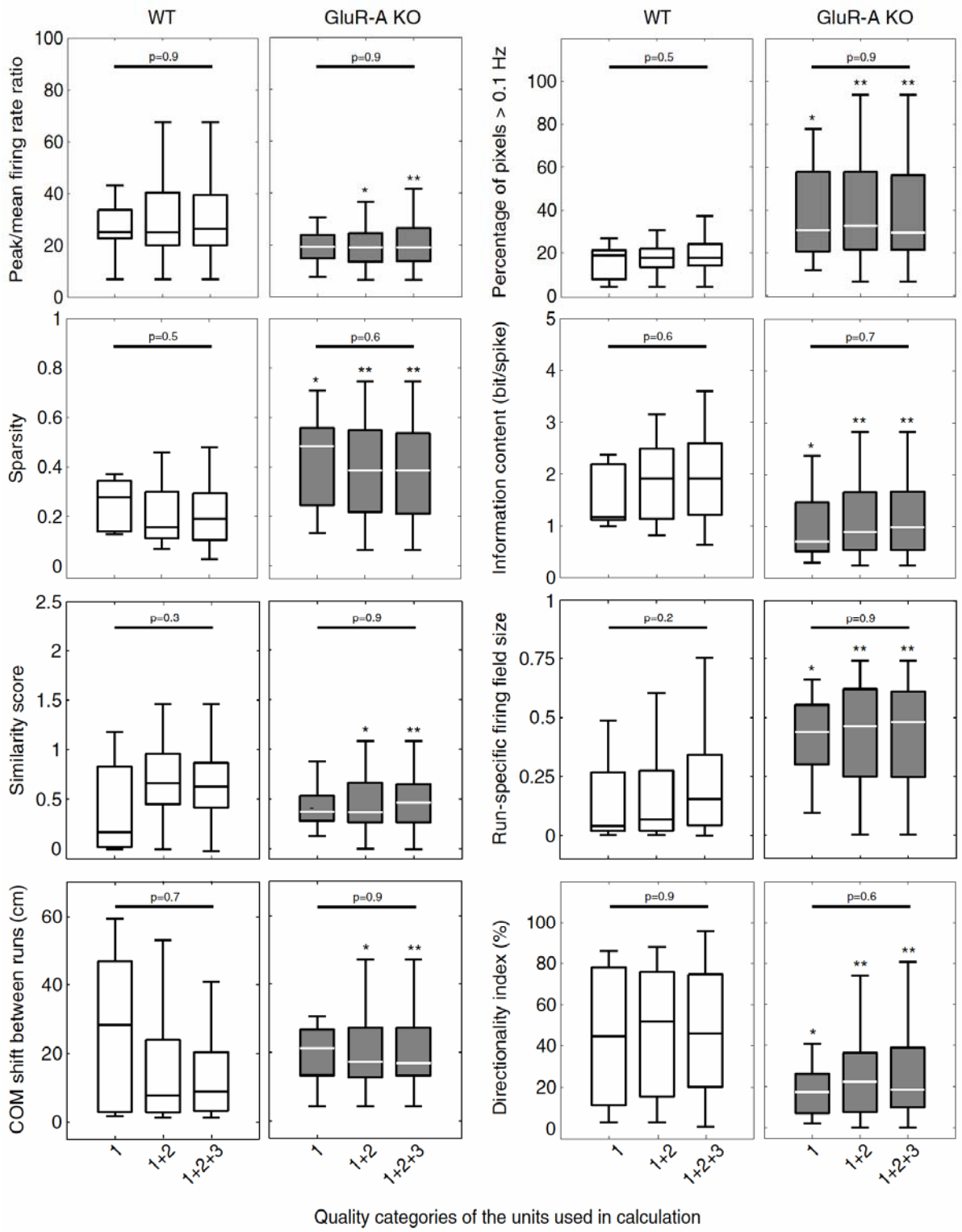
WT
GluR-A KO
WT
GluR-A KO
Peak/mean firing rate ratio
Percentage of pixels > 0.1 Hz
Sparsity
Information content (bit/spike)
Similarity score
Run-specific firing field size
COM shift between runs (cm)
Directionality index (%)
p=0.9
p=0.9
p=0.5
p=0.9
p=0.5
p=0.6
p=0.6
p=0.7
p=0.3
p=0.9
p=0.2
p=0.9
p=0.7
p=0.9
p=0.9
p=0.6
1
1+2
1+2+3
Quality categories of the units used in calculation

Figure 3.16. Change in the parameter statistics when cells of different isolation quality are analyzed (isolation quality was estimated by isolation distance).
Each horizontal pair of panels shows descriptive statistics of a certain firing parameter calculated for the cells of different isolation quality in WT (left panel within the pair, open bars) and GluR-A KO (right panel within the pair, filled bars) mice. Descriptive statistics is represented by median values (horizontal lines inside boxes), interquartile range (boxes), upper and lower limits of the values distribution. All the cells in each genotype were categorized on the basis of their isolation quality so, that the quality worsened from the category 1 ('best isolation') to the category 3 ('weak isolation'). Isolation quality of the cells was estimated by computing 'isolation distance' measure (see Figure 3.14B). X axis labels depict three groups of cells used in the analysis: '1' – only cells from the category 1; '1+2' – only cells from the categories 1 and 2; '1+2+3' – cells from all three categories. Horizontal lines with p-values above the median boxes show results of statistical comparisons across the groups of cells within a given genotype (Kruskal-Wallis one way analysis of variance on ranks). Asterisks above the median boxes show results of statistical comparisons across the genotypes within a given cellular group (Mann-Whitney rank sum test, *$p<0.05$; **$p<0.001$).

3.3. Study of theta rhythm in CA1 on a linear track

Spatial representation of the environment has been suggested to be encoded in the hippocampus not only by the firing rate of pyramidal cell assemblies, but also by the timing of action potentials with respect to each other and to the hippocampal theta rhythm (Buzsaki and Chrobak, 1995; Konig et al., 1996; Lisman and Idiart, 1995; Mehta et al., 2002; Mehta et al., 2000; Riehle et al., 1997; Skaggs et al., 1996). If so, deficit either in theta rhythm, which is the population oscillation in 6-14 Hz range seen during locomotion in rodents (Buzsáki, 2002; Vanderwolf, 1969), or in temporal relationship between spikes and theta rhythm should lead to impaired hippocampus-dependent learning. Indeed, numerous studies have shown that disruption of the hippocampal theta correlated with deficient performance in spatial memory tasks (Givens and Olton, 1994; Markowska et al., 1995; Mizumori et al., 1990b; Pan and McNaughton, 1997; Winson, 1978). Furthermore, reduced spike timing coordination has been shown to be responsible for cannabinoid-induced spatial memory deficits (Robbe et al., 2006).

Considering the impaired spatial learning in GluR-A KO mice, I hypothesized that there might be some differences either in the hippocampal theta and/or in spike-theta synchrony between WT and GluR-A KO mice during behavior. As in the case of place cells, basic properties of theta rhythm and its interplay with neuronal firing were evaluated in the simplest paradigm - on the linear track. Figure 3.17A shows typical recordings of the hippocampal EEG in WT and GluR-A KO mice during locomotion. The rhythmic, sine-wave like pattern in each example is a typical theta oscillation, whose frequency range varies from 6 to 12 Hz. Theta properties were evaluated based on the analysis of power spectra of the EEG recordings (PSD-based analysis). A power spectrum allows us to see the relative power of the EEG signal in each frequency band. Two representative power

spectra from one recording session in both genotypes are shown in Figure 3.17B. In both groups, there is a large power peak in the range of 6–12 Hz derived from the hippocampal theta rhythm. Fitting the Gaussian function to this peak allows me to estimate the dominant theta frequency (mean of the gaussian fit) and theta peak power (peak of the gaussian fit). Theta integral power was determined as an integral of the spectrum over the range of 6-12 Hz, normalized by the total power in the 1-400 Hz range.

3.3.1. Inconsistent relationship between theta rhythm and running speed of the mice

Frequency of theta rhythm has been shown to be positively correlated with animal's speed in rats (McFarland et al., 1975; McNaughton et al., 1983a; Zhang et al., 1998). To examine the relationship between theta frequency and running speed of the mice, I applied regression and correlation analyses for each recording session. In this analysis theta frequency and animal's speed were determined every 1 s and, then, Pearson's correlation coefficient and best linear fit were computed for combined 1s-values from the entire session (Figure 3.17C). There were two food reward locations on the linear track, at which the EEG changed from predominantly theta to large irregular activity (LIA), when the mice stopped to eat (Vanderwolf et al., 1975). Therefore, to prevent the contamination of theta rhythm by LIA, the measurements when the speed was <2 cm/s were excluded from the analysis. In order to match speed ranges across the animals, the measurements when the speed was > 30 cm/s (the highest speed common for all the animals), were also eliminated. In general, the relationship between theta frequency and the speed was quiet variable across sessions and animals. Twenty-nine of 62 (47%) sessions recorded from WT mice and 21 of 41 (51%) sessions recorded from GluR-A KO mice exhibited weak, but statistically significant correlations (either positive or negative) between the speed and theta frequency ($p<0.05$). Furthermore, among the sessions with significant correlation between the speed and theta frequency, the correlation was negative in 26 of 29 (90%) sessions in WT mice and in 18 of 21 (86%) sessions in GluR-A KO mice. This means that theta frequency reduced with increased speed. This is the _opposite_ of what has been reported in the literature. How can that be? The relationship between theta power and running speed of the mice was also examined, using the same EEG and regression analysis. Fifty of 62 (81%) sessions recorded from WT mice and 28 of 41 (68%) sessions recorded from GluR-A KO mice exhibited statistically significant correlations (either

positive or negative) between the speed and theta power ($p<0.05$). Furthermore, among the sessions with significant correlation between the speed and theta power, the correlation was negative in 29 of 50 (58%) sessions in WT mice and only in 3 of 28 (11%) sessions in GluR-A KO mice. This too is opposite of published literature. To avoid complexities in the further analysis due to the ambiguous theta - speed relationship found in the mice, intercepts of the corresponding regression lines in a given session were used as a mean theta frequency and mean theta power in the session (Figure 3.17C, black circles on the Y axes). The intercepts reflected values of the theta parameters without the influence of any movement.

You should restrict the above anlysis to only the middle of the track where the mouse runs reliably, and then restrict to only those data where he was running above 20cm/s to see if theta frequency and power as a function of speed. Data from goal locations and when the mouse sits are contaminated by head movement artifacts that give spuriously large speeds. Same for the following section.

3.3.2. Slightly reduced frequency of theta rhythm in GluR-A KO mice

The mean frequency, peak power and integral power of theta rhythm during running on the linear track were compared between WT and GluR-A KO mice (Figure 3.18). As the mean theta frequency in a given session, the intercept of the corresponding regression line in that session was taken. These intercept values were averaged over all sessions for each animal, then, over all animals to obtain the mean frequency for each genotype. The mean peak power and mean integral power of theta rhythm were determined and averaged in the same way. Frequency of theta rhythm was slightly, but significantly lower in GluR-A KO (8.0 ± 0.1 Hz, mean ± SEM) than in WT (8.4 ± 0.1 Hz, mean ± SEM) mice ($p=0.036$, Student's t test) (Figure 3.18A). There was no significant difference in either theta peak power (WT: 0.33 ± 0.02; KO: 0.40 ± 0.03; mean ± SEM; $p=0.09$, Student's t test) (Figure 3.18B) or theta integral power (WT: 0.72 ± 0.05; KO: 0.79 ± 0.04; mean ± SEM; $p=0.27$, Student's t test) (Figure 3.18C) between WT and GluR-A KO mice. Notably, both peak power and integral power of theta rhythm were quite variable between individual mice of both genotypes, presumably because the power is sensitive to the exact location of the EEG electrode (Buzsáki, 2002). As a consequence of such variability, the statistical powers of the performed tests (0.25 and 0.08) were below the desired level of 0.8, indicating that the genotype-related differences in theta power could not be detected

with 7 animals in each group although such differences may existed. The power analysis has shown that in order to detect a difference of 0.1 in mean theta power with significance level 5% and observed variability in the data, Student's t test would require 17-21 animals in each genotype group.

As an additional control, the frequency and amplitude of theta rhythm were estimated also by a so called oscillation-based method. In this method occurrences of theta oscillation in the band-pass (6-12 Hz) filtered EEG recordings were detected, so that theta properties could be determined directly from the period and amplitude of the oscillation cycles. Theta frequency was defined as the inverse of the time between successive peaks of the filtered EEG. Theta amplitude was defined as the height of the peaks of the filtered EEG to the baseline (μV) and was equivalent to the theta power used in the power spectrum-based analysis. These parameters were averaged, first, over all cycles within a single theta occurrence, then over all theta occurrences within a single session, then over all sessions within a given animal, and, finally, over all animals to obtain the mean values for each genotype. Oscillation-based analysis found no significant difference in either theta frequency (WT: 8.24 ± 0.04 Hz; KO: 8.13 ± 0.05 Hz; mean ± SEM; p=0.2, Student's t test) (Figure 3.18D) or theta amplitude (WT: 106 ± 6 μV; KO: 97 ± 4 μV; mean ± SEM; p=0.3, Student's t test) (Figure 3.18E) between WT and GluR-A KO mice. Similar to the power spectrum-based analysis, the statistical powers of the performed tests (0.2 and 0.06) were below the desired level of 0.8, indicating that the genotype-related differences could be not detected with 7 animals in each group even when they actually existed. As mentioned above, restrict the analysis to place and time when the mouse runs reliably to see if there are any remaining differences in theta on cycle by cycle basis.

Thus, frequency of theta rhythm was somewhat (~5%) reduced in GluR-A KO mice compared to WT mice. No difference in theta power was found with the size of animal groups (n=7) used in this study.

3.3.3. Depth of theta modulation of cell firing is not altered in GluR-A KO mice

Considering the negligible difference in the frequency of hippocampal theta rhythm between the genotypes, it was of interest to examine the temporal relationship between theta and spiking of CA1 pyramidal cells. The temporal analysis was performed for EEG recorded locally from the same tetrode with which the spiking activity of the cells of interests was recorded. The pyramidal cells which have shown a marked rhythmicity at 6–

12 Hz were classified as theta-modulated. Figure 3.19A shows a representative EEG trace, along with the simultaneously recorded action potentials of one theta-modulated pyramidal cell. As can be seen, spikes of this cell occurred preferentially around the trough of the theta oscillation. Such structured neuronal firing is termed common 'phase locked' to a certain phase ('preferred phase') of the ongoing theta oscillation.

A conventional way to visualize the depth of theta modulation of a cell is to calculate its temporal autocorrelation histogram (autocorrelogram). Averaged autocorrelograms for the pyramidal cells from WT and GluR-A KO mice are shown in Figure 3.19B. Characteristic peaks in the 83-166 ms bin range reflect periodicity in the firing of the cells at 6-12 Hz, corresponding to the theta rhythm. Depth of the firing modulation was quantified using a theta modulation index (TMI), derived from the autocorrelogram. The TMI was computed as the difference between the theta modulation trough (defined as mean of autocorrelogram bins, 50–71 ms) and the theta modulation peak (mean of autocorrelogram bins, 83–166 ms) over their sum. Figure 3.19C shows distributions and mean TMI values for WT and GluR-A KO mice. The majority of the pyramidal cells from both WT and GluR-A KO animals were modulated by the ongoing theta rhythm. No significant difference was found in the theta modulation depth, measured by TMI, between WT (0.08 ± 0.02, mean ± SEM) and GluR-A KO (0.13 ± 0.03, mean ± SEM) mice ($p=0.2$, Student's t test).

3.3.4. Cell firing in WT and GluR-A KO mice is locked to the same theta phase

Considering theta modulated activity of the pyramidal cells in both genotypes, I examined further whether the cells in WT and GluR-A KO mice were locked to the same phase of the ongoing theta rhythm. A theta phase value from 0 to 359° was assigned to each spike that occurred during EEG epochs showing clear theta. Intuitively, if the firing of a given neuron is independent of the theta rhythm, the distribution of its phase values will be random and uniformly distributed throughout the cycle (0-360°) (Figure 3.20A, left panel). Conversely, if the firing of a given neuron is phase locked to the theta rhythm, its phase distribution will be unimodal and centered on a certain phase of the cycle (Figure 3.20A, right panel). Theta phase distribution for each cell was tested for uniformity, using the Rayleigh test ($p<0.05$). Approximately 44% (33 of 75) of the CA1 pyramidal cells in WT and 67% (39 of 58) of the cells in GluR-A KO mice were significantly phase locked to the hippocampal theta rhythm. A more detailed relationship between theta activity and cell

firing was studied quantitatively in two different, but complementary ways. First, discharge probability vs. theta phase histograms were calculated and averaged across neurons. In this calculation method all recorded cells contributed to the overall average histogram, independent from whether the cell was phase locked or not (Figure 3.20B). The histogram revealed that the average theta phase distributions of spikes for WT and GluR-A KO pyramidal cells were similar. Fitting the distributions with a cosine function has shown that the discharge probability of the WT cells reached its maximum at ~60°, while that of the GluR-A KO cells at ~100°, corresponding to a ~14 ms delay in latency of action potential in respect to theta cycle. Secondly, the 'preferred' phase of the theta cycle for a given neuron was determined quantitatively and the preferred phase values for all the cells were displayed in a histogram (Figure 3.20C). For this histograms only cells which were significantly phase locked ($p<0.05$, Rayleigh test) were included. There was no significant difference in the 'preferred' theta phase between WT (67 ± 14°, circular mean ± SEM) and GluR-A KO (102° ± 10°, circular mean ± SEM) cells ($p=0.7$, test for the equality of circular means). Thus, most of the CA1 pyramidal cells in both genotypes had preferred phases on the falling edge of the theta cycle (Figure 3.20B,C), as it has been previously reported (Buzsáki, 2002). Does this work when you restrict the data to spikes within place cells, away from goal locations when the mouse is running above 20cm/s?

As in case of place cells, a number of additional controls were done. Neither theta modulation depth nor mean 'preferred' theta phase changed significantly when the WT cells with high (> 20 Hz) peak firing rate were eliminated or when stricter criteria for unit selection were applied (data not shown). No difference in the parameter values was found also for the opposite running directions (data not shown).

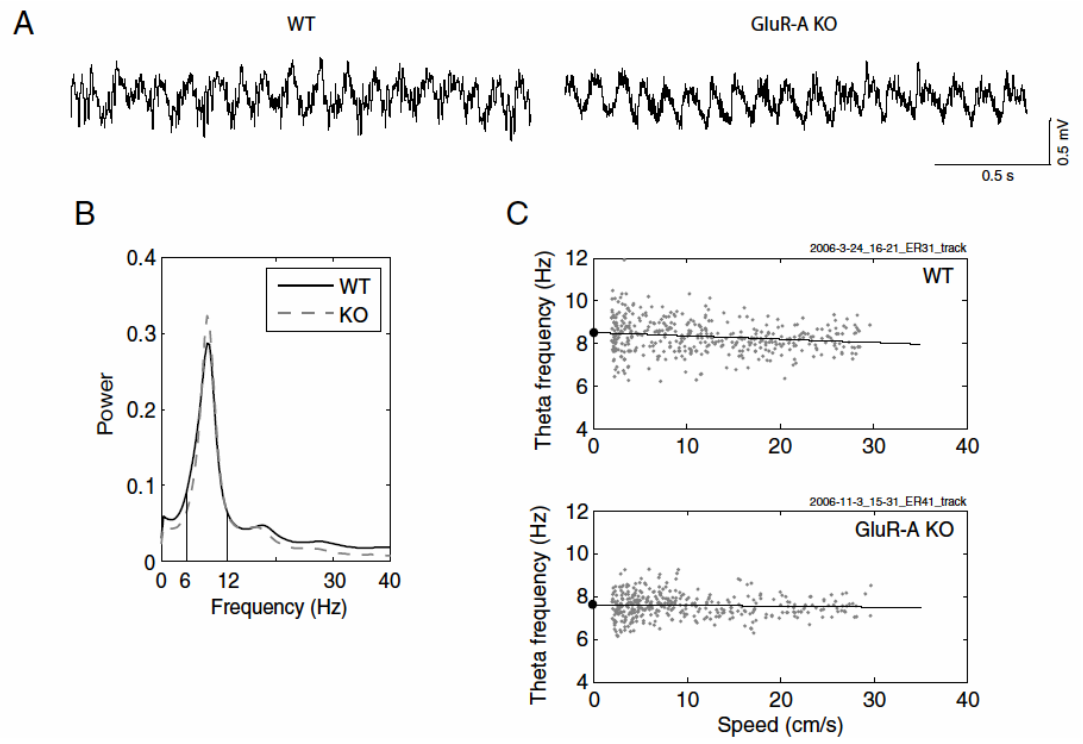

Figure 3.17. Comparative analysis of theta rhythm in WT and GluR-A KO mice.
A) Typical recordings of the hippocampal EEG from a WT (left trace) and a GluR-A KO (right trace) mouse during running on the linear track. The rhythmic, sine-like pattern in each example is a typical theta oscillation, whose frequency range varies from 6 to 12 Hz. B) Typical power spectra of the hippocampal EEG from a WT (black solid line) and a GluR-A KO (gray dashed line) mouse during running on the linear track. The power of each frequency was normalized to the power over 1 - 400 Hz. In both groups, there is a large power in the range of 6–12 Hz derived from the hippocampal theta rhythm. C) Two representative examples, one from a WT mouse, the other from a GluR-A KO mouse, for the regression analysis of the relationship between theta frequency and running speed in a single recording session. Low-speed data (<2 cm/s) were excluded to prevent contamination of results with nontheta mode EEG (LIA). High-speed data (> 30 cm/s) were also excluded to match speed ranges across the animals. An intercept of the regression line (black circles on the Y axes) in a given session was used as a mean theta frequency in the session, reflecting the theta frequency without the influence of any movement.

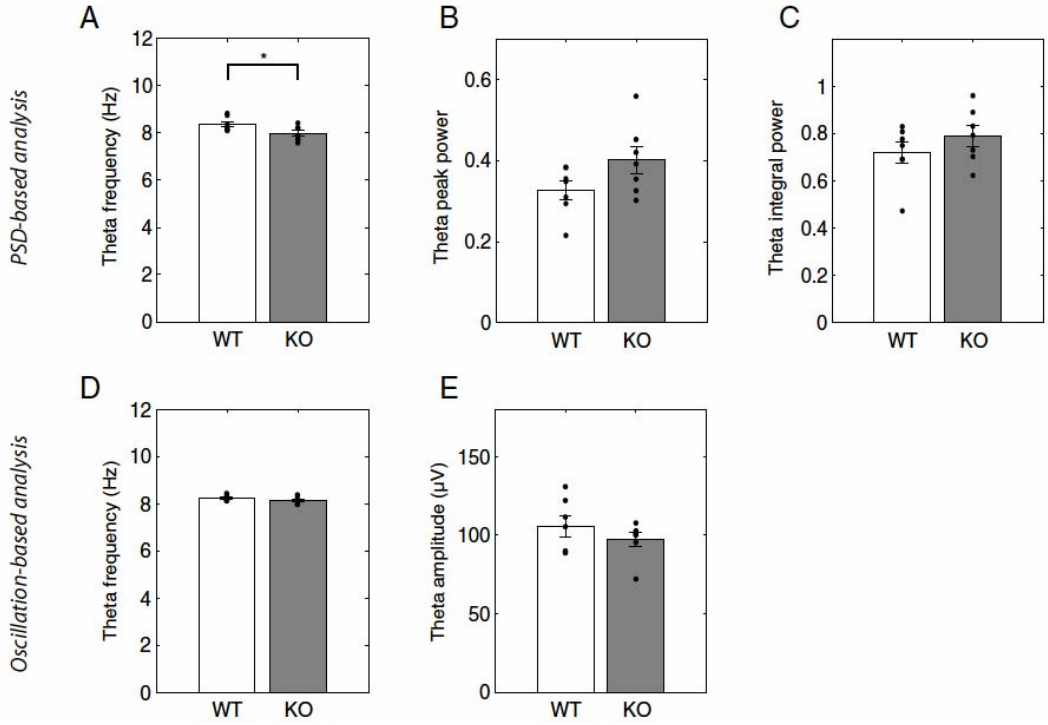

Figure 3.18. Comparison of theta rhythm properties between WT and GluR-A KO mice.
Two complementary methods were used to evaluate properties of theta rhythm: power spectrum (PSD)-based (A,B,C) and oscillation-based methods (D,E). The same data from 7 WT and 7 GluR-A KO mice were used to compute frequency (A), peak power (B) and integral power (C) of the theta rhythm by the PSD-based method and frequency (D) and amplitude (E) of the theta rhythm by the oscillation-based method. Data are represented as mean±SEM. Each black dot depicts a parameter value from one animal. Statistical evaluation was done by a Student's *t* test (*p=0.036). Note that peak power, integral power and amplitude of the theta rhythm were quiet variable between individual mice of both genotypes, presumably because of the fact that they are sensitive to the exact location of the EEG electrode. As a consequence of the across-animals variability in the theta power and theta amplitude values, the statistical power of the performed tests (0.06 - 0.25) was below the desired level of 0.8, indicating that the genotype-related differences could be not detected with 7 animals in each group even when they actually existed. Thus, no difference in theta power or theta amplitude was found with the size of animal groups (n=7) used in this study. Frequency of the theta rhythm was somewhat (~5%) reduced in GluR-A KO mice compared to WT mice as determined by the PSD-based method.

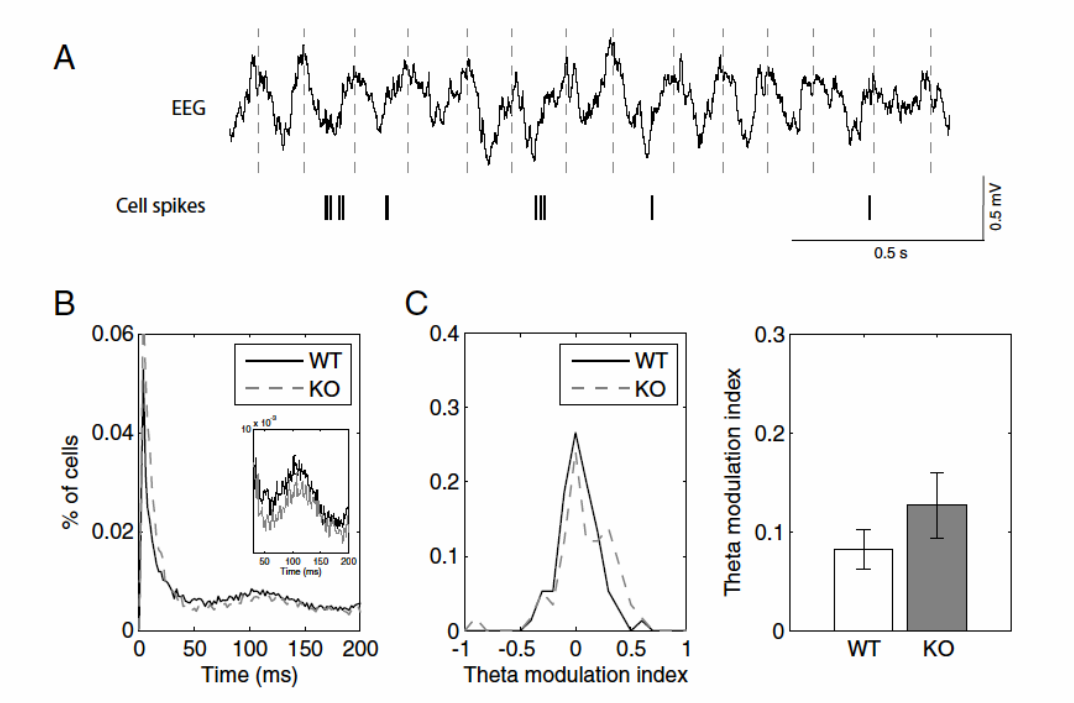

Figure 3.19. Similar theta modulation of cell firing in WT and GluR-A KO mice.
A) Simultaneously recorded EEG from the CA1 pyramidal layer and the spike activity of one pyramidal cell (ticks). Dashed vertical lines depict positive peaks of theta waves. B) Average autocorrelation histograms for the WT and GluR-A KO cells. Insert shows the same histograms, but zoomed in. Characteristic peaks in the 83-166 ms range reflect periodicity in the firing of the cells at 6-12 Hz, corresponding to the theta rhythm. Depth of theta modulation of cell firing was quantified using a theta modulation index (TMI), derived from the autocorrelogram. C) Distributions of the TMI values (left panel) and their means (right panel) for the WT (black solid line, n=75) and GluR-A KO (gray dashed line, n=58) pyramidal cells. Data are represented as mean±SEM. Statistical evaluation was done by a Student's *t* test ($p<0.05$). The pyramidal cells in WT and GluR-A KO mice had similar depth of theta modulation.

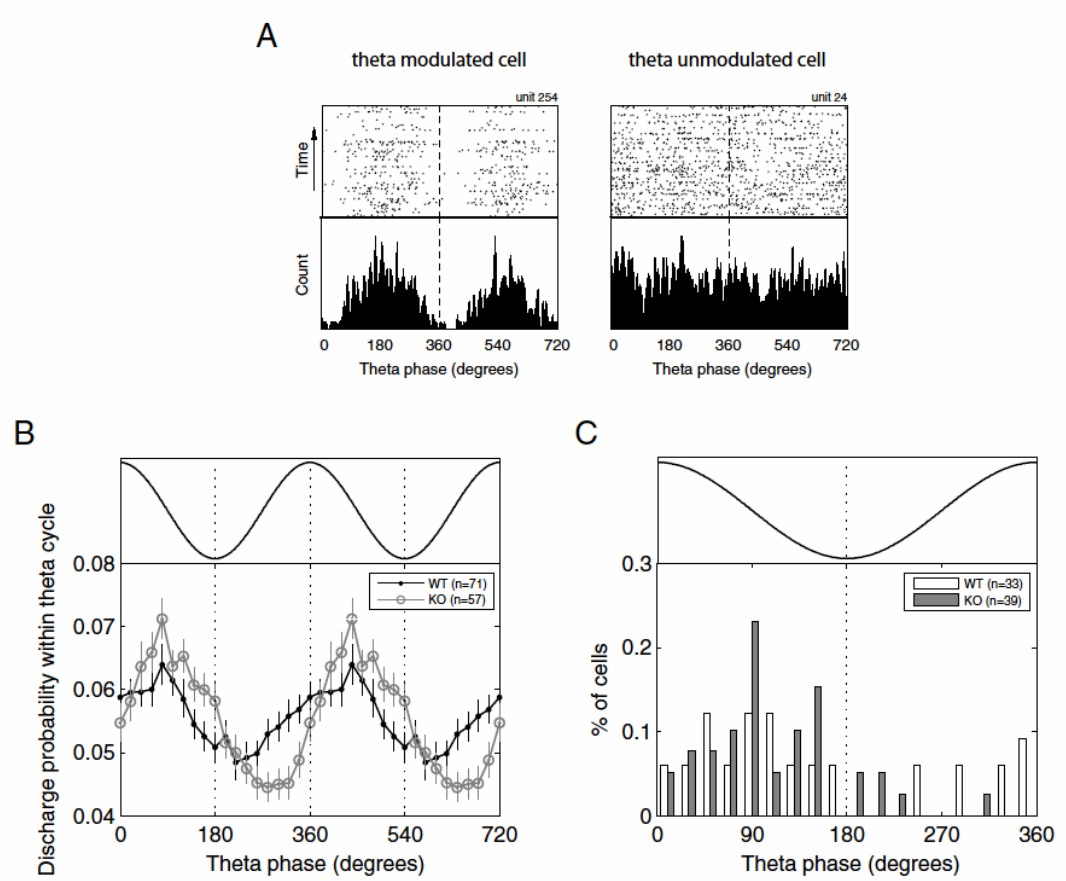

Figure 3.20. Cell firing in WT and GluR-A KO mice is locked to the same theta phase
A) Examples of different phase locking to the hippocampal theta rhythm for two CA1 pyramidal cells. The spike trains of individual cells were broken up at the peaks of the hippocampal theta rhythm and the resulting segments were stacked up to form the theta-triggered rasters shown on top. Below are the corresponding phase value distributions. B) Discharge probability of the pyramidal cells during the theta cycle. Two theta cycles are shown to facilitate the phase vs. cell-discharge comparison. Hypothetical theta oscillation is shown on top. Zero phase was assigned to a positive peak of locally recorded theta waves. Note the similar probability of discharge of the WT (black line with dots) and GluR-A KO (gray line with circles) cells. Fitting the distributions with a cosine function has shown that the discharge probability of the WT cells reached its maximum at ~60°, while that of the GluR-A KO cells at ~100°, corresponding to a ~14 ms delay in latency of action potential in respect to theta cycle. C) Distributions of the preferred theta phase for the WT (open bars) and GluR-A KO (gray bars) cells. The preferred phase of a given cell was determined by averaging of phase values across all spikes of the cell. Only neurons with significant phase modulation are shown ($p<0.05$, Rayleigh test). There was no significant difference in the preferred theta phase between WT (67 ± 14°, circular mean ± SEM) and GluR-A KO (102° ± 10°, circular mean ± SEM) cells (test for the equality of circular means, $p=0.7$).

3.4. Impaired place-specific activity of the GluR-A KO pyramidal cells in an open field

In general, an open field is the enclosure where the animal can freely run and explore the environment. Behavior of animals in the open field is similar to that in the Morris water maze, one of the most frequently used tasks for measuring spatial reference memory in rodents, where animals learn to explore and orient themselves in the environment using extra and intramaze cues. Therefore, the open field is a conventional paradigm that correlates place cell activity of the animals with their spatial abilities. In this project open field recording was made while the mice foraged for crumbled chocolate pellets randomly scattered over a square wooden box.

I recorded activity of 89 CA1 pyramidal cells from 4 WT mice and 100 from 6 GluR-A KO mice while the animals explored the open field. Figure 3.21 shows representative trajectories of two different mice recorded during food-motivated running in the open field (20-30 min/session). In a novel environment, rodents display thigmotaxis and preferentially explore the area close to the walls (Save et al., 1992). Such exploration pattern was observed also in GluR-A KO mice as seen in the Figure 3.21 (right panel) where the mouse has left the middle part of the environment unvisited, i.e. undersampled. Undersampling of a particular area in the environment results in the lack of information about firing of the cell in that area, which in turn can be misinterpreted as an absence of the firing. To overcome this problem I applied an additional criterion for selection of the recording sessions: the area visited by the animal during the recording session must be ≥ 80% of the total open field area. Only 25 pyramidal cells in WT mice and 21 pyramidal cells in GluR-A KO mice met the cell selection criteria (well isolated cluster, ≥150 spikes, mean firing rate > 0.1 Hz) together with the sampling criterion.

The impaired place-specific firing of the GluR-A KO pyramidal cells observed on the linear track was also impaired in the open field. Difference in spatial firing patterns can be seen in Figure 3.22, on which a firing rate map for each of the representative 5 WT (B) and 5 GluR-A KO (D) cells recorded in the open field are shown. In contrast to the WT cells, the GluR-A KO cells revealed diffused firing fields with multiple peaks. Among the selected cells, 2 WT and 3 GluR-A KO cells were recorded in both the linear track and the open field paradigms. Although these numbers of cells do not allow us to make a general conclusion, the spatial firing patterns of these 2 WT and 3 GluR-A KO cells were maintained across different environments. In both paradigms WT cells formed compact

place fields, while the GluR-A KO cells showed rather diffuse firing patterns. The firing rate maps of these 2 WT cells on the linear track are shown in Figures 3.4 (units 292 and 285) and those in the open field – in Figure 3.22 (units 350 and 344, corresponding to units 292 and 285 recorded on the linear track). The firing rate maps of the 3 GluR-A KO cells on the linear track are shown in Figures 3.4 (units 254, 406 and 407) and those in the open field – in Figure 3.22 (units 234, 592 and 593, corresponding to units 254, 406 and 407 recorded on the linear track).

To quantify the properties of the firing fields in the open field I used the same parameters as for the linear track (Table 3.1). Selectivity (measured by a peak/mean firing rate ratio) and size (measured by a percentage of pixels > 0.1 Hz) of the firing fields in the open field were not significantly altered in the GluR-A KO animals compared to the WT animals. Genotype-related differences in the other firing field properties were similar to those found on the linear track: the pyramidal cells in GluR-A KO mice showed less selective, broader and less stable firing fields in the open field (Table 3.1).

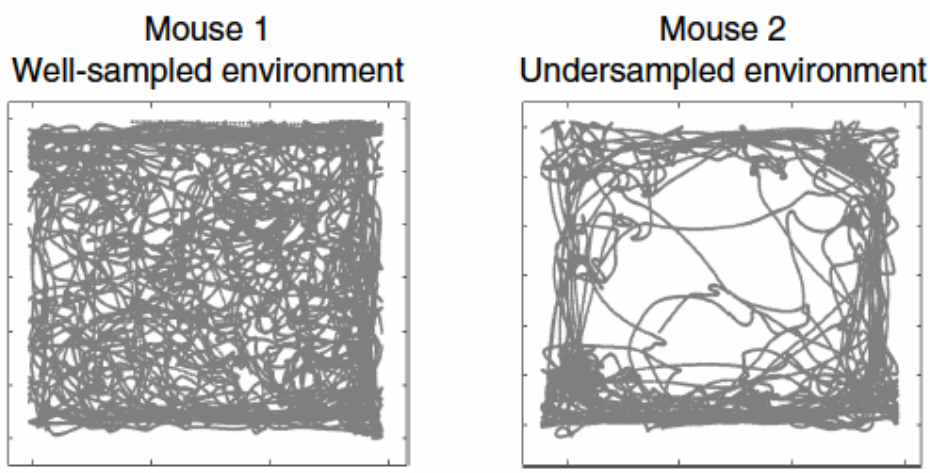

Figure 3.21. Examples of the mouse's trajectory in an open field.
Representative trajectories of two mice during food-motivated running in a square enclosure (open field), demonstrating different fraction of the environment visited by the animals over the same time period (20-30 min). Undersampling of a particular area in the environment results in the lack of information about firing of the cell in that area, which, in turn, can be misinterpreted as an absence of the firing. Only recording sessions in which the animal has visited ≥ 80% of the total open field area were used in the analysis.

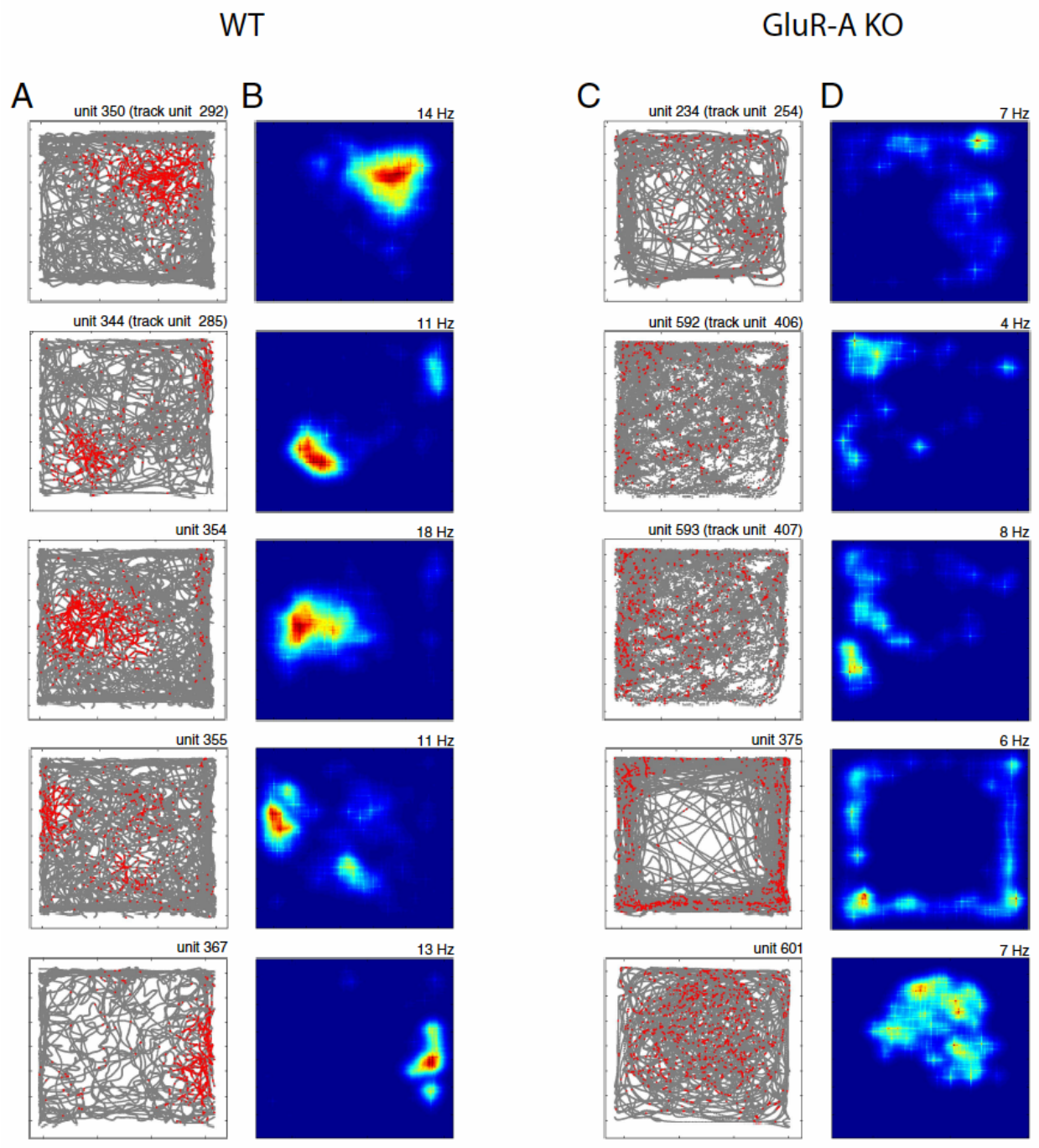

Figure 3.22. Impaired place-specific activity of the GluR-A KO cells in an open field
Data from WT mice are shown in the left two columns (A,B) and data from the GluR-A KO mice - in the right two columns (C,D). Different rows show data from different cells recorded in different sessions and tetrodes. A) Spikes (red) from single cells superimposed on the mouse's trajectories (gray) during food-motivated running in an open field. B) Firing rate of the neurons in (A) as a function of the animal's position in the open field (top-down view). Red indicates maximum firing rates, which are different for each cell and shown in the upper right corners, and dark blue indicates no firing. C,D) Similar data as (A,B), but from GluR-A KO mice. By visual inspection, it is clear that activity of the CA1 pyramidal cells in GluR-A KO mice is more diffuse than that in WT mice.

3.5. Impaired place-specific activity of the GluR-A KO pyramidal cells in a T-maze

The T-maze alternation task is a behavioral paradigm which has originally revealed a profound spatial working memory impairment in GluR-A KO mice (Reisel et al., 2002). Therefore, it was of particular interest to examine place cell properties while the animals were performing the T-maze task. I recorded activity of 45 CA1 pyramidal cells from 2 WT mice and 73 from 4 GluR-A KO mice while the animals performed the alternation task in the T-maze. Among these neurons, only 26 pyramidal cells in WT mice and 41 pyramidal cells in GluR-A KO mice met the cell selection criteria (well isolated cluster, ≥100 spikes, mean firing rate > 0.1 Hz), and the analysis was performed only on these cells. Figure 3.23A shows a representative trajectory of the mouse recorded during running in the maze. Asymptotic performance level that the WT and GluR-A KO mice have reached to the beginning of recording is represented in Figure 3.23B. Mean percent correct responses of the WT mice (81 ± 2, n=2, mean±SEM) was significantly higher than that of the GluR-A KO mice (52 ± 4, n=4, mean±SEM), as reported previously (Reisel et al., 2002). The impaired place-specific firing of the GluR-A KO pyramidal cells observed on the linear track was also preserved in the T-maze. Difference in spatial firing patterns can be seen in Figure 3.24, on which a firing rate map for each of the representative 6 WT (A) and 6 GluR-A KO (B) cells recorded in the T-maze is shown. In contrast to the WT cells, the GluR-A KO cells revealed diffused firing fields with multiple peaks. The quantified properties of the firing fields in the T-maze are shown in Table 3.2. Genotype-related differences in the properties of the T-maze firing fields were similar to those of the linear track firing fields (Table 3.1). Moreover, for some parameters the discrepancy between WT and GluR-A KO mice was essentially larger compared to the linear track: 10 versus 2 times difference in sparsity; 3 versus 1.2 times difference in similarity score; 6 versus 2 times difference in information content.

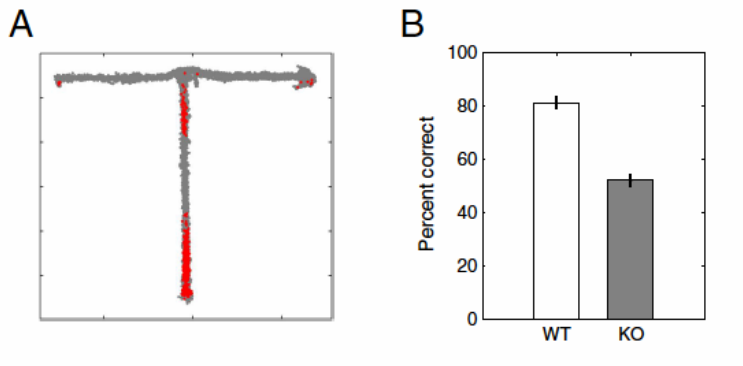

Figure 3.23. Example of the mouse's trajectory in a T-maze
A) Locations of spikes from one cell (red) are superimposed on the mouse's trajectory (gray) while it performed the T-maze alternation task. B) Asymptotic performance level in the T-maze task that the WT (n=2) and GluR-A KO (n=4) mice have reached at the moment of the recording start (mean±SEM). It is seen that GluR-A KO mice are impaired on a spatial working memory task in the T-maze.

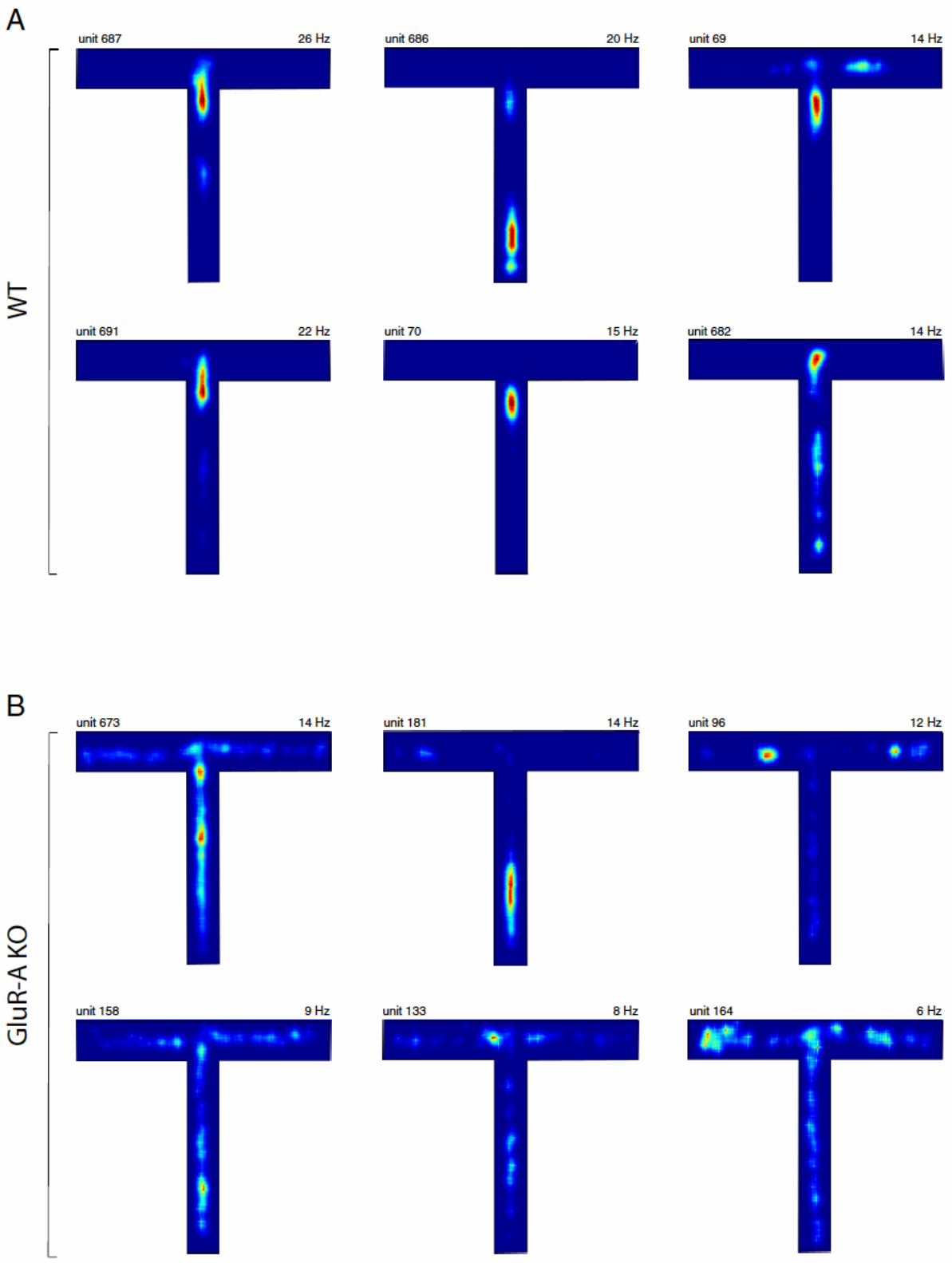
A
WT
unit 687
26 Hz
unit 686
20 Hz
unit 69
14 Hz
unit 691
22 Hz
unit 70
15 Hz
unit 682
14 Hz
B
GluR-A KO
unit 673
14 Hz
unit 181
14 Hz
unit 96
12 Hz
unit 158
9 Hz
unit 133
8 Hz
unit 164
6 Hz

Figure 3.24. Impaired place-specific activity of the GluR-A KO cells in a T-maze
Data from WT mice are shown in the upper two rows (A) and data from the GluR-A KO mice - in the bttom two rows (B). Firing rate of the neurons is represented as a function of the animal's position on the T-maze (top-down view). Red indicates maximum firing rates, which are different for each cell and shown in the upper right corners, and dark blue indicates no firing. By visual inspection, it is clear that activity of the CA1 pyramidal cells in GluR-A KO mice is more diffuse than that in WT mice.

3.6. Context-related differences in the firing field properties

Different behavioral paradigms used in the study provided the animals with a different context, the combination of the background cues making up the environment and cognitive demands of the paradigm (Jeffery et al., 2004; Mizumori et al., 1999). Changes in the animal's context, in turn, have been shown to evoke various alterations in the activity of the CA1 place cells (Lever et al., 2002; Mizumori et al., 1999; Shapiro et al., 1997; Skaggs and McNaughton, 1998; Tanila et al., 1997b). To examine how discrete changes in the environmental context influenced the activity of CA1 place cells, I compared properties of the firing fields for the cells from both genotypes across the used behavioral paradigms: linear track, open field and T-maze (Table 3.2).

Mean firing rate of the pyramidal cells from both genotypes was significantly different across the paradigms: 0.90 ± 0.04 Hz (n=133) on the linear track, 0.57 ± 0.07 Hz (n=46) in the open field and 0.31 ± 0.06 Hz (n=67) in the T-maze ($p \leq 0.003$, 2-way ANOVA and Holm-Sidak test for post hoc pairwise comparisons). Similarly, peak firing rate of the cells was significantly different across the paradigms: 12.2 ± 0.5 Hz on the linear track, 6.7 ± 0.9 Hz in the open field and 9.6 ± 0.8 Hz in the T-maze ($p \leq 0.013$, 2-way ANOVA and Holm-Sidak test). The firing rate of CA1 pyramidal cells was shown to correlate positively with the animal's running speed (Czurkó et al., 1999; Ekstrom et al., 2001; Huxter et al., 2003; McNaughton et al., 1983a). Hence, the differences in the firing rates across the paradigms can be, at least partly, attributed to the corresponding differences in running speed of the WT and GluR-A KO animals: 19 ± 2 cm/s (n=14) on the linear track, 8.3 ± 0.4 cm/s (n=10) in the open field and 20 ± 3 cm/s (n=6) in the T-maze ($p<0.001$, 1-way ANOVA on ranks). Significant differences in the animals speed were found between the linear track and open field ($p<0.001$, post hoc Holm-Sidak test) and between the T-maze and open field ($p<0.001$, post hoc Holm-Sidak test), but not between the linear track and T-maze ($p=0.3$, post hoc Holm-Sidak test).

Spatial selectivity of the firing fields (as measured by the peak/mean firing rate ratio) was maximal in the T-maze (38 ± 2, n=67) and minimal in the open field (14 ± 3, n=46) ($p \leq 0.0011$, 2-way ANOVA and Holm-Sidak test).

Size of the firing fields (as measured by the percentage of pixels >0.1 Hz) was minimal in the T-maze (25 ± 2%, n=67) and maximal in the open field (52 ± 2%, n=46) suggesting that the size of the CA1 receptive fields changes with the environment. Significant differences in the field size were also found between the open field and linear track ($p<0.001$, post hoc Holm-Sidak test) and the open field and T-maze ($p<0.001$, post hoc Holm-Sidak test). In contrast, sparsity of the firing fields was similar across the behavioral tasks: 0.29 ± 0.01 (n=133) on the linear track, 0.33 ± 0.03 (n=46) in the open field and 0.26 ± 0.02 (n=67) in the T-maze ($p=0.16$, 2-way ANOVA) supporting the conclusion that the shape but not the size of the place fields is hard-wired and does not depend on the immediate environment of the animal.

Stability of the firing fields (as measured by the similarity score) was significantly higher in the T-maze (0.96 ± 0.05, n=67) than in the open field (0.56 ± 0.05, n=46) and linear track (0.56 ± 0.03, n=133) ($p<0.001$, 2-way ANOVA and Holm-Sidak test). No statistical difference was found in the stability between the open field and linear track ($p=0.98$, Holm-Sidak test).

Despite the lack of stability of firing fields in the open field relative to those in the T-maze, the place fields preserved their coherence in this environment (2.60 ± 0.05, n=46). Coherence of the firing fields was maximal in the T-maze (2.73 ± 0.04, n=67) and minimal on the linear track (1.98 ± 0.03, n=133) ($p \leq 0.038$, 2-way ANOVA and Holm-Sidak test).

Location specificity of the pyramidal cell firing (as measured by the information content) also changed across the environments. Information content of the firing fields was maximal in the T-maze (2.3 ± 0.1, n=67) and minimal in the open field (1.4 ± 0.1, n=46) ($p<0.001$, 2-way ANOVA and Holm-Sidak test). No statistical difference was found in the information content between the open field and linear track ($p=0.16$, Holm-Sidak test).

Table 3.1. Spatial firing properties of CA1 pyramidal cells in WT and GluR-A KO mice in different behavioral paradigms

	Linear track			Open field			T-maze		
	WT (n = 75)	GluR-A KO (n = 58)	*p*	WT (n = 25)	GluR-A KO (n = 21)	*p*	WT (n = 26)	GluR-A KO (n = 41)	*p*
Mean firing rate (Hz)	0.8 (0.5 - 1.1)	0.7 (0.5 - 1.3)	0.7	0.4 (0.3 - 0.9)	0.4 (0.2 - 0.6)	0.2	0.3 (0.3 - 0.4)	0.2 (0.2 - 0.3)	0.9
Peak firing rate (Hz)	12 (8 - 17)	10 (7 - 13)	0.001*	7 (4 - 13)	4 (3 - 7)	0.03*	12 (10 - 16)	6 (4 - 7)	<0.001*
Peak/mean firing rate ratio	26 (20 - 39)	19 (14 - 26)	<0.001*	14 (11 - 17)	11 (9 - 14)	0.1	42 (34 - 56)	22 (18 - 30)	<0.001*
Percentage of pixels > 0.1	18 (14 - 24)	29 (21 - 56)	<0.001*	46 (29 - 72)	56 (38 - 68)	0.3	18 (11 - 23)	30 (21 - 39)	<0.001*
Sparsity	0.2 (0.1 - 0.3)	0.4 (0.2 - 0.5)	<0.001*	0.2 (0.2 - 0.3)	0.4 (0.3 - 0.6)	<0.001*	0.04 (0.03 - 0.07)	0.4 (0.2 - 0.6)	<0.001*
Similarity score	0.6 (0.4 - 0.9)	0.5 (0.3 - 0.7)	0.007*	0.9 (0.5 - 1.14)	0.3 (0.1 - 0.4)	<0.001*	0.9 (0.5 - 1.14)	0.3 (0.1 - 0.4)	<0.001*
Coherence	2.1 (1.9 - 2.3)	1.8 (1.7 - 2.0)	<0.001*	2.9 (2.5 - 3.2)	2.4 (2.2 - 2.5)	<0.001*	3.1 (3.0 - 3.3)	2.4 (2.2 - 2.5)	<0.001*
Information content (bit/spike)	1.9 (1.2 - 2.6)	0.9 (0.5 - 1.7)	<0.001*	1.7 (1.3 - 2.1)	0.9 (0.5 - 1.2)	<0.001*	4 (3 - 5)	0.7 (0.4 - 1.5)	<0.001*

Please refer to the methods section for the detailed description of the parameters studied. Data are represented as median (interquartile range). Statistical evaluation was done either by a Mann-Whitney rank sum test or by a Student's *t* test as appropriate (*statistically significant effect).

Table 3.2. Spatial firing properties of CA1 pyramidal cells in both genotypes in different behavioral paradigms

	Linear track (n=133)	Open field (n=46)	T-maze (n=67)	*p*
Mean firing rate (Hz)	0.90 ± 0.04	0.57 ± 0.07	0.31 ± 0.06	<0.001*
Peak firing rate (Hz)	12.2 ± 0.5	6.7 ± 0.9	9.6 ± 0.8	<0.001*
Peak/mean firing rate ratio	29 ± 2	14 ± 3	38 ± 2	<0.001*
Percentage of pixels > 0.1 Hz (%)	29 ± 1	52 ± 2	25 ± 2	<0.001*
Sparsity	0.29 ± 0.01	0.33 ± 0.03	0.26 ± 0.02	0.16
Similarity score	0.56 ± 0.03	0.56 ± 0.05	0.96 ± 0.05	<0.001*
Coherence	1.98 ± 0.03	2.60 ± 0.05	2.73 ± 0.04	<0.001*
Information content (bit/spike)	1.6 ± 0.1	1.4 ± 0.1	2.3 ± 0.1	<0.001*

Please refer to the methods section for the detailed description of the parameters studied. Data are represented as mean±SEM. Statistical evaluation was done by a 2-way ANOVA (*statistically significant effect).

4. DISCUSSION

Genetically modified mice lacking GluR-A-containing AMPAR are deficient in a tetanus-induced hippocampal CA3-CA1 LTP and have also reduced AMPAR-mediated somatic (10-fold) and synaptic (2-fold) currents (Andrasfalvy et al., 2003; Jensen et al., 2003; Zamanillo et al., 1999). These mice exhibit normal spatial reference memory performance but, at the same time, show a dramatic spatial working memory impairment as tested in a variety of the behavioral tasks (Reisel et al., 2002; Schmitt et al., 2004; Schmitt et al., 2003; Schmitt et al., 2005; Zamanillo et al., 1999). The ability of the animals to learn these spatial tasks strongly requires an intact hippocampus (Deacon et al., 2002; Morris et al., 1982; Rawlins and Olton, 1982), a brain region which is believed to be primarily involved in generating a neural representation of the immediate environment by means of spatially restricted activity of pyramidal neurons known as place cells (O'Keefe and Nadel, 1978). Firing rate of the place cells and timing of their action potentials with respect to the hippocampal theta rhythm are hypothesized to be the variables used to encode the environment (Buzsaki and Chrobak, 1995; Konig et al., 1996; Lisman and Idiart, 1995; Riehle et al., 1997; Skaggs et al., 1996). Considering the spatial working memory deficit in the GluR-A KO mice and the presumed role of hippocampal activity in establishing a cognitive representation of the space across time, it could be hypothesized that the behavioral deficits observed following GluR-A deletion might be due to altered place representation in the hippocampus. Therefore the current study addressed how representation of space by hippocampal CA1 place cells is modified following GluR-A deletion. Towards this goal the activity of place cells was analyzed in several behavioral paradigms with different complexity (linear track, T-maze and open field).

4.1. Impaired place fields without AMPAR-mediated synaptic plasticity

Under all the behavioral conditions examined in this study, spatial firing patterns of the place cells in the GluR-A KO mice differed from those of the place cells in WT mice. Specifically, after GluR-A deletion, place cells have become less selective to a particular location and were significantly larger. The irregular structure of the place fields following GluR-A deletion was accompanied by the loss of directional selectivity in a linear environment and lack of stability within a recording session (20-30 min). The spatial specificity of the most GluR-A KO pyramidal cells was so weak that it was hard to think of them as true place cells. The impaired place field representation in the CA1 region of

the mice lacking GluR-A-containing AMPARs clearly indicates the essential role of the AMPAR-mediated synaptic plasticity and synaptic transmission in the place field formation.

CA1 pyramidal cells receive synaptic input mainly from CA3 and layer III of the entorhinal cortex (ECIII). In principle, there might be two possible explanation for the defects in spatial firing of the GluR-A KO CA1 place cells: (1) CA1 place cells can not integrate properly the information coming from the upstream structures (CA3 and ECIII); and/or (2) CA1 place cells just relay results of the improper information processing in those upstream structures. Given that deletion of the GluR-A gene is not hippocampus-specific (Zamanillo et al., 1999), there is no reason to believe that the deficit in spatial representation is restricted to the CA1 pyramidal cells. It can be already impaired in the entorhinal cortex or/and CA3 region. Additional experiments are needed in order to locate the neural circuit underlying such impairments in spatial representation.

If the deficiency of GluR-A KO place fields was not due to loci upstream to the CA1 how could the observed changes in place field have arisen? Potentially, both the abolished LTP (Zamanillo et al., 1999) and the reduced basal AMPAR-mediated transmission in CA3-CA1 synapses (Andrasfalvy et al., 2003; Jensen et al., 2003) can contribute to the place field deficit in GluR-A KO mice. To illustrate one possible mechanism, I have constructed a simple model of the CA3 network connected to a single postsynaptic CA1 cell via direct excitatory afferents and via interneurons that provide feed-forward inhibition of the CA1 cell (Figure 4.1). For simplicity input from ECIII was not considered. In general, this basic model can be applied to any neuronal network connected via excitatory and inhibitory afferents to the CA1 cell. The model was based on two assumptions: (1) place fields in CA3 are intact; (2) The discharge rate of the CA1 cell at any given position depends on the balanced excitatory and inhibitory inputs to the cell at that position. Therefore, I took one possible configuration of the synaptic inputs to the WT CA1 cell which would shape its place field. In this configuration the connections between the CA3 cells 1 and 3 and the CA1 cell were dominated by inhibition, while the connection between the CA3 cell 2 and the CA1 cell - by excitation. Such connection pattern can arise in WT animals as a result of experience-induced plastic changes in CA3-CA1 synapses (Dragoi et al., 2003; Kentros et al., 1998). In this model, successive activation of the CA3 place cells as the animal moves through a region of space would lead to a spatially specific firing of the CA1 place cell. In GluR-A KO mice the proper configuration of the synaptic

connections is disrupted due to impaired long-term potentiation in the CA3-CA1 synapses and reduced AMPAR-mediated excitability of the interneurons and the CA1 cell (Figure 4.1, left). The CA3 cells 1 and 3 lose their dominating inhibiting effect, while the CA3 cell 2 – its excitatory effect on the CA1 neuron. As a result of such disorganized synaptic input, the GluR-A KO CA1 cell spontaneously generates spikes over the entire environment, forming a diffuse firing field.

Recently it has been shown, that despite the lack of tetanus-induced CA3-CA1 LTP in GluR-A KO mice, slowly developing (over 20-40 min) long-lasting synaptic potentiation could still be evoked by a modified induction protocol (Hoffman et al., 2002). In principle, this GluR-A-independent form of LTP can also contribute to shaping of place fields in the CA1. If so, in both genotypes one could expect to observe firing fields, which are more diffuse at the beginning of the session, but get sharper over the time required for LTP to develop. However, no improvement in the place field quality was detected in the current study at least over a single recording session (20-30 min). Thus, the contribution of the GluR-A-independent form of LTP to the formation of place fields in CA1 seems to be negligible.

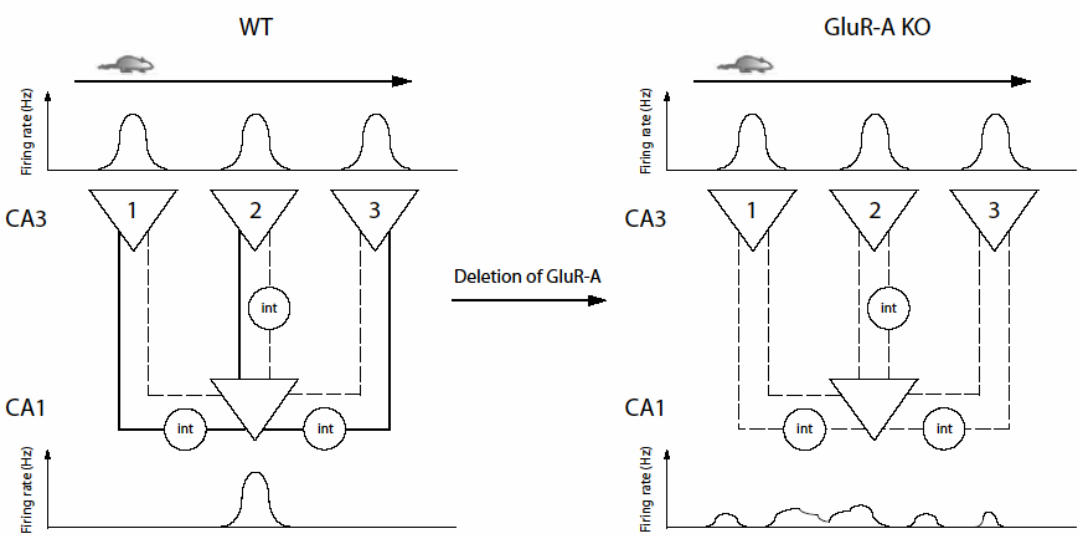

Figure 4.1. Basic two-layer model of CA3-CA1 connections, illustrating possible mechanism of CA1 place field deficit in GluR-A KO mice.
Three CA3 pyramidal cells (upper triangles) are connected to a single postsynaptic CA1 cell (bottom triangle) via direct excitatory afferents and via interneurons (circles) that provide feed-forward inhibition of the CA1 cell. Triangles depict pyramidal cells, while circles – interneurons. Solid lines depict strong synaptic input, while dashed lines – weak synaptic input. For simplicity, input from the entorhinal cortex was not considered. Place fields of the CA3 cells were assumed to be intact. Left) In WT mice configuration of the synaptic inputs to the CA1 cell shapes its place field as the mouse moves through the environment: the connections between CA3 cells 1 and 3 and the CA1 cell were dominated by inhibition, while the connection between CA3 cell 2 and the CA1 cell - by excitation. Right) In GluR-A KO mice the proper configuration of the synaptic connections is disrupted due to impaired long-term plasticity in CA3-CA1 synapses and reduced AMPAR-mediated excitability of the interneurons and the CA1 cell. As a result of the disorganized synaptic input, the GluR-A KO CA1 cell spontaneously generates spikes over the entire environment, forming a diffuse firing field.

Another mechanism which can potentially mediate impaired place-specific firing of CA1 place cells in GluR-A KO mice is related with the recent discovery that a large subpopulation of CA1 interneurons possess location-specific firing fields, which are similar to the fields of pyramidal cells (Ego-Stengel and Wilson, 2006; Wilent and Nitz, 2007). It was hypothesized, that a spatially modulated inhibitory and/or disinhibitory output of the local interneurons may directly shape the place-specific firing fields of principal neurons in the CA1. If so, GluR-A KO interneurons with elevated excitation threshold would show a smaller variation in their firing rates, which, in turn, would reduces the strength of spatial modulation of CA1 pyramidal cells.

4.2. Link between the impaired place fields, impaired working and intact spatial reference memories

How can the impaired place fields in the CA1 region of GluR-A KO mice be linked to the behavioral deficits reported for these animals? In a recent study, Reisel *et al.*(2005) have demonstrated that GluR-A KO mice exhibit impaired working memory not only in spatial (Reisel et al., 2002; Schmitt et al., 2003), but also in the non-spatial domain. The pattern of impaired working but spared reference memory performance in GluR-A KO mice suggested the existence of two distinct information processing mechanisms which may co-exist within the hippocampus: (1) a mechanism that encodes the spatial (where) as well as temporal (when) context of an event or episode and (2) a separate, independent mechanism for encoding information about spatial locations that is relevant across many trials. This hypothesis is in agreement with other evidences coming from lesion studies, that the hippocampus is important for the encoding of spatial as well as non-spatial information (Fortin et al., 2002; Kesner et al., 2002). Furthermore, the existence of such information processing mechanisms was supported by the results of Leutgeb et al. (2005) who have shown that the same hippocampal place cells may simultaneously represent spatial (where an animal is located) and episodic (what is currently present in that location) information.

Within this framework, the data obtained in the present study suggest some conclusions: (1) Although in the present study no place cell recording was done while the animals performed a spatial reference memory task, the consistent dysfunction of the place cells across several behavioral paradigms (linear track, open field, T-maze) allows to assume that this dysfunction is, in principle, invariant in respect to the context and

cognitive demands of the task; (2) The lack of correlation between spatial reference memory performance and CA1 place field quality in GluR-A KO mice indicates that the animals do not require place fields in CA1 for successful navigation. To my knowledge, the current study is the first study on mutant mice reporting preserved spatial reference memory (as studied in Morris water maze) despite the disrupted place fields in the CA1.

Previous data from different laboratories indicate that hippocampal place fields are highly sensitive to the animal's context, even when the context is defined by abstract task demands rather than the spatial geometry of the environment (Kentros, 2006; Smith and Mizumori, 2006). On the basis of these findings, it was proposed that place fields reflect a more general context processing in hippocampus, which involves many kinds of information and resembles an episodic memory. In line with this viewpoint, our experiments revealed that the profound deficit in both spatial (Reisel et al., 2002; Schmitt et al., 2003) and temporal (Reisel et al., 2005) aspects of the working memory was accompanied by disrupted CA1 place fields in GluR-A KO mice. This finding is one more evidence challenging the cognitive map theory, which suggests a purely spatial function for the hippocampal place cells (O'Keefe and Nadel, 1978). The defects in place cell activity observed in the GluR-A KO mice have features that might allow to account for the behavioral deficits. Pyramidal cells that form very dispersed place fields without a true salient peak could generate inaccurate representation of the animal's context which is relayed further to the downstream brain structures. Furthermore, a lack of stability in place representations over short time intervals might indicate that the GluR-A KO animals are not able to maintain the stored representation of the current context, which is necessary for developing a task solving strategy, especially in working memory paradigms. However, it can not be excluded that the defects in spatial and/or temporal encoding of the spatial context found in GluR-A KO mice might also arise via some other mechanisms, not directly related with the deficient place cells in CA1. In a recent study, for example, Young and McNaughton (2000) have demonstrated that the activity of a considerable proportion of CA1 pyramidal cells in rats was correlated with temporal aspects of the differential reinforcement of low rates (DRL) task, the task which has earlier revealed non-spatial working memory impairment in GluR-A KO mice (Reisel et al., 2005). Therefore, it is also possible that working memory deficit in GluR-A KO mice is related with impaired temporal rather than spatial control over the firing of CA1 neurons.

Other genetically modified mice (Cho et al., 1998; McHugh et al., 1996; Rotenberg et al., 2000; Rotenberg et al., 1996) with impaired performance in spatial reference memory tasks have shown smaller alterations in the properties of place fields as compared to GluR-A KO animals. Considering the results of the current study, I propose that the behavioral deficit found in those mice, although correlating with quality of the place fields, is likely to arise via another, place field-independent, mechanism. It would be interesting to examine, in future experiments, whether smaller place field defects in those mice are associated with correspondingly smaller working memory impairment.

4.3. Context-related differences in the place field properties

I found that quality of the place fields, quantified by a number of parameters, was different between the behavioral paradigms (Table 3.2). In general, the most compact, selective and stable place fields were observed while the animals performed the T-maze alternation task. The place fields on the linear track showed intermediate characteristics, while those in the open field possessed the minimal selectivity and the largest size across all the paradigms studied. In fact, it is not surprising that different behavioral contexts alter activity of the CA1 place cells differently (Lever et al., 2002; Mizumori et al., 1999; Shapiro et al., 1997; Skaggs and McNaughton, 1998; Tanila et al., 1997b). For example, the larger (~2 times) place fields in the open field relative to those on the linear track or T-maze could be explained by the known correlation between place field size and dimensions of the environment where this field is observed (Muller and Kubie, 1987; O'Keefe and Burgess, 1996). However, the geometric factor can not account for the change in the other place field properties. Recently it has been shown that the firing patterns of hippocampal neurons undergo an attentional modulation (Kentros et al., 2004; McEchron and Disterhoft, 1999; Olypher et al., 2002). For example, the place cells of rats actively performing a spatial task appeared to be more spatially selective than those recorded from rats that are randomly foraging in the same environment (Zinyuk et al., 2000). Consistent with these results, I hypothesized that the better place field representation in the T-maze could be due to necessity for the animals to pay essentially more attention to their immediate context in order to successfully perform the task.

4.4. Theta rhythm and phase-locking without AMPAR-mediated synaptic plasticity

In the current study I have shown that elimination of AMPAR-mediated fast synaptic excitation does not alter the depth of theta modulation, temporal relationship between spiking of CA1 cells and theta cycles, although the lack of GluR-A containing AMPARs slightly (~5%) reduces the average theta frequency.

It has long been suggested that the hippocampal theta rhythm is driven by two theta-frequency inputs on CA1 pyramidal cells - a proximal (perisomatic) inhibitory input and a distal (dendritic) excitatory input (Buzsaki et al., 1983). The proximal inhibitory input is provided by a rhythmic discharge of the basket and chandelier interneurons (Fox, 1989; Kamondi et al., 1998; Leung and Yim, 1986; Ylinen et al., 1995b). These interneurons are driven by GABAergic and cholinergic inputs from the medial septum (Freund and Buzsaki, 1996). The distal excitatory input on the CA1 pyramidal cells is provided by dendritic excitation of the cells by the perforant pathway from the entorhinal cortex and also drives the theta rhythms in CA1 (Brankack et al., 1993; Buzsaki and Eidelberg, 1982; Buzsaki et al., 1983; Leung, 1998). CA1 theta may also be driven, perhaps to a smaller degree, by an independent pacemaker in CA3 as shown by *in vitro* experiments (Fischer et al., 2002; Konopacki et al., 1987; MacVicar and Tse, 1989; Sik et al., 1995). What are knockout-related alterations in these theta-generating pathways that might explain the slight reduction in the theta frequency found in the GluR-A KO mice? Considering that the entorhinal input to CA1 is mediated mostly by NMDAR (Colbert and Levy, 1992; Otmakhova and Lisman, 2000), deletion of AMPAR-mediated component in EPSPs would have a minimal effect on it. Furthermore, any change in AMPAR-mediated transmission should not affect the rhythmic activity of GABAergic interneurons in CA1, which are driven by GABAergic and cholinergic afferents from the medial septum. In contrast, the CA3 region as a circuit that strongly depends on recurrent excitation or inhibition should be sensitive to AMPAR deletion. If so, defects in CA3 together with the impaired CA3-CA1 transmission (Jensen et al., 2003) would abolish the theta drive coming from CA3. This suggestion is consistent with the *in vitro* experiments, which have shown that intrinsic generation of theta rhythm in CA3 was blocked by CNQX, a competitive AMPAR antagonist (Fellous and Sejnowski, 2000; but see also Leung and Shen, 2004; Williams and Kauer, 1997). A small magnitude (5%) of the reduction in theta frequency found in GluR-A KO mice might reflect a minor contribution of CA3 theta generator under the

experimental conditions used. Similarly, multiple studies have led to the hypothesis that a major part of the extracellular currents underlying theta oscillation derive from rhythmic excitation of the distal dendrites by the entorhinal input (Brankack et al., 1993; Buzsaki et al., 1986; Buzsaki et al., 1983; Lopes da Silva et al., 1990; Winson, 1974; Ylinen et al., 1995b).

Pyramidal cell firing is determined by the interaction between the convergent dendritic excitatory inputs and the rhythmic oscillatory hyperpolarizing forces at the perisomatic region provided by theta (Kamondi et al., 1998). Assuming a stochastic synaptic input, pyramidal cells can be discharged with the least amount of excitation during the negative phase of field theta in the pyramidal layer (i.e., when the soma is least hyperpolarized) (Kamondi et al., 1998). This might explain why the peak discharge of the CA1 pyramidal cells is phase-locked to the negative peak of the local theta in rats (Buzsáki, 2002; Buzsaki et al., 1983; Csicsvari et al., 1999; Fox et al., 1986). In the present study I have confirmed results of the previous report (Buzsáki et al., 2003), and showed that in WT mice most CA1 pyramidal cells discharge on the negative phase of local theta waves. The difference in precise phase value between two species may be related with distinct species-specific features of theta oscillation (e.g. theta amplitude is notably higher in mice, Buzsáki et al., 2003) or/and distinct excitatory input to the dendrites of CA1 pyramidal cells. Stronger depolarization due to dendritic excitation may discharge the cell at an earlier phase of the clock signal and vice versa (Buzsaki and Chrobak, 1995; Hopfield, 1995; Kamondi et al., 1998). This also explains my observation that peak in discharge probability of the GluR-A KO cells was ~14 ms delayed (although it was not statistically significant) in respect to theta cycle compared to that of the WT cells. Reduced excitatory input into CA1 pyramidal cells due to disrupted AMPAR-mediated synaptic transmission resulted in a small shift of the 'preferred' theta phase from 67° in the WT mice to 102° in the GluR-A KO mice.

5. CONCLUSIONS

1. Place-specific activity of the CA1 pyramidal cells was significantly impaired in the GluR-A KO mice. The pyramidal cells in the GluR-A KO mice formed firing fields, that were: significantly larger (160-200%), less spatially selective (73%), less direction selective (39%), less stable (53%) and carried less information about the animal's position (47%) than those in wild-type mice, across all the behavioral paradigms studied.

2. The defects in the properties of the GluR-A KO place fields were consistent across different behavioral paradigms (linear track, open field, T-maze) independent from their spatial complexity.

3. In both genotypes CA1 pyramidal cells formed more compact and selective place fields when the mice performed spatial T-maze alternation task, than when they ran on the linear track and in the open field.

4. Frequency, but not amplitude of the hippocampal theta rhythm was slightly, but significantly reduced (5%) in the GluR-A KO mice relative to that in WT mice. Depth of theta modulation of the CA1 pyramidal cells was not altered in the GluR-A KO mice. Temporal relationship between spikes of the CA1 pyramidal cells and the theta rhythm was not altered in the GluR-A KO mice. Most of the CA1 pyramidal cells in both genotypes had preferred phases on the falling edge of the theta cycle.

5. These results demonstrate that GluR-A-dependent tetanus-induced LTP in the CA3-CA1 synapses is necessary for the proper place-specific activity of place cells in the CA1 region of the mouse hippocampus.

6. The lack of correlation between spatial reference memory performance and CA1 place field quality in GluR-A KO mice indicates that the animals do not require place fields in CA1 for successful navigation.

6. REFERENCE LIST

Abel, T., Nguyen, P.V., Barad, M., Deuel, T.A., Kandel, E.R., and Bourtchouladze, R. (1997). Genetic demonstration of a role for PKA in the late phase of LTP and in hippocampus-based long-term memory. Cell *88*, 615-626.

Abraham, W.C., Mason-Parker, S.E., Williams, J., and Dragunow, M. (1995). Analysis of the decremental nature of LTP in the dentate gyrus. Brain Res Mol Brain Res *30*, 367–372.

Adey, W.R., Dunlop, C.W., and Hendrix, C.E. (1960). Hippocampal slow waves. Distribution and phase relationships in the course of approach learning. Arch Neurol *3*, 74-90.

Agnihotri, N.T., Hawkins, R.D., Kandel, E.R., and Kentros, C. (2004). The long-term stability of new hippocampal place fields requires new protein synthesis. Proc Natl Acad Sci U S A *101*, 3656-3661.

Andrasfalvy, B.K., Smith, M.A., Borchardt, T., Sprengel, R., and Magee, J.C. (2003). Impaired regulation of synaptic strength in hippocampal neurons from GluR1-deficient mice. J Physiol *552*, 35-45.

Ascher, P., and Nowak, L. (1986). A patch-clamp study of excitatory amino acid activated channels. . Adv Exp Med Biol *203*, 507–511.

Bagal, A.A., Kao, J.P., Tang, C.M., and Thompson, S.M. (2005). Long-term potentiation of exogenous glutamate responses at single dendritic spines. Proc Natl Acad Sci U S A *102*, 14434-14439.

Bannerman, D.M., Deacon, R.M.J., Brady, S., Bruce, A., Sprengel, R., Seeburg, P.H., and Rawlins, J.N.P. (2004). A comparison of GluR-A-deficient and wild-type mice on a test battery assessing sensorimotor, affective, and cognitive behaviors. Behav Neurosci *118*, 643-647.

Bannerman, D.M., Good, M.A., Butcher, S.P., Ramsay, M., and Morris, R.G. (1995). Distinct components of spatial learning revealed by prior training and NMDA receptor blockade. Nature *378*, 182-186.

Barnes, C.A. (1979). Memory deficits associated with senescence: a neurophysiological and behavioral study in the rat. J Comp Physiol Psychol *93*, 74-104.

Barnes, C.A., Jung, M.W., McNaughton, B.L., Korol, D.L., Andreasson, K., and Worley, P.F. (1994). LTP saturation and spatial learning disruption: effects of task variables and saturation levels. J Neurosci *14*, 5793-5806.

Barnes, C.A., McNaughton, B.L., Mizumori, S.J., Leonard, B.W., and Lin, L.H. (1990). Comparison of spatial and temporal characteristics of neuronal activity in sequential stages of hippocampal processing. Prog Brain Res *83*, 287-300.

Barnes, C.A., Suster, M.S., Shen, J., and McNaughton, B.L. (1997). Multistability of cognitive maps in the hippocampus of old rats. Nature *388*, 272-275.

Barria, A., Muller, D., Derkach, V., Griffith, L.C., and Soderling, T.R. (1997). Regulatory phosphorylation of AMPA-type glutamate receptors by CaM-KII during long-term potentiation. Science *276*, 2042-2045.

Battaglia, F.P., and Treves, A. (1998). Attractor neural networks storing multiple space representations: A model for hippocampal place fields. . Phys Rev E *58*, 7738–7753.

Berger, H. (1929). Über das Elektroenkephalogramm des Menschen., Vol 87.

Berry, S.D., and Thompson, R.F. (1978). Prediction of learning rate from the hippocampal electroencephalogram. Science *200*, 1298-1300.

Best, P.J., White, A.M., and Minai, A. (2001). Spatial processing in the brain: the activity of hippocampal place cells. Annu Rev Neurosci *24*, 459-486.

Bland, B.H. (1986). The physiology and pharmacology of hippocampal formation theta rhythms. Prog Neurobiol *26*, 1-54.

Bland, B.H., and Oddie, S.D. (2001). Theta band oscillation and synchrony in the hippocampal formation and associated structures: the case for its role in sensorimotor integration. Behav Brain Res *127*, 119-136.

Bliss, T.V. (1996). LTP and spatial learning. J Physiol Paris *90*, 335.

Bliss, T.V.P., and Collinridge, G.L. (1993). A synaptic model of memory: long-term potentiation in the hipocampus. Nature *361*, 31–39.

Bliss, T.V.P., and Lømo, T. (1973). Long-lasting potentiation of synaptic transmission in the dentate area of the anaesthetized rabbit following stimulation of the perforant path. J. Physiol (Lond) *232*, 331–356.

Bodizs, R., Kantor, S., Szabo, G., Szucs, A., Eross, L., and Halasz, P. (2001). Rhythmic hippocampal slow oscillation characterizes REM sleep in humans. Hippocampus *11*, 747-753.

Bostock, E., Muller, R.U., and Kubie, J.L. (1991). Experience-dependent modifications of hippocampal place cell firing. Hippocampus *1*, 193-205.

Bourtchuladze, R., Frenguelli, B., Blendy, J., Cioffi, D., Schutz, G., and Silva, A.J. (1994). Deficient long-term memory in mice with a targeted mutation of the cAMP-responsive element-binding protein. Cell *79*, 59-68.

Bragin, A., Jando, G., Nadasdy, Z., Hetke, J., Wise, K., and Buzsaki, G. (1995). Gamma (40-100 Hz) oscillation in the hippocampus of the behaving rat. J Neurosci *15*, 47-60.

Brankack, J., Seidenbecher, T., and Muller-Gartner, H.W. (1996). Task-relevant late positive component in rats: is it related to hippocampal theta rhythm? Hippocampus *6*, 475-482.

Brankack, J., Stewart, M., and Fox, S.E. (1993). Current source density analysis of the hippocampal theta rhythm: associated sustained potentials and candidate synaptic generators. Brain Res *615*, 310-327.

Brazhnik, E.S., Muller, R.U., and Fox, S.E. (2003). Muscarinic blockade slows and degrades the location-specific firing of hippocampal pyramidal cells. J Neurosci *23*, 611-621.

Brown, E.N., Frank, L.M., Tang, D., Quirk, M.C., and Wilson, M.A. (1998). A statistical paradigm for neural spike train decoding applied to position prediction from ensemble firing patterns of rat hippocampal place cells. J Neurosci *18*, 7411-7425.

Brun, V.H., Otnass, M.K., Molden, S., Steffenach, H.-A., Witter, M.P., Moser, M.-B., and Moser, E.I. (2002). Place cells and place recognition maintained by direct entorhinal-hippocampal circuitry. Science *296*, 2243-2246.

Bullock, T.H., Buzsaki, G., and McClune, M.C. (1990). Coherence of compound field potentials reveals discontinuities in the CA1-subiculum of the hippocampus in freely-moving rats. Neuroscience *38*, 609-619.

Buno, W., Jr., and Velluti, J.C. (1977). Relationships of hippocampal theta cycles with bar pressing during self-stimulation. Physiol Behav *19*, 615-621.

Bures, J., Fenton, A.A., Kaminsky, Y., and Zinyuk, L. (1997). Place cells and place navigation. Proc Natl Acad Sci U S A *94*, 343-350.

Buzsaki, G. (1996). The hippocampo-neocortical dialogue. Cereb Cortex *6*, 81-92.

Buzsáki, G. (1986). Hippocampal sharp waves: their origin and significance. Brain Res *398*, 242-252.

Buzsáki, G. (2002). Theta oscillations in the hippocampus. Neuron *33*, 325-340.

Buzsáki, G., Buhl, D.L., Harris, K.D., Csicsvari, J., Czéh, B., and Morozov, A. (2003). Hippocampal network patterns of activity in the mouse. Neuroscience *116*, 201-211.

Buzsaki, G., and Chrobak, J.J. (1995). Temporal structure in spatially organized neuronal ensembles: a role for interneuronal networks. Curr Opin Neurobiol *5*, 504-510.

Buzsaki, G., Czopf, J., Kondakor, I., and Kellenyi, L. (1986). Laminar distribution of hippocampal rhythmic slow activity (RSA) in the behaving rat: current-source density analysis, effects of urethane and atropine. Brain Res *365*, 125-137.

Buzsaki, G., and Eidelberg, E. (1982). Convergence of associational and commissural pathways on CA1 pyramidal cells of the rat hippocampus. Brain Res *237*, 283-295.

Buzsaki, G., Horvath, Z., Urioste, R., Hetke, J., and Wise, K. (1992). High-frequency network oscillation in the hippocampus. Science *256*, 1025-1027.

Buzsáki, G., Horvath, Z., Urioste, R., Hetke, J.F., and Wise, K.D. (1992). High-frequency network oscillation in the hippocampus. Science *256*, 1025-1027.

Buzsaki, G., Leung, L.W., and Vanderwolf, C.H. (1983). Cellular bases of hippocampal EEG in the behaving rat. Brain Res *287*, 139-171.

Cacucci, F., Lever, C., Wills, T.J., Burgess, N., and O'Keefe, J. (2004). Theta-modulated place-by-direction cells in the hippocampal formation in the rat. J Neurosci *24*, 8265-8277.

Cajal, Y.R. (1913). Histologie du Systeme Nerveux de l'Homme et des Vertebras. . Paris: Maloine.

Cammarota, M., Bernabeu, R., Izquierdo, I., and Medina, J.H. (1996). Reversible changes in hippocampal 3H-AMPA binding following inhibitory avoidance training in the rat. Neurobiol Learn Mem *66*, 85-88.

Cammarota, M., Bernabeu, R., Levi De Stein, M., Izquierdo, I., and Medina, J.H. (1998). Learning-specific, time-dependent increases in hippocampal Ca2+/calmodulin-dependent protein kinase II activity and AMPA GluR1 subunit immunoreactivity. Eur J Neurosci *10*, 2669-2676.

Cammarota, M., Izquierdo, I., Wolfman, C., Levi de Stein, M., Bernabeu, R., Jerusalinsky, D., and Medina, J.H. (1995). Inhibitory avoidance training induces rapid and selective changes in 3[H]AMPA receptor binding in the rat hippocampal formation. Neurobiol Learn Mem *64*, 257-264.

Carroll, R., Lissin, D., Von Zastrow, M., Nicoll, R., and Malenka, R. (1999). Rapid redistribution of glutamate receptors contributes to long-term depression in hippocampal cultures. Nat Neurosci *2*, 454–460.

Chapman, C.A., and Lacaille, J.C. (1999a). Cholinergic induction of theta-frequency oscillations in hippocampal inhibitory interneurons and pacing of pyramidal cell firing. J Neurosci *19*, 8637-8645.

Chapman, C.A., and Lacaille, J.C. (1999b). Intrinsic theta-frequency membrane potential oscillations in hippocampal CA1 interneurons of stratum lacunosum-moleculare. J Neurophysiol *81*, 1296-1307.

Chen, H.X., Otmakhov, N., and Lisman, J. (1999). Requirements for LTP induction by pairing in hippocampal CA1 pyramidal cells. J Neurophysiol *82*, 526-532.

Cho, Y.H., Giese, K.P., Tanila, H., Silva, A.J., and Eichenbaum, H. (1998). Abnormal hippocampal spatial representations in alphaCaMKIIT286A and CREBalphaDelta- mice. Science *279*, 867-869.

Chrobak, J.J., and Buzsáki, G. (1996). High-frequency oscillations in the output networks of the hippocampal-entorhinal axis of the freely behaving rat. J Neurosci *16*, 3056-3066.

Coan, E.J., and Collingridge, G.L. (1987). Characterization of an N-methyl-D-aspartate receptor component of synaptic transmission in rat hippocampal slices. Neuroscience *22*, 1-8.

Cohen, N.J., and Eichenbaum, H. (1993). Memory, amnesia and the hippocampal system. Cambridge, MA: MIT Press.

Colbert, C.M., and Levy, W.B. (1992). Electrophysiological and pharmacological characterization of perforant path synapses in CA1: mediation by glutamate receptors. J Neurophysiol *68*, 1-8.

Colby, C.L., and Goldberg, M.E. (1999). Space and attention in parietal cortex. Annu Rev Neurosci *22*, 319-349.

Collingridge, G.L., Isaac, J.T.R., and Wang, Y.T. (2004). Receptor trafficking and synaptic plasticity. Nat Rev Neurosci *5*, 952-962.

Collingridge, G.L., Kehl, S.J., and McLennan, H. (1983). Excitatory amino acids in synaptic transmission in the Schaffer collateral-commissural pathway of the rat hippocampus. . J Physiol *334*, 33–46.

Cooper, B.G., and Mizumori, S.J. (2001). Temporary inactivation of the retrosplenial cortex causes a transient reorganization of spatial coding in the hippocampus. J Neurosci *21*, 3986-4001.

Cressant, A., Muller, R.U., and Poucet, B. (1997). Failure of centrally placed objects to control the firing fields of hippocampal place cells. J Neurosci *17*, 2531-2542.

Cressant, A., Muller, R.U., and Poucet, B. (1999). Further study of the control of place cell firing by intra-apparatus objects. Hippocampus *9*, 423-431.

Csicsvari, J., Hirase, H., Czurko, A., Mamiya, A., and Buzsaki, G. (1999). Oscillatory coupling of hippocampal pyramidal cells and interneurons in the behaving Rat. J Neurosci *19*, 274-287.

Csicsvari, J., Jamieson, B., Wise, K.D., and Buzsaki, G. (2003). Mechanisms of gamma oscillations in the hippocampus of the behaving rat. Neuron *37*, 311-322.

Czurkó, A., Hirase, H., Csicsvari, J., and Buzsáki, G. (1999). Sustained activation of hippocampal pyramidal cells by 'space clamping' in a running wheel. Eur J Neurosci *11*, 344-352.

Davis, H.P., and Squire, L.R. (1984). Protein synthesis and memory: a review. Psychol Bull *96*, 518-559.

Deacon, R.M.J., Bannerman, D.M., Kirby, B.P., Croucher, A., and Rawlins, J.N.P. (2002). Effects of cytotoxic hippocampal lesions in mice on a cognitive test battery. Behav Brain Res *133*, 57-68.

Dement, W., and Kleitman, N. (1957). Cyclic variations in EEG during sleep and their relation to eye movements, body motility, and dreaming. Electroencephalogr Clin Neurophysiol Suppl *9*, 673-690.

Derkach, V.A., Oh, M.C., Guire, E.S., and Soderling, T.R. (2007). Regulatory mechanisms of AMPA receptors in synaptic plasticity. Nat Rev Neurosci *8*, 101-113.

Diamond, D.M., Dunwiddie, T.V., and Rose, G.M. (1988). Characteristics of hippocampal primed burst potentiation in vitro and in the awake rat. J Neurosci *8*, 4079–4088.

Dingledine, R., Borges, K., Bowie, D., and Traynelis, S.F. (1999). The glutamate receptor ion channels. Pharmacol Rev *51*, 7-61.

Dragoi, G., Harris, K.D., and Buzsáki, G. (2003). Place representation within hippocampal networks is modified by long-term potentiation. Neuron *39*, 843-853.

Ego-Stengel, V., and Wilson, M.A. (2006). Spatial selectivity and theta phase precession in CA1 interneurons. Hippocampus.

Ego-Stengel, V., and Wilson, M.A. (2007). Spatial selectivity and theta phase precession in CA1 interneurons. Hippocampus.

Eichenbaum, H., Wiener, S.I., Shapiro, M.L., and Cohen, N.J. (1989). The organization of spatial coding in the hippocampus: a study of neural ensemble activity. J Neurosci *9*, 2764-2775.

Ekstrom, A.D., Kahana, M.J., Caplan, J.B., Fields, T.A., Isham, E.A., Newman, E.L., and Fried, I. (2003). Cellular networks underlying human spatial navigation. Nature *425*, 184-188.

Ekstrom, A.D., Meltzer, J., McNaughton, B.L., and Barnes, C.A. (2001). NMDA receptor antagonism blocks experience-dependent expansion of hippocampal "place fields". Neuron *31*, 631-638.

Errington, M.L., Lynch, M.A., and Bliss, T.V. (1987). Long-term potentiation in the dentate gyrus: induction and increased glutamate release are blocked by D(-)aminophosphonovalerate. Neuroscience *20*, 279-284.

Fellous, J.M., and Sejnowski, T.J. (2000). Cholinergic induction of oscillations in the hippocampal slice in the slow (0.5-2 Hz), theta (5-12 Hz), and gamma (35-70 Hz) bands. Hippocampus *10*, 187-197.

Fischer, Y., Wittner, L., Freund, T.F., and Gahwiler, B.H. (2002). Simultaneous activation of gamma and theta network oscillations in rat hippocampal slice cultures. J Physiol *539*, 857-868.

Fisher, N.I. (1993). Statistical analysis of circular data. Cambridge: Cambridge University Press.

Forbes, W.B., and Macrides, F. (1984). Temporal matching of sensory-motor behavior and limbic theta rhythm deteriorates in aging rats. Neurobiol Aging *5*, 7-17.

Fortin, N.J., Agster, K.L., and Eichenbaum, H.B. (2002). Critical role of the hippocampus in memory for sequences of events. Nat Neurosci *5*, 458-462.

Foster, T.C., Castro, C.A., and McNaughton, B.L. (1989). Spatial selectivity of rat hippocampal neurons: dependence on preparedness for movement. Science *244*, 1580-1582.

Fox, S.E. (1989). Membrane potential and impedance changes in hippocampal pyramidal cells during theta rhythm. Exp Brain Res *77*, 283-294.

Fox, S.E., and Ranck, J.B. (1981). Electrophysiological characteristics of hippocampal complex spike cells and theta cells. Exp Brain Res *41*, 399-410.

Fox, S.E., and Ranck, J.B., Jr. (1975). Localization and anatomical identification of theta and complex spike cells in dorsal hippocampal formation of rats. Exp Neurol *49*, 299-313.

Fox, S.E., Wolfson, S., and Ranck, J.B., Jr. (1986). Hippocampal theta rhythm and the firing of neurons in walking and urethane anesthetized rats. Exp Brain Res *62*, 495-508.

Frankland, P.W., O'Brien, C., Ohno, M., Kirkwood, A., and Silva, A.J. (2001). Alpha-CaMKII-dependent plasticity in the cortex is required for permanent memory. Nature *411*, 309-313.

Freund, T.F., and Antal, M. (1988). GABA-containing neurons in the septum control inhibitory interneurons in the hippocampus. Nature *336*, 170-173.

Freund, T.F., and Buzsaki, G. (1996). Interneurons of the hippocampus. Hippocampus *6*, 347-470.

Frey, U., Krug, M., Reymann, K.G., and Matthies, H. (1988). Anisomycin, an inhibitor of protein synthesis, blocks late phases of LTP phenomena in the hippocampal CA1 region in vitro. Brain Res *452*, 57-65.

Frotscher, M., and Leranth, C. (1985). Cholinergic innervation of the rat hippocampus as revealed by choline acetyltransferase immunocytochemistry: a combined light and electron microscopic study. J Comp Neurol *239*, 237-246.

Fyhn, M., Molden, S., Witter, M.P., Moser, E.I., and Moser, M.-B. (2004). Spatial representation in the entorhinal cortex. Science *305*, 1258-1264.

Gallagher, M., and Burwell, R.D. (1989). Relationship of age-related decline across several behavioral domains. Neurobiol Aging *10*, 691-708.

Gavrilov, V.V., Wiener, S.I., and Berthoz, A. (1995). Enhanced hippocampal theta EEG during whole body rotations in awake restrained rats. Neurosci Lett *197*, 239-241.

Geiger, J.R., Melcher, T., Koh, D.S., Sakmann, B., Seeburg, P.H., Jonas, P., and Monyer, H. (1995). Relative abundance of subunit mRNAs determines gating and Ca2+ permeability of AMPA receptors in principal neurons and interneurons in rat CNS. Neuron *15*, 193-204.

Gerlai, R., Henderson, J.T., Roder, J.C., and Jia, Z. (1998). Multiple behavioral anomalies in GluR2 mutant mice exhibiting enhanced LTP. Behav Brain Res *95*, 37-45.

Giese, K.P., Fedorov, N.B., Filipkowski, R.K., and Silva, A.J. (1998). Autophosphorylation at Thr286 of the alpha calcium-calmodulin kinase II in LTP and learning. Science *279*, 870-873.

Gillies, M.J., Traub, R.D., LeBeau, F.E., Davies, C.H., Gloveli, T., Buhl, E.H., and Whittington, M.A. (2002). A model of atropine-resistant theta oscillations in rat hippocampal area CA1. J Physiol *543*, 779-793.

Givens, B. (1996). Stimulus-evoked resetting of the dentate theta rhythm: relation to working memory. Neuroreport *8*, 159-163.

Givens, B., and Olton, D.S. (1994). Local modulation of basal forebrain: effects on working and reference memory. J Neurosci *14*, 3578-3587.

Givens, B.S., and Olton, D.S. (1990). Cholinergic and GABAergic modulation of medial septal area: effect on working memory. Behav Neurosci *104*, 849-855.

Gothard, K.M., Skaggs, W.E., Moore, K.M., and McNaughton, B.L. (1996). Binding of hippocampal CA1 neural activity to multiple reference frames in a landmark-based navigation task. J Neurosci *16*, 823-835.

Gouaux, E. (2004). Structure and function of AMPA receptors. J Physiol *554*, 249-253.

Granger, R., Staubli, U., Davis, M., Perez, Y., Nilsson, L., Rogers, G.A., and Lynch, G. (1993). A drug that facilitates glutamatergic transmission reduces exploratory activity and improves performance in a learning-dependent task. Synapse *15*, 326-329.

Grastyan, E., Karmos, G., Vereczkey, L., and Kellenyi, L. (1966). The hippocampal electrical correlates of the homeostatic regulation of motivation. Electroencephalogr Clin Neurophysiol *21*, 34-53.

Grastyan, E., Lissak, K., Madarasz, I., and Donhoffer, H. (1959). Hippocampal electrical activity during the development of conditioned reflexes. Electroencephalogr Clin Neurophysiol Suppl *11*, 409-430.

Green, J.D., and Arduini, A.A. (1954). Hippocampal electrical activity in arousal. J Neurophysiol *17*, 533-557.

Greenstein, Y.J., Pavlides, C., and Winson, J. (1988a). Long-term potentiation in the dentate gyrus is preferentially induced at theta rhythm periodicity. Brain Res *438*, 331-334.

Greenstein, Y.J., Pavlides, C., and Winson, J. (1988b). Long-term potentiation in the dentate gyrus is preferentially induced at theta rhythm periodicity. . Brain Res *438*, 331–334.

Grover, L.M., and Teyler, T.J. (1990). Two components of long-term potentiation induced by different patterns of afferent activation. Nature *347*, 477-479.

Guzowski, J.F., McNaughton, B.L., Barnes, C.A., and Worley, P.F. (1999). Environment-specific expression of the immediate-early gene Arc in hippocampal neuronal ensembles. Nat Neurosci *2*, 1120-1124.

Hafting, T., Fyhn, M., Molden, S., Moser, M.B., and Moser, E.I. (2005). Microstructure of a spatial map in the entorhinal cortex. Nature *436*, 801-806.

Hajos, M., Hoffmann, W.E., Robinson, D.D., Yu, J.H., and Hajos-Korcsok, E. (2003). Norepinephrine but not serotonin reuptake inhibitors enhance theta and gamma activity of the septo-hippocampal system. Neuropsychopharmacology *28*, 857-864.

Harris, K.D., Henze, D.A., Hirase, H., Leinekugel, X., Dragoi, G., Czurko, A., and Buzsaki, G. (2002). Spike train dynamics predicts theta-related phase precession in hippocampal pyramidal cells. Nature *417*, 738-741.

Harris, K.D., Hirase, H., Leinekugel, X., Henze, D.A., and Buzsáki, G. (2001). Temporal interaction between single spikes and complex spike bursts in hippocampal pyramidal cells. Neuron *32*, 141-149.

Hasselmo, M.E. (1999). Neuromodulation: acetylcholine and memory consolidation. Trends Cogn Sci *3*, 351-359.

Hayashi, Y., Shi, S.H., Esteban, J.A., Piccini, A., Poncer, J.C., and Malinow, R. (2000). Driving AMPA receptors into synapses by LTP and CaMKII: requirement for GluR1 and PDZ domain interaction. Science *287*, 2262-2267.

Hebb, D.O. (1949). The organization of the behavior. . New York: Wiley.

Hill, A.J. (1978). First occurrence of hippocampal spatial firing in a new environment. Exp Neurol *62*, 282-297.

Hill, A.J., and Best, P.J. (1981). Effects of deafness and blindness on the spatial correlates of hippocampal unit activity in the rat. Exp Neurol *74*, 204-217.

Hoffman, D.A., Sprengel, R., and Sakmann, B. (2002). Molecular dissection of hippocampal theta-burst pairing potentiation. Proc Natl Acad Sci U S A *99*, 7740-7745.

Hölscher, C. (1999). Synaptic plasticity and learning and memory: LTP and beyond. J Neurosci Res *58*, 62–75.

Holscher, C., Anwyl, R., and Rowan, M.J. (1997). Stimulation on the positive phase of hippocampal theta rhythm induces long-term potentiation that can Be depotentiated by stimulation on the negative phase in area CA1 in vivo. J Neurosci *17*, 6470-6477.

Hopfield, J.J. (1995). Pattern recognition computation using action potential timing for stimulus representation. Nature *376*, 33-36.

Hori, E., Tabuchi, E., Matsumura, N., Tamura, R., Eifuku, S., Endo, S., Nishijo, H., and Ono, T. (2003). Representation of place by monkey hippocampal neurons in real and virtual translocation. Hippocampus *13*, 190-196.

Huang, Y.Y., Nguyen, P.V., Abel, T., and Kandel, E.R. (1996). Long-lasting forms of synaptic potentiation in the mammalian hippocampus. Learn Mem *3*, 74-85.

Huerta, P.T., and Lisman, J.E. (1993). Heightened synaptic plasticity of hippocampal CA1 neurons during a cholinergically induced rhythmic state. Nature *364*, 723-725.

Huerta, P.T., and Lisman, J.E. (1995). Bidirectional synaptic plasticity induced by a single burst during cholinergic theta oscillation in CA1 in vitro. Neuron *15*, 1053-1063.

Huxter, J., Burgess, N., and O'Keefe, J. (2003). Independent rate and temporal coding in hippocampal pyramidal cells. Nature *425*, 828-832.

Isaac, J., Nicoll, R., and Malenka, R. (1995). Evidence for silent synapses: implications for the expression of LTP. Neuron *15*, 427–434.

Jarrard, L.E., Okaichi, H., Steward, O., and Goldschmidt, R.B. (1984). On the role of hippocampal connections in the performance of place and cue tasks: comparisons with damage to hippocampus. Behav Neurosci *98*, 946-954.

Jeffery, K.J., Anderson, M.I., Hayman, R., and Chakraborty, S. (2004). A proposed architecture for the neural representation of spatial context. Neurosci Biobehav Rev *28*, 201-218.

Jeffery, K.J., Gilbert, A., Burton, S., and Strudwick, A. (2003). Preserved performance in a hippocampal-dependent spatial task despite complete place cell remapping. Hippocampus *13*, 175-189.

Jeffery, K.J., and Hayman, R. (2004). Plasticity of the hippocampal place cell representation. Rev Neurosci *15*, 309-331.

Jensen, O. (2001). Information transfer between rhythmically coupled networks: reading the hippocampal phase code. Neural Comput *13*, 2743-2761.

Jensen, O. (2005). Reading the hippocampal code by theta phase-locking. Trends Cogn Sci *9*, 551-553.

Jensen, O., and Lisman, J.E. (2000). Position reconstruction from an ensemble of hippocampal place cells: contribution of theta phase coding. J Neurophysiol *83*, 2602-2609.

Jensen, V., Kaiser, K.M., Borchardt, T., Adelmann, G., Rozov, A., Burnashev, N., Brix, C., Frotscher, M., Andersen, P., Hvalby, O., *et al.* (2003). A juvenile form of postsynaptic hippocampal long-term potentiation in mice deficient for the AMPA receptor subunit GluR-A. J Physiol *553*, 843-856.

Jerusalinsky, D., Ferreira, M.B., Walz, R., Da Silva, R.C., Bianchin, M., Ruschel, A.C., Zanatta, M.S., Medina, J.H., and Izquierdo, I. (1992). Amnesia by post-training infusion of glutamate receptor antagonists into the amygdala, hippocampus, and entorhinal cortex. Behav Neural Biol *58*, 76-80.

Jia, Z., Agopyan, N., Miu, P., Xiong, Z., Henderson, J., Gerlai, R., Taverna, F.A., Velumian, A., MacDonald, J., Carlen, P., *et al.* (1996). Enhanced LTP in mice deficient in the AMPA receptor GluR2. Neuron *17*, 945-956.

Jonas, P., and Burnashev, N. (1995). Molecular mechanisms controlling calcium entry through AMPA-type glutamate receptor channels. Neuron *15*, 987-990.

Jouvet, M. (1969). Biogenic amines and the states of sleep. Science *163*, 32-41.

Jung, M.W., and McNaughton, B.L. (1993). Spatial selectivity of unit activity in the hippocampal granular layer. Hippocampus *3*, 165-182.

Kahana, M.J., Seelig, D., and Madsen, J.R. (2001). Theta returns. Curr Opin Neurobiol *11*, 739-744.

Kamondi, A., Acsády, L., Wang, X.J., and Buzsáki, G. (1998). Theta oscillations in somata and dendrites of hippocampal pyramidal cells in vivo: activity-dependent phase-precession of action potentials. Hippocampus *8*, 244-261.

Kask, K., Zamanillo, D., Rozov, A., Burnashev, N., Sprengel, R., and Seeburg, P.H. (1998). The AMPA receptor subunit GluR-B in its Q/R site-unedited form is not essential for brain development and function. Proc Natl Acad Sci U S A *95*, 13777-13782.

Kentros, C. (2006). Hippocampal place cells: the "where" of episodic memory? Hippocampus *16*, 743-754.

Kentros, C., Hargreaves, E., Hawkins, R.D., Kandel, E.R., Shapiro, M., and Muller, R.V. (1998). Abolition of long-term stability of new hippocampal place cell maps by NMDA receptor blockade. Science *280*, 2121-2126.

Kentros, C.G., Agnihotri, N.T., Streater, S., Hawkins, R.D., and Kandel, E.R. (2004). Increased attention to spatial context increases both place field stability and spatial memory. Neuron *42*, 283-295.

Kesner, R.P., Gilbert, P.E., and Barua, L.A. (2002). The role of the hippocampus in memory for the temporal order of a sequence of odors. Behav Neurosci *116*, 286-290.

King, C., Recce, M., and O'Keefe, J. (1998). The rhythmicity of cells of the medial septum/diagonal band of Broca in the awake freely moving rat: relationships with behaviour and hippocampal theta. Eur J Neurosci *10*, 464-477.

Kinney, G.G., Patino, P., Mermet-Bouvier, Y., Starrett, J.E., Jr., and Gribkoff, V.K. (1999). Cognition-enhancing drugs increase stimulated hippocampal theta rhythm amplitude in the urethane-anesthetized rat. J Pharmacol Exp Ther *291*, 99-106.

Kiss, T., Orbán, G., Lengyel, M., and Érdi, P. (2001). Intrahippocampal gamma and theta rhythm generation in a network model of inhibitory interneurons. . Neurocomputing *38-40*, 713–719.

Klausberger, T., Magill, P.J., Márton, L.F., Roberts, J.D.B., Cobden, P.M., Buzsáki, G., and Somogyi, P. (2003). Brain-state- and cell-type-specific firing of hippocampal interneurons in vivo. Nature *421*, 844-848.

Klimesch, W. (1999). EEG alpha and theta oscillations reflect cognitive and memory performance: a review and analysis. Brain Res Brain Res Rev *29*, 169-195.

Knierim, J.J., McNaughton, B.L., and Poe, G.R. (2000). Three-dimensional spatial selectivity of hippocampal neurons during space flight. Nat Neurosci *3*, 209-210.

Kocsis, B., Bragin, A., and Buzsaki, G. (1999). Interdependence of multiple theta generators in the hippocampus: a partial coherence analysis. J Neurosci *19*, 6200-6212.

Kogan, J.H., Frankland, P.W., Blendy, J.A., Coblentz, J., Marowitz, Z., Schutz, G., and Silva, A.J. (1997). Spaced training induces normal long-term memory in CREB mutant mice. Curr Biol *7*, 1-11.

Komisaruk, B.R. (1970). Synchrony between limbic system theta activity and rhythmical behavior in rats. J Comp Physiol Psychol *70*, 482-492.

Konig, P., Engel, A.K., and Singer, W. (1996). Integrator or coincidence detector? The role of the cortical neuron revisited. Trends Neurosci *19*, 130-137.

Konopacki, J., Bland, B.H., MacIver, M.B., and Roth, S.H. (1987). Cholinergic theta rhythm in transected hippocampal slices: independent CA1 and dentate generators. Brain Res *436*, 217-222.

Kramis, R., Vanderwolf, C.H., and Bland, B.H. (1975). Two types of hippocampal rhythmical slow activity in both the rabbit and the rat: relations to behavior and effects of atropine, diethyl ether, urethane, and pentobarbital. Exp Neurol *49*, 58-85.

Kubie, J.L., Muller, R.U., Hawley, E.S., and Jia, C.P. (1992). Evidence that hippocampal place cell representations in multiple ments are not strictly topographic. Soc. Neurosci. Abstr. 18, 1062.

Larson, J., Wong, D., and Lynch, G. (1986a). Patterned stimulation at the theta frequency is optimal for the induction of hippocampal long-term potentiation. Brain Res *368*, 347-350.

Larson, J., Wong, D., and Lynch, G. (1986b). Patterned stimulation at the theta frequency is optimal for the induction of hippocampal long-term potentiation. . Brain Res *368*, 347–350.

Lee, I., Yoganarasimha, D., Rao, G., and Knierim, J.J. (2004). Comparison of population coherence of place cells in hippocampal subfields CA1 and CA3. Nature *430*, 456-459.

Lenck-Santini, P.P., Save, E., and Poucet, B. (2001). Evidence for a relationship between place-cell spatial firing and spatial memory performance. Hippocampus *11*, 377-390.

Leung, L.S. (1998). Generation of theta and gamma rhythms in the hippocampus. Neurosci Biobehav Rev *22*, 275-290.

Leung, L.S., and Shen, B. (2004). Glutamatergic synaptic transmission participates in generating the hippocampal EEG. Hippocampus *14*, 510-525.

Leung, L.S., and Yim, C.Y. (1986). Intracellular records of theta rhythm in hippocampal CA1 cells of the rat. Brain Res *367*, 323-327.

Leutgeb, S., Leutgeb, J.K., Barnes, C.A., Moser, E.I., McNaughton, B.L., and Moser, M.-B. (2005). Independent codes for spatial and episodic memory in hippocampal neuronal ensembles. Science *309*, 619-623.

Leutgeb, S., Leutgeb, J.K., Treves, A., Moser, M.-B., and Moser, E.I. (2004). Distinct ensemble codes in hippocampal areas CA3 and CA1. Science *305*, 1295-1298.

Leutgeb, S., and Mizumori, S.J. (1999). Excitotoxic septal lesions result in spatial memory deficits and altered flexibility of hippocampal single-unit representations. J Neurosci *19*, 6661-6672.

Lever, C., Wills, T., Cacucci, F., Burgess, N., and O'Keefe, J. (2002). Long-term plasticity in hippocampal place-cell representation of environmental geometry. Nature *416*, 90-94.

Liao, D., Hessler, N., and Malinow, R. (1995). Activation of postsynaptically silent synapses during pairing-induced LTP in CA1 region of hippocampal slice. Nature *375*, 400–404.

Lisman, J.E., and Idiart, M.A. (1995). Storage of 7 +/- 2 short-term memories in oscillatory subcycles. Science *267*, 1512-1515.

Lisman, J.E., and Otmakhova, N.A. (2001). Storage, recall, and novelty detection of sequences by the hippocampus: elaborating on the SOCRATIC model to account for normal and aberrant effects of dopamine. Hippocampus *11*, 551-568.

Lissin, D.V., Gomperts, S.N., Carroll, R.C., Christine, C.W., Kalman, D., Kitamura, M., Hardy, S., Nicoll, R.A., Malenka, R.C., and von Zastrow, M. (1998). Activity differentially regulates the surface expression of synaptic AMPA and NMDA glutamate receptors. Proc Natl Acad Sci U S A *95*, 7097-7102.

Liu, S.Q., and Cull-Candy, S.G. (2000). Synaptic activity at calcium-permeable AMPA receptors induces a switch in receptor subtype. Nature *405*, 454-458.

Lopes da Silva, F.H., Witter, M.P., Boeijinga, P.H., and Lohman, A.H. (1990). Anatomic organization and physiology of the limbic cortex. Physiol Rev *70*, 453-511.

Ludvig, N., Tang, H.M., Gohil, B.C., and Botero, J.M. (2004). Detecting location-specific neuronal firing rate increases in the hippocampus of freely-moving monkeys. Brain Res *1014*, 97-109.

Lynch, G.S., Dunwiddie, T., and Gribkoff, V. (1977). Heterosynaptic depression: postsynaptic correlate of long-term potentiation. . Nature *266*, 737–739.

Lynch, M.A. (2004). Long-term potentiation and memory. Physiol Rev *84*, 87-136.

Maaswinkel, H., and Whishaw, I.Q. (1999). Homing with locale, taxon, and dead reckoning strategies by foraging rats: sensory hierarchy in spatial navigation. Behav Brain Res *99*, 143-152.

Mack, V., Burnashev, N., Kaiser, K.M., Rozov, A., Jensen, V., Hvalby, O., Seeburg, P.H., Sakmann, B., and Sprengel, R. (2001). Conditional restoration of hippocampal synaptic potentiation in Glur-A-deficient mice. Science *292*, 2501-2504.

Macrides, F. (1975). Temporal relationships between hippocampal slow waves and exploratory sniffing in hamsters. Behav Biol *14*, 295-308.

MacVicar, B.A., and Tse, F.W. (1989). Local neuronal circuitry underlying cholinergic rhythmical slow activity in CA3 area of rat hippocampal slices. J Physiol *417*, 197-212.

Madison, D.V., Lancaster, B., and Nicoll, R.A. (1987). Voltage clamp analysis of cholinergic action in the hippocampus. J Neurosci *7*, 733-741.

Magee, J.C., and Cook, E.P. (2000). Somatic EPSP amplitude is independent of synapse location in hippocampal pyramidal neurons. Nat Neurosci *3*, 895-903.

Magee, J.C., and Johnston, D. (1997). A synaptically controlled, associative signal for Hebbian plasticity in hippocampal neurons. Science *275*, 209-213.

Malenka, R.C., and Nicoll, R.A. (1999). Long-term potentiation--a decade of progress? Science *285*, 1870-1874.

Malinow, R., and Malenka, R.C. (2002). AMPA receptor trafficking and synaptic plasticity. Annu Rev Neurosci *25*, 103-126.

Manabe, T., Noda, Y., Mamiya, T., Katagiri, H., Houtani, T., Nishi, M., Noda, T., Takahashi, T., Sugimoto, T., Nabeshima, T., and Takeshima, H. (1998). Facilitation of

long-term potentiation and memory in mice lacking nociceptin receptors. Nature *394*, 577-581.

Markowska, A.L., Olton, D.S., and Givens, B. (1995). Cholinergic manipulations in the medial septal area: age-related effects on working memory and hippocampal electrophysiology. J Neurosci *15*, 2063-2073.

Markus, E.J., Qin, Y.L., Leonard, B., Skaggs, W.E., McNaughton, B.L., and Barnes, C.A. (1995). Interactions between location and task affect the spatial and directional firing of hippocampal neurons. J Neurosci *15*, 7079-7094.

Martin, S.J., Grimwood, P.D., and Morris, R.G. (2000). Synaptic plasticity and memory: an evaluation of the hypothesis. Annu Rev Neurosci *23*, 649-711.

Matsumura, N., Nishijo, H., Tamura, R., Eifuku, S., Endo, S., and Ono, T. (1999). Spatial- and task-dependent neuronal responses during real and virtual translocation in the monkey hippocampal formation. J Neurosci *19*, 2381-2393.

Matsuzaki, M., Honkura, N., Ellis-Davies, G.C.R., and Kasai, H. (2004). Structural basis of long-term potentiation in single dendritic spines. Nature *429*, 761-766.

Matthews, D.A., Cotman, C., and Lynch, G. (1976). An electron microscopic study of lesion-induced synaptogenesis in the dentate gyrus of the adult rat. II. Reappearance of morphologically normal synaptic contacts. Brain Res *115*, 23-41.

Mayford, M., Mansuy, I.M., Muller, R.U., and Kandel, E.R. (1997). Memory and behavior: a second generation of genetically modified mice. Curr Biol *7*, R580-589.

McEchron, M.D., and Disterhoft, J.F. (1999). Hippocampal encoding of non-spatial trace conditioning. Hippocampus *9*, 385-396.

McFarland, W.L., Teitelbaum, H., and Hedges, E.K. (1975). Relationship between hippocampal theta activity and running speed in the rat. J Comp Physiol Psychol *88*, 324-328.

McHugh, T.J., Blum, K.I., Tsien, J.Z., Tonegawa, S., and Wilson, M.A. (1996). Impaired hippocampal representation of space in CA1-specific NMDAR1 knockout mice. Cell *87*, 1339-1349.

McNaughton, B.L., Barnes, C.A., Meltzer, J., and Sutherland, R.J. (1989). Hippocampal granule cells are necessary for normal spatial learning but not for spatially-selective pyramidal cell discharge. Exp Brain Res *76*, 485-496.

McNaughton, B.L., Barnes, C.A., and O'Keefe, J. (1983a). The contributions of position, direction, and velocity to single unit activity in the hippocampus of freely-moving rats. Exp Brain Res *52*, 41-49.

McNaughton, B.L., Battaglia, F.P., Jensen, O., Moser, E.I., and Moser, M.B. (2006). Path integration and the neural basis of the 'cognitive map'. Nat Rev Neurosci *7*, 663-678.

McNaughton, B.L., O'Keefe, J., and Barnes, C.A. (1983b). The stereotrode: a new technique for simultaneous isolation of several single units in the central nervous system from multiple unit records. J Neurosci Methods *8*, 391-397.

Mehta, M.R., Barnes, C.A., and McNaughton, B.L. (1997). Experience-dependent, asymmetric expansion of hippocampal place fields. Proc Natl Acad Sci U S A *94*, 8918-8921.

Mehta, M.R., Lee, A.K., and Wilson, M.A. (2002). Role of experience and oscillations in transforming a rate code into a temporal code. Nature *417*, 741-746.

Mehta, M.R., and McNaughton, B.L. (1997). Absence of experience dependent place field expansion and shift in the dentate gyrus and the NMDA deprived CA1. Soc. Neurosci. Abs. #196.7.

Mehta, M.R., Quirk, M.C., and Wilson, M.A. (2000). Experience-dependent asymmetric shape of hippocampal receptive fields. Neuron *25*, 707-715.

Mizumori, S.J., Barnes, C.A., and McNaughton, B.L. (1990a). Behavioral correlates of theta-on and theta-off cells recorded from hippocampal formation of mature young and aged rats. Exp Brain Res *80*, 365-373.

Mizumori, S.J., McNaughton, B.L., Barnes, C.A., and Fox, K.B. (1989). Preserved spatial coding in hippocampal CA1 pyramidal cells during reversible suppression of CA3c output: evidence for pattern completion in hippocampus. J Neurosci *9*, 3915-3928.

Mizumori, S.J., Perez, G.M., Alvarado, M.C., Barnes, C.A., and McNaughton, B.L. (1990b). Reversible inactivation of the medial septum differentially affects two forms of learning in rats. Brain Res *528*, 12-20.

Mizumori, S.J., Ragozzino, K.E., Cooper, B.G., and Leutgeb, S. (1999). Hippocampal representational organization and spatial context. Hippocampus *9*, 444-451.

Mizumori, S.J., Ward, K.E., and Lavoie, A.M. (1992). Medial septal modulation of entorhinal single unit activity in anesthetized and freely moving rats. Brain Res *570*, 188-197.

Molnár, E., Baude, A., Richmond, S.A., Patel, P.B., Somogyi, P., and McIlhinney, R.A. (1993). Biochemical and immunocytochemical characterization of antipeptide antibodies to a cloned GluR1 glutamate receptor subunit: cellular and subcellular distribution in the rat forebrain. Neuroscience *53*, 307-326.

Morris, R.G., Anderson, E., Lynch, G.S., and Baudry, M. (1986). Selective impairment of learning and blockade of long-term potentiation by an N-methyl-D-aspartate receptor antagonist, AP5. Nature *319*, 774–776.

Morris, R.G., Garrud, P., Rawlins, J.N., and O'Keefe, J. (1982). Place navigation impaired in rats with hippocampal lesions. Nature *297*, 681-683.

Morris, R.G.M., Moser, E.I., Riedel, G., Martin, S.J., Sandin, J., Day, M., and O'Carroll, C. (2003). Elements of a neurobiological theory of the hippocampus: the role of activity-dependent synaptic plasticity in memory. Philos Trans R Soc Lond B Biol Sci *358*, 773-786.

Moser, E.I., Krobert, K.A., Moser, M.B., and Morris, R.G. (1998). Impaired spatial learning after saturation of long-term potentiation. Science *281*, 2038-2042.

Muller, R.U., and Kubie, J.L. (1987). The effects of changes in the environment on the spatial firing of hippocampal complex-spike cells. J Neurosci *7*, 1951-1968.

Muller, R.U., and Kubie, J.L. (1989). The firing of hippocampal place cells predicts the future position of freely moving rats. J Neurosci *9*, 4101-4110.

Muller, R.U., Kubie, J.L., and Ranck, J.B., Jr. (1987). Spatial firing patterns of hippocampal complex-spike cells in a fixed environment. J Neurosci *7*, 1935-1950.

Muller, R.U., Stead, M., and Pach, J. (1996). The hippocampus as a cognitive graph. J Gen Physiol *107*, 663-694.

Nakazawa, K., McHugh, T.J., Wilson, M.A., and Tonegawa, S. (2004). NMDA receptors, place cells and hippocampal spatial memory. Nat Rev Neurosci *5*, 361-372.

Nakazawa, K., Quirk, M.C., Chitwood, R.A., Watanabe, M., Yeckel, M.F., Sun, L.D., Kato, A., Carr, C.A., Johnston, D., Wilson, M.A., and Tonegawa, S. (2002). Requirement for hippocampal CA3 NMDA receptors in associative memory recall. Science *297*, 211-218.

Niedermeyer, E. (1999). The normal EEG of the waking adult. In: Niedermeyer E, Lopes da Silva F, editors. Electroencephalography: basic principles, clinical applications, and related fields, Philadelphia, PA: Lippincott Williams and Wilkins, Fourth edition., 149–173.

Nishi, M., Houtani, T., Noda, Y., Mamiya, T., Sato, K., Doi, T., Kuno, J., Takeshima, H., Nukada, T., Nabeshima, T.*, et al.* (1997). Unrestrained nociceptive response and disregulation of hearing ability in mice lacking the nociceptin/orphaninFQ receptor. Embo J *16*, 1858-1864.

Nunez, A., Garcia-Austt, E., and Buno, W., Jr. (1987). Intracellular theta-rhythm generation in identified hippocampal pyramids. Brain Res *416*, 289-300.

O'Keefe, J. (1976). Place units in the hippocampus of the freely moving rat. Exp Neurol *51*, 78-109.

O'Keefe, J. (1999). Do hippocampal pyramidal cells signal non-spatial as well as spatial information? Hippocampus *9*, 352-364.

O'Keefe, J., and Burgess, N. (1996). Geometric determinants of the place fields of hippocampal neurons. Nature *381*, 425-428.

O'Keefe, J., and Burgess, N. (1999). Theta activity, virtual navigation and the human hippocampus. Trends Cogn Sci *3*, 403-406.

O'Keefe, J., and Conway, D.H. (1978). Hippocampal place units in the freely moving rat: why they fire where they fire. Exp Brain Res *31*, 573-590.

O'Keefe, J., and Dostrovsky, J. (1971). The hippocampus as a spatial map. Preliminary evidence from unit activity in the freely-moving rat. Brain Res *34*, 171-175.

O'Keefe, J., and Nadel, L. (1978). The hippocampus as a cognitive map.Oxford: Clarendon Press.

O'Keefe, J., and Recce, M. (1993a). Phase relationship between hippocampal place units and the EEG theta rhythm. Hippocampus *3*, 317-330.

O'Keefe, J., and Recce, M.L. (1993b). Phase relationship between hippocampal place units and the EEG theta rhythm. Hippocampus *3*, 317-330.

O'Keefe, J., and Speakman, A. (1987). Single unit activity in the rat hippocampus during a spatial memory task. Exp Brain Res *68*, 1-27.

Oler, J.A., and Markus, E.J. (1998). Age-related deficits on the radial maze and in fear conditioning: hippocampal processing and consolidation. Hippocampus *8*, 402-415.

Oler, J.A., and Markus, E.J. (2000). Age-related deficits in the ability to encode contextual change: a place cell analysis. Hippocampus *10*, 338-350.

Olypher, A.V., Lansky, P., and Fenton, A.A. (2002). Properties of the extra-positional signal in hippocampal place cell discharge derived from the overdispersion in location-specific firing. Neuroscience *111*, 553-566.

Ono, T., Tamura, R., and Nakamura, K. (1991). The hippocampus and space: are there "place neurons" in the monkey hippocampus? Hippocampus *1*, 253-257.

Orban, G., Kiss, T., Lengyel, M., and Erdi, P. (2001). Hippocampal rhythm generation: gamma-related theta-frequency resonance in CA3 interneurons. Biol Cybern *84*, 123-132.

Orr, G., Rao, G., Houston, F.P., McNaughton, B.L., and Barnes, C.A. (2001). Hippocampal synaptic plasticity is modulated by theta rhythm in the fascia dentata of adult and aged freely behaving rats. Hippocampus *11*, 647-654.

Otmakhova, N.A., and Lisman, J.E. (2000). Dopamine, serotonin, and noradrenaline strongly inhibit the direct perforant path-CA1 synaptic input, but have little effect on the Schaffer collateral input. Ann N Y Acad Sci *911*, 462-464.

Otnaess, M.K., Brun, V.H., Moser, M.B., and Moser, E.I. (1999). Pretraining prevents spatial learning impairment after saturation of hippocampal long-term potentiation. J Neurosci *19*, RC49.

Pan, W.X., and McNaughton, N. (1997). The medial supramammillary nucleus, spatial learning and the frequency of hippocampal theta activity. Brain Res *764*, 101-108.

Pavlides, C., Greenstein, Y.J., Grudman, M., and Winson, J. (1988). Long-term potentiation in the dentate gyrus is induced preferentially on the positive phase of theta-rhythm. Brain Res *439*, 383-387.

Petralia, R.S., and Wenthold, R.J. (1992). Light and electron immunocytochemical localization of AMPA-selective glutamate receptors in the rat brain. J Comp Neurol *318*, 329-354.

Petsche, H., Stumpf, C., and Gogolak, G. (1962). [The significance of the rabbit's septum as a relay station between the midbrain and the hippocampus. I. The control of hippocampus arousal activity by the septum cells.]. Electroencephalogr Clin Neurophysiol *14*, 202-211.

Pike, F.G., Meredith, R.M., Olding, A.W., and Paulsen, O. (1999). Rapid report: postsynaptic bursting is essential for 'Hebbian' induction of associative long-term potentiation at excitatory synapses in rat hippocampus. J Physiol *518 (Pt 2)*, 571-576.

Poucet, B., Save, E., and Lenck-Santini, P.P. (2000). Sensory and memory properties of hippocampal place cells. Rev Neurosci *11*, 95-111.

Puryear, C.B., King, M., and Mizumori, S.J. (2006). Specific changes in hippocampal spatial codes predict spatial working memory performance. Behav Brain Res *169*, 168-175.

Quirk, G.J., Muller, R.U., Kubie, J.L., and Ranck, J.B., Jr. (1992). The positional firing properties of medial entorhinal neurons: description and comparison with hippocampal place cells. J Neurosci *12*, 1945-1963.

Ramón y Cajal, S. (1893). Estructura del asta de Ammon y fascia dentata. An Soc Esp Hist Nat *22*.

Ranck, J.B. (1973a). Studies on single neurons in dorsal hippocampal formation and septum in unrestrained rats. I. behavioral correlates and firing repertoires. Exp Neurol *41*, 461-531.

Ranck, J.B., Jr. (1973b). Studies on single neurons in dorsal hippocampal formation and septum in unrestrained rats. I. Behavioral correlates and firing repertoires. Exp Neurol *41*, 461-531.

Rawlins, J.N., and Olton, D.S. (1982). The septo-hippocampal system and cognitive mapping. Behav Brain Res *5*, 331-358.

Redish, A.D. (1999). Beyond the cognitive map: from place cells to episodic memory, A Bradford Book. Cambridge, MA: The MIT Press.

Redish, A.D., Battaglia, F.P., Chawla, M.K., Ekstrom, A.D., Gerrard, J.L., Lipa, P., Rosenzweig, E.S., Worley, P.F., Guzowski, J.F., McNaughton, B.L., and Barnes, C.A. (2001). Independence of firing correlates of anatomically proximate hippocampal pyramidal cells. J Neurosci *21*, RC134.

Reisel, D., Bannerman, D.M., Deacon, R.M., Sprengel, R., Seeburg, P.H., and Rawlins, J.N. (2005). GluR-A-dependent synaptic plasticity is required for the temporal encoding of nonspatial information. Behav Neurosci *119*, 1298-1306.

Reisel, D., Bannerman, D.M., Schmitt, W.B., Deacon, R.M., Flint, J., Borchardt, T., Seeburg, P.H., and Rawlins, J.N. (2002). Spatial memory dissociations in mice lacking GluR1. Nat Neurosci *5*, 868-873.

Riehle, A., Grun, S., Diesmann, M., and Aertsen, A. (1997). Spike synchronization and rate modulation differentially involved in motor cortical function. Science *278*, 1950-1953.

Robbe, D., Montgomery, S.M., Thome, A., Rueda-Orozco, P.E., McNaughton, B.L., and Buzsaki, G. (2006). Cannabinoids reveal importance of spike timing coordination in hippocampal function. Nat Neurosci *9*, 1526-1533.

Robinson, T.E. (1980). Hippocampal rhythmic slow activity (RSA; theta): a critical analysis of selected studies and discussion of possible species-differences. Brain Res *203*, 69-101.

Rolls, E.T. (1999). Spatial view cells and the representation of place in the primate hippocampus. Hippocampus *9*, 467-480.

Rolls, E.T., Robertson, R.G., and Georges-Francois, P. (1997). Spatial view cells in the primate hippocampus. Eur J Neurosci *9*, 1789-1794.

Rose, G.M., and Dunwiddie, T.V. (1986). Induction of hippocampal long-term potentiation using physiologically patterned stimulation. Neurosci Lett *69*, 244–248.

Rotenberg, A., Abel, T., Hawkins, R.D., Kandel, E.R., and Muller, R.U. (2000). Parallel instabilities of long-term potentiation, place cells, and learning caused by decreased protein kinase A activity. J Neurosci *20*, 8096-8102.

Rotenberg, A., Mayford, M., Hawkins, R.D., Kandel, E.R., and Muller, R.U. (1996). Mice expressing activated CaMKII lack low frequency LTP and do not form stable place cells in the CA1 region of the hippocampus. Cell *87*, 1351-1361.

Sakimura, K., Kutsuwada, T., Ito, I., Manabe, T., Takayama, C., Kushiya, E., Yagi, T., Aizawa, S., Inoue, Y., and Sugiyama, H. (1995). Reduced hippocampal LTP and spatial learning in mice lacking NMDA receptor epsilon 1 subunit. Nature *373*, 151-155.

Samsonovich, A., and McNaughton, B.L. (1997). Path integration and cognitive mapping in a continuous attractor neural network model. J Neurosci *17*, 5900-5920.

Sanchis-Segura, C., Borchardt, T., Vengeliene, V., Zghoul, T., Bachteler, D., Gass, P., Sprengel, R., and Spanagel, R. (2006). Involvement of the AMPA receptor GluR-C subunit in alcohol-seeking behavior and relapse. J Neurosci *26*, 1231-1238.

Sargolini, F., Fyhn, M., Hafting, T., McNaughton, B.L., Witter, M.P., Moser, M.B., and Moser, E.I. (2006). Conjunctive representation of position, direction, and velocity in entorhinal cortex. Science *312*, 758-762.

Saucier, D., and Cain, D.P. (1995). Spatial learning without NMDA receptor-dependent long-term potentiation. Nature *378*, 186-189.

Save, E., Cressant, A., Thinus-Blanc, C., and Poucet, B. (1998). Spatial firing of hippocampal place cells in blind rats. J Neurosci *18*, 1818-1826.

Save, E., Nerad, L., and Poucet, B. (2000). Contribution of multiple sensory information to place field stability in hippocampal place cells. Hippocampus *10*, 64-76.

Save, E., Poucet, B., Foreman, N., and Buhot, M.C. (1992). Object exploration and reactions to spatial and nonspatial changes in hooded rats following damage to parietal cortex or hippocampal formation. Behav Neurosci *106*, 447-456.

Schmitt, W.B., Deacon, R.M., Reisel, D., Sprengel, R., Seeburg, P.H., Rawlins, J.N., and Bannerman, D.M. (2004). Spatial reference memory in GluR-A-deficient mice using a novel hippocampal-dependent paddling pool escape task. Hippocampus *14*, 216-223.

Schmitt, W.B., Deacon, R.M., Seeburg, P.H., Rawlins, J.N., and Bannerman, D.M. (2003). A within-subjects, within-task demonstration of intact spatial reference memory and

impaired spatial working memory in glutamate receptor-A-deficient mice. J Neurosci *23*, 3953-3959.

Schmitt, W.B., Sprengel, R., Mack, V., Draft, R.W., Seeburg, P.H., Deacon, R.M., Rawlins, J.N., and Bannerman, D.M. (2005). Restoration of spatial working memory by genetic rescue of GluR-A-deficient mice. Nat Neurosci *8*, 270-272.

Schmitzer-Torbert, N., Jackson, J., Henze, D., Harris, K., and Redish, A.D. (2005). Quantitative measures of cluster quality for use in extracellular recordings. Neuroscience *131*, 1-11.

Scoville, W.B., and Milner, B. (1957). Loss of recent memory after bilateral hippocampal lesions. J Neurol Neurosurg Psychiatry *20*, 11-21.

Seager, M.A., Johnson, L.D., Chabot, E.S., Asaka, Y., and Berry, S.D. (2002). Oscillatory brain states and learning: Impact of hippocampal theta-contingent training. Proc Natl Acad Sci U S A *99*, 1616-1620.

Shapiro, M.L., Tanila, H., and Eichenbaum, H. (1997). Cues that hippocampal place cells encode: dynamic and hierarchical representation of local and distal stimuli. Hippocampus *7*, 624-642.

Sharp, P.E. (1996). Multiple spatial/behavioral correlates for cells in the rat postsubiculum: multiple regression analysis and comparison to other hippocampal areas. Cereb Cortex *6*, 238-259.

Sharp, P.E. (1999). Subicular place cells expand or contract their spatial firing pattern to fit the size of the environment in an open field but not in the presence of barriers: comparison with hippocampal place cells. Behav Neurosci *113*, 643-662.

Sharp, P.E. (2002). The neural basis of navigation. Dordrecht, The Netherlands: Kluwer.

Sharp, P.E. (2006). Subicular place cells generate the same "map" for different environments: Comparison with hippocampal cells. Behav Brain Res.

Sharp, P.E., and Green, C. (1994). Spatial correlates of firing patterns of single cells in the subiculum of the freely moving rat. J Neurosci *14*, 2339-2356.

Shen, J., Barnes, C.A., McNaughton, B.L., Skaggs, W.E., and Weaver, K.L. (1997). The effect of aging on experience-dependent plasticity of hippocampal place cells. J Neurosci *17*, 6769-6782.

Shi, S., Hayashi, Y., Esteban, J., and Malinow, R. (2001). Subunit-specific rules governing AMPA receptor trafficking to synapses in hippocampal pyramidal neurons. Cell *105*, 331–343.

Shimshek, D.R., Jensen, V., Celikel, T., Geng, Y., Schupp, B., Bus, T., Mack, V., Marx, V., Hvalby, O., Seeburg, P.H., and Sprengel, R. (2006). Forebrain-specific glutamate receptor B deletion impairs spatial memory but not hippocampal field long-term potentiation. J Neurosci *26*, 8428-8440.

Shin, J., and Talnov, A. (2001). A single trial analysis of hippocampal theta frequency during nonsteady wheel running in rats. Brain Res *897*, 217-221.

Siapas, A.G., and Wilson, M.A. (1998). Coordinated interactions between hippocampal ripples and cortical spindles during slow-wave sleep. Neuron *21*, 1123-1128.

Sik, A., Penttonen, M., Ylinen, A., and Buzsaki, G. (1995). Hippocampal CA1 interneurons: an in vivo intracellular labeling study. J Neurosci *15*, 6651-6665.

Silva, A.J., Kogan, J.H., Frankland, P.W., and Kida, S. (1998). CREB and memory. Annu Rev Neurosci *21*, 127-148.

Sirota, A., Csicsvari, J., Buhl, D., and Buzsáki, G. (2003). Communication between neocortex and hippocampus during sleep in rodents. Proc Natl Acad Sci U S A *100*, 2065-2069.

Skaggs, W.E., and McNaughton, B.L. (1998). Spatial firing properties of hippocampal CA1 populations in an environment containing two visually identical regions. J Neurosci *18*, 8455-8466.

Skaggs, W.E., McNaughton, B.L., Gothard, K.M., and Markus, E.J. (1993). An Information-Theoretic Approach to Deciphering the Hippocampal Code. Advances in Neural Information Processing Systems *5*, 1030-1037.

Skaggs, W.E., McNaughton, B.L., Wilson, M.A., and Barnes, C.A. (1996). Theta phase precession in hippocampal neuronal populations and the compression of temporal sequences. Hippocampus *6*, 149-172.

Smith, D.M., and Mizumori, S.J. (2006). Hippocampal place cells, context, and episodic memory. Hippocampus.

Sprengel, R. (2006). Role of AMPA receptors in synaptic plasticity. Cell Tissue Res *326*, 447-455.

Squire, L.R., Stark, C.E.L., and Clark, R.E. (2004). The medial temporal lobe. Annu Rev Neurosci *27*, 279-306.

Staubli, U., Rogers, G., and Lynch, G. (1994). Facilitation of glutamate receptors enhances memory. Proc Natl Acad Sci U S A *91*, 777-781.

Stewart, M., and Fox, S.E. (1989). Two populations of rhythmically bursting neurons in rat medial septum are revealed by atropine. J Neurophysiol *61*, 982-993.

Stewart, M., and Fox, S.E. (1990). Do septal neurons pace the hippocampal theta rhythm? Trends Neurosci *13*, 163-168.

Sun, Y., Olson, R., Horning, M., Armstrong, N., Mayer, M., and Gouaux, E. (2002). Mechanism of glutamate receptor desensitization. Nature *417*, 245-253.

Tang, Y.P., Shimizu, E., Dube, G.R., Rampon, C., Kerchner, G.A., Zhuo, M., Liu, G., and Tsien, J.Z. (1999). Genetic enhancement of learning and memory in mice. Nature *401*, 63-69.

Tang, Y.P., Wang, H., Feng, R., Kyin, M., and Tsien, J.Z. (2001). Differential effects of enrichment on learning and memory function in NR2B transgenic mice.
. Neuropharmacology *41*, 779–790.

Tanila, H., Shapiro, M., Gallagher, M., and Eichenbaum, H. (1997a). Brain aging: changes in the nature of information coding by the hippocampus. J Neurosci *17*, 5155-5166.

Tanila, H., Shapiro, M.L., and Eichenbaum, H. (1997b). Discordance of spatial representation in ensembles of hippocampal place cells. Hippocampus *7*, 613-623.

Tanila, H., Sipila, P., Shapiro, M., and Eichenbaum, H. (1997c). Brain aging: impaired coding of novel environmental cues. J Neurosci *17*, 5167-5174.

Taube, J.S. (1995). Place cells recorded in the parasubiculum of freely moving rats. Hippocampus *5*, 569-583.

Taverna, F.A., Georgiou, J., McDonald, R.J., Hong, N.S., Kraev, A., Salter, M.W., Takeshima, H., Muller, R.U., and Roder, J.C. (2005). Defective place cell activity in nociceptin receptor knockout mice with elevated NMDA receptor-dependent long-term potentiation. J Physiol *565*, 579-591.

Tesche, C.D., and Karhu, J. (2000). Theta oscillations index human hippocampal activation during a working memory task. Proc Natl Acad Sci U S A *97*, 919-924.

Thompson, L.T., and Best, P.J. (1989). Place cells and silent cells in the hippocampus of freely-behaving rats. J Neurosci *9*, 2382-2390.

Thompson, L.T., and Best, P.J. (1990). Long-term stability of the place-field activity of single units recorded from the dorsal hippocampus of freely behaving rats. Brain Res *509*, 299-308.

Tocco, G., Devgan, K.K., Hauge, S.A., Weiss, C., Baudry, M., and Thompson, R.F. (1991). Classical conditioning selectively increases AMPA receptor binding in rabbit hippocampus. Brain Res *559*, 331-336.

Tolman, E.C. (1948). Cognitive maps in rats and men. Psychol Rev *55*, 189–208.

Tonegawa, S., Nakazawa, K., and Wilson, M.A. (2003). Genetic neuroscience of mammalian learning and memory. Philos Trans R Soc Lond B Biol Sci *358*, 787-795.

Toth, K., Freund, T.F., and Miles, R. (1997). Disinhibition of rat hippocampal pyramidal cells by GABAergic afferents from the septum. J Physiol *500 (Pt 2)*, 463-474.

Tropp Sneider, J., Chrobak, J.J., Quirk, M.C., Oler, J.A., and Markus, E.J. (2006). Differential behavioral state-dependence in the burst properties of CA3 and CA1 neurons. Neuroscience *141*, 1665-1677.

Tsien, J.Z., Huerta, P.T., and Tonegawa, S. (1996). The essential role of hippocampal CA1 NMDA receptor-dependent synaptic plasticity in spatial memory. Cell *87*, 1327-1338.

Vanderwolf, C.H. (1969). Hippocampal electrical activity and voluntary movement in the rat. Electroencephalogr Clin Neurophysiol *26*, 407-418.

Vanderwolf, C.H., Kramis, R., Gillespie, L.A., and Bland, B.H. (1975). Hippocampal rhythmical slow activity and neocortical low voltage fast activity: relation to behavior. In: The hippocampus: Neurophysiology and behavior, Vol 2 (Isaacson RL, Pribram KH, eds), New York: Plenum. 101-128.

Vazdarjanova, A., and Guzowski, J.F. (2004). Differences in hippocampal neuronal population responses to modifications of an environmental context: evidence for distinct, yet complementary, functions of CA3 and CA1 ensembles. J Neurosci *24*, 6489-6496.

Vertes, R.P., and Kocsis, B. (1997). Brainstem-diencephalo-septohippocampal systems controlling the theta rhythm of the hippocampus. Neuroscience *81*, 893-926.

Vinogradova, O.S., Brazhnik, E.S., Karanov, A.M., and Zhadina, S.D. (1980). Neuronal activity of the septum following various types of deafferentation. Brain Res *187*, 353-368.

Wallenstein, G.V., Eichenbaum, H., and Hasselmo, M.E. (1998). The hippocampus as an associator of discontiguous events. Trends Neurosci *21*, 317-323.

Wang, Y., Rowan, M.J., and Anwyl, R. (1997). Induction of LTD in the dentate gyrus in vitro is NMDA receptor independent, but dependent on Ca2+ influx via low-voltage-activated Ca2+ channels and release of Ca2+ from intracellular stores. J Neurophysiol *77*, 812-825.

Wenthold, R.J., Petralia, R.S., Blahos, J., II, and Niedzielski, A.S. (1996). Evidence for multiple AMPA receptor complexes in hippocampal CA1/CA2 neurons. J Neurosci *16*, 1982-1989.

Whitlock, J.R., Heynen, A.J., Shuler, M.G., and Bear, M.F. (2006). Learning induces long-term potentiation in the hippocampus. Science *313*, 1093-1097.

Wiener, S.I., Paul, C.A., and Eichenbaum, H. (1989). Spatial and behavioral correlates of hippocampal neuronal activity. J Neurosci *9*, 2737-2763.

Wilent, W.B., and Nitz, D.A. (2007). Discrete place fields of hippocampal formation interneurons. J Neurophysiol.

Williams, J.H., and Kauer, J.A. (1997). Properties of carbachol-induced oscillatory activity in rat hippocampus. J Neurophysiol *78*, 2631-2640.

Wilson, M.A., and McNaughton, B.L. (1993). Dynamics of the hippocampal ensemble code for space. Science *261*, 1055-1058.

Wilson, M.A., and Tonegawa, S. (1997). Synaptic plasticity, place cells and spatial memory: study with second generation knockouts. Trends Neurosci *20*, 102-106.

Winson, J. (1974). Patterns of hippocampal theta rhythm in the freely moving rat. Electroencephalogr Clin Neurophysiol *36*, 291-301.

Winson, J. (1978). Loss of hippocampal theta rhythm results in spatial memory deficit in the rat. Science *201*, 160-163.

Wood, E.R., Dudchenko, P.A., and Eichenbaum, H. (1999). The global record of memory in hippocampal neuronal activity. Nature *397*, 613-616.

Wood, E.R., Dudchenko, P.A., Robitsek, R.J., and Eichenbaum, H. (2000). Hippocampal neurons encode information about different types of memory episodes occurring in the same location. Neuron *27*, 623-633.

Yan, J., Zhang, Y., Jia, Z., Taverna, F.A., McDonald, R.J., Muller, R.U., and Roder, J.C. (2002). Place-cell impairment in glutamate receptor 2 mutant mice. J Neurosci *22*, RC204.

Ylinen, A., Bragin, A., Nádasdy, Z., Jandó, G., Szabó, I., Sik, A., and Buzsáki, G. (1995a). Sharp wave-associated high-frequency oscillation (200 Hz) in the intact hippocampus: network and intracellular mechanisms. J Neurosci *15*, 30-46.

Ylinen, A., Soltesz, I., Bragin, A., Penttonen, M., Sik, A., and Buzsaki, G. (1995b). Intracellular correlates of hippocampal theta rhythm in identified pyramidal cells, granule cells, and basket cells. Hippocampus *5*, 78-90.

Young, B., and McNaughton, N. (2000). Common firing patterns of hippocampal cells in a differential reinforcement of low rates of response schedule. J Neurosci *20*, 7043-7051.

Zamanillo, D., Sprengel, R., Hvalby, O., Jensen, V., Burnashev, N., Rozov, A., Kaiser, K.M., Köster, H.J., Borchardt, T., Worley, P.*, et al.* (1999). Importance of AMPA receptors for hippocampal synaptic plasticity but not for spatial learning. Science *284*, 1805-1811.

Zhang, K., Ginzburg, I., McNaughton, B.L., and Sejnowski, T.J. (1998). Interpreting neuronal population activity by reconstruction: unified framework with application to hippocampal place cells. J Neurophysiol *79*, 1017-1044.

Zinyuk, L., Kubik, S., Kaminsky, Y., Fenton, A.A., and Bures, J. (2000). Understanding hippocampal activity by using purposeful behavior: place navigation induces place cell discharge in both task-relevant and task-irrelevant spatial reference frames. Proc Natl Acad Sci U S A *97*, 3771-3776.